

Sensitivity Study of a Computer Model Based Leak Detection System in Liquid Pipelines

by

Sergio Pabon

A thesis submitted in partial fulfillment of the requirements for the degree of

Master of Science

in

Water Resources Engineering

Department of Civil and Environmental Engineering  
University of Alberta

© Sergio Pabon, 2015

## **Abstract**

Computer model based leak detection technique is extensively applied in the energy pipeline industry. However, its effectiveness is often limited by the ability of the computer models to accurately reproduce the complex real-world pipeline systems and by inaccurate and insufficient measured data. Therefore, it is important to evaluate the impact of various factors and identify those which have the largest effect on leak detection. This sensitivity study investigated the effect of leak rate, the R factor (which includes pipeline, instrument and operating variables), leak location, transient type and severity, pressure and flow noise level in instruments on the response of the leak detection system. Datasets of simulated leaks on a virtual pipeline were created and used to test this sensitivity for various leak scenarios and data without and with instrument noise. The output variables of the tests revealed the leak detection system is more sensitive to R factor than to flow state, noise of instruments, and the transient severity. Leak location seems to have a smaller impact on the leak detection system. Leaks are easier to detect in pipeline systems with low R factor or during flow decrease transient events. These results are valuable to prioritize future improvement on the computer model, instruments, or the SCADA system in pipeline systems with low R factor or flow decrease transient events.

## **Acknowledgments**

The author expresses his gratitude to his supervisors, Dr. Mark Loewen and Dr. Yuntong She, for their kind assistance, guidance, time and effort in all aspects of this project. Thank you as well to Dr. Huazhou Li for being on the oral examining committee and chairing the exam.

This research was supported by an industry partner, and their contribution is gratefully acknowledged.

The author would also like to thank God and his family for their love, support and inspiration.

## Table of Contents

Chapter 1:	Introduction.....	1
1.1	Background.....	1
1.2	Research Impetus.....	2
1.3	Objective.....	4
1.4	Thesis Structure.....	4
Chapter 2:	Literature Review of Leak Detection Methods.....	6
2.1	Inspection.....	6
2.2	External Systems.....	7
2.3	Internally Based Computational Pipeline Monitoring Systems.....	8
2.3.1	Balance Methods.....	9
2.3.2	Other Methods.....	10
2.3.3	Real-Time Transient Model Based Methods.....	11
Chapter 3:	Methodology.....	18
3.1	Simulated Leak Test .....	18
3.1.1	<i>Simulator</i> Model Configuration.....	19
3.1.1.1	Pump and Valve Simulation.....	20
3.1.1.2	Leak Simulation.....	20
3.1.2	Instrument Noise Generation.....	21
3.1.3	Leak Detection System Response Testing.....	21
3.2	Pipeline Testing .....	26
3.2.1	Similitude Parameters.....	26
3.2.1.1	<i>R</i> Factor.....	26
3.2.1.2	Transient Severity.....	27

3.2.2	Idealized Study Pipeline.....	28
3.2.3	Discretization.....	29
3.3	Design Testing Scenarios.....	29
3.3.1	<i>R</i> Factor.....	30
3.3.2	Transient Type.....	30
3.3.3	Transient Severity.....	31
3.3.4	Noise Level.....	31
3.4	Diagnostic Flow.....	32
Chapter 4:	Discussion of Results.....	37
4.1	Sensitivity to Leak Rate.....	38
4.1.1	Perfect Data.....	38
4.1.2	Noisy Data.....	39
4.2	Sensitivity to <i>R</i> Factor.....	40
4.2.1	Perfect Data.....	40
4.2.2	Noisy Data.....	41
4.3	Sensitivity to Leak Location.....	42
4.3.1	Perfect Data.....	42
4.3.2	Noisy Data.....	43
4.4	Sensitivity to Transient Severity.....	44
4.4.1	Perfect Data.....	45
4.4.2	Noisy Data.....	45
4.5	Sensitivity to Flow State.....	48
4.5.1	Perfect Data.....	48
4.5.2	Noisy Data.....	48
4.6	Sensitivity to Noise Level in Flow .....	50

Chapter 5: Conclusions .....	79
5.1 Sensitivity to Leak Rate and Data Noise.....	80
5.2 Sensitivity to <i>R</i> Factor.....	80
5.3 Sensitivity to Flow State and Transient Severity.....	81
5.4 Sensitivity to Leak Location.....	81
5.5 Significance.....	82
References.....	84
Appendices.....	89
Appendix A: Sample Check List of Tests.....	89
Appendix B: List of Tests.....	90
Appendix C: Supplementary Plots of Diagnostic Flow.....	98
Appendix D: Best Tuning Parameters of the Leak Detection System.....	123

**List of Tables**

Table 3-1: Values and flow conditions of the tested variables.....36

## List of Figures

Figure 3-1: Simulated leak test system and its analogy to the real test system (Industry partner, 2013).....	33
Figure 3-2: Pipeline system layout for the idealized case in the Simulator model. Steel pipeline with a diameter of 30 inches, length of 150 km and Colebrook roughness of 0.0001 inches.....	33
Figure 3-3: Leak rate versus time for the orifice and the fixed leak rate methods. Flow decrease condition, leak size of 1%, $V_o = 2$ m/s, $R = 2.20$ , $V_f = 1$ m/s, duration = 5 s, TSV = 0.5. Perfect data. Leak starts at 04:00:00.....	34
Figure 3-4: Non-dimensional diagnostic flow DDF versus time for different sets of R factors, velocities and friction factors; leak size of 5%, steady state condition, perfect data, leak at midpoint. ....	34
Figure 3-5: Non-dimensional diagnostic flow DDF versus time for perfect data and noisy data, 1% noise levels, leak size of 1%, steady state condition, $V_o = 0.3$ m/s, $R = 0.49$ , leak at midpoint, leak starts at 04:00:00.....	35
Figure 4-1: Non-dimensional diagnostic flow DDF versus time for perfect data, leak sizes of 1%, 10%, 20% and 30%, steady flow conditions, $V_o = 0.3$ m/s, $R = 0.49$ , leak at midpoint.....	52
Figure 4-2: Non-dimensional diagnostic flow DDF versus time for perfect data, leak sizes of 1%, 10%, 20% and 30%, steady flow conditions, $V_o = 1$ m/s, $R = 1.26$ , leak at midpoint.....	52
Figure 4-3: Non-dimensional diagnostic flow DDF versus time for perfect data, leak sizes of 1%, 10%, 20% and 30%, steady flow conditions, $V_o = 2$ m/s, $R = 2.20$ , leak at midpoint.....	53

Figure 4-4: Non-dimensional diagnostic flow DDF versus time for perfect data, leak sizes of 1%, 10%, 20% and 30%, steady flow conditions,  $V_o = 3$  m/s,  $R = 3.08$ , leak at midpoint.....53

Figure 4-5: Non-dimensional diagnostic flow DDF versus time for perfect data, leak sizes of 1%, 10%, 20% and 30%, flow increase transient,  $V_o = 2$  m/s,  $V_f = 3$  m/s,  $R = 2.20$ ,  $TSV = 0.5$ , duration = 5 s, leak at midpoint.....54

Figure 4-6: Non-dimensional diagnostic flow DDF versus time for perfect data, leak sizes of 1%, 10%, 20% and 30%, flow decrease transient,  $V_o = 2$  m/s,  $V_f = 1$  m/s,  $R = 2.20$ ,  $TSV = 0.5$ , duration = 5 s, leak at midpoint.....54

Figure 4-7: Non-dimensional time-averaged diagnostic flow DDFTAVE versus time for 1% noise levels, leak sizes of 1% and 30% and steady flow conditions,  $V_o = 0.3$  m/s,  $R = 0.49$ , leak at midpoint.....55

Figure 4-8: Non-dimensional time-averaged diagnostic flow DDFTAVE versus time for 1% noise levels, leak sizes of 1% and 30% and flow increase transient,  $V_o = 2$  m/s,  $V_f = 3$  m/s,  $R = 2.20$ ,  $TSV = 0.5$ , duration = 5 s, leak at midpoint....55

Figure 4-9: Non-dimensional time-averaged diagnostic flow DDFTAVE versus time for 1% noise levels, leak sizes of 1% and 30%, flow decrease transient,  $V_o = 2$  m/s,  $V_f = 1$  m/s,  $R = 2.20$ ,  $TSV = 0.5$ , duration = 5 s, leak at midpoint....56

Figure 4-10: Non-dimensional diagnostic flow DDF versus time for perfect data and noisy data, 1% noise levels, leak size of 1%, steady flow conditions,  $V_o = 0.3$  m/s,  $R = 0.49$ , leak at midpoint.....56

Figure 4-11: Non-dimensional diagnostic flow DDF versus time for perfect data and noisy data, 1% noise levels, leak size of 30%, steady flow conditions,  $V_o = 0.3$  m/s,  $R = 0.49$ , leak at midpoint.....57

Figure 4-12: Non-dimensional diagnostic flow DDF versus time for perfect data, leak size of 1%, R factors of 0.49, 1.26, 2.20 and 3.08, steady flow conditions, leak at midpoint.....57

Figure 4-13: Non-dimensional diagnostic flow DDF versus time for perfect data, leak size of 1%, R factors of 0.49, 1.26 and 2.20, flow increase transient, duration = 5 s, leak at midpoint, TSV = 0.5.....58

Figure 4-14: Non-dimensional diagnostic flow DDF versus time for perfect data, leak size of 1%, R factors of 0.49, 1.26, 2.20 and 3.08, flow decrease transient, duration = 5 s, leak at midpoint, TSV = 0.5.....58

Figure 4-15: Non-dimensional time-averaged diagnostic flow DDFTAVE versus time for 1% noise levels, leak size of 30%, R factors of 0.49 and 2.20, steady flow conditions, leak at midpoint.....59

Figure 4-16: Non-dimensional time-averaged diagnostic flow DDFTAVE versus time for 1% noise levels, leak size of 1%, R factors of 0.49 and 2.20, steady flow conditions, leak at midpoint.....59

Figure 4-17: Non-dimensional time-averaged diagnostic flow DDFTAVE versus time for 1% noise levels, leak size of 30%, R factors of 0.49 and 2.20, flow increase transient, duration = 5 s, TSV = 0.5, leak at midpoint.....60

Figure 4-18: Non-dimensional time-averaged diagnostic flow DDFTAVE versus time for 1% noise levels, leak size of 1%, R factors of 0.49 and 2.20, flow increase transient, duration = 5 s, TSV = 0.5, leak at midpoint.....60

Figure 4-19: Non-dimensional time-averaged diagnostic flow DDFTAVE versus time for 1% noise levels, leak sizes of 1% and 30%, R factors of 0.49 and 2.20, flow decrease transient, duration = 5 s, TSV = 0.5, leak at midpoint.....61

Figure 4-20: Non-dimensional diagnostic flow DDF versus time for perfect data, leak size of 1%, leaks at first quarter, midpoint and third quarter of pipeline length, steady flow conditions,  $V_o = 0.3$  m/s,  $R = 0.49$ .....61

Figure 4-21: Non-dimensional diagnostic flow DDF versus time for perfect data, leak size of 1%, leaks at first quarter, midpoint and third quarter of pipeline length, steady flow conditions,  $V_o = 2$  m/s,  $R = 2.20$ .....62

Figure 4-22: Non-dimensional diagnostic flow DDF versus time for perfect data, leak size of 1%, leaks at first quarter, midpoint and third quarter of pipeline length, flow increase transient, duration = 5 s,  $R = 0.49$ ,  $V_o = 0.3$  m/s,  $TSV = 0.5$ .....62

Figure 4-23: Non-dimensional diagnostic flow DDF versus time for perfect data, leak size of 1%, leaks at first quarter, midpoint and third quarter of pipeline length, flow increase transient, duration = 5 s,  $R = 2.20$ ,  $V_o = 2.0$  m/s,  $TSV = 0.5$ .....63

Figure 4-24: Non-dimensional diagnostic flow DDF versus time for perfect data, leak size of 1%, leaks at first quarter, midpoint and third quarter of pipeline length, flow decrease transient, duration = 5 s,  $TSV = 0.5$ ,  $R = 0.49$ ,  $V_o = 0.3$  m/s.....63

Figure 4-25: Non-dimensional diagnostic flow DDF versus time for perfect data, leak size of 1%, leaks at first quarter, midpoint and third quarter of pipeline length, flow decrease transient, duration = 5 s,  $TSV = 0.5$ ,  $R = 2.20$ ,  $V_o = 2.0$  m/s.....64

Figure 4-26: Non-dimensional time-averaged diagnostic flow DDFTAVE versus time for 1% noise levels, leak size of 30%, leaks at first quarter, midpoint and third quarter of pipeline length, steady flow conditions,  $V_o = 0.3$  m/s,  $R = 0.49$ .....64

Figure 4-27: Non-dimensional time-averaged diagnostic flow DDFTAVE versus time for 1% noise levels, leak size of 30%, leaks at first quarter, midpoint and third quarter of pipeline length, steady flow conditions,  $V_o = 2$  m/s,  $R = 2.20$ ....65

Figure 4-28: Non-dimensional time-averaged diagnostic flow DDFTAVE versus time for 1% noise levels, leak size of 1%, leaks at first quarter, midpoint and third quarter of pipeline length, steady flow conditions,  $V_o = 0.3$  m/s,  $R = 0.49$ .....65

Figure 4-29: Non-dimensional time-averaged diagnostic flow DDFTAVE versus time for 1% noise levels, leak size of 1%, leaks at first quarter, midpoint and third quarter of pipeline length, steady flow conditions,  $V_o = 2$  m/s,  $R = 2.20$ .....66

Figure 4-30: Non-dimensional time-averaged diagnostic flow DDFTAVE versus time for 1% noise levels, leak size of 30%, leaks at first quarter, midpoint and third quarter of pipeline length, flow increase transient,  $V_o = 0.30$  m/s,  $R = 0.49$ ,  $V_f = 0.45$  m/s, duration = 5 s, TSV = 0.5.....66

Figure 4-31: Non-dimensional time-averaged diagnostic flow DDFTAVE versus time for 1% noise levels, leak size of 30%, leaks at first quarter, midpoint and third quarter of pipeline length, flow increase transient,  $V_o = 2$  m/s,  $R = 2.20$ ,  $V_f = 3$  m/s, duration = 5s, TSV = 0.5.....67

Figure 4-32: Non-dimensional time-averaged diagnostic flow DDFTAVE versus time for 1% noise levels, leak size of 1%, leaks at first quarter, midpoint and third quarter of pipeline length, flow increase transient,  $V_o = 0.30$  m/s,  $R = 0.49$ ,  $V_f = 0.45$  m/s, duration = 5 s, TSV = 0.5.....67

Figure 4-33: Non-dimensional time-averaged diagnostic flow DDFTAVE versus time for 1% noise levels, leak size of 1%, leaks at first quarter, midpoint and third quarter of pipeline length, flow increase transient,  $V_o = 2$  m/s,  $R = 2.20$ ,  $V_f = 3$  m/s, duration = 5 s, TSV = 0.5.....68

Figure 4-34: Non-dimensional time-averaged diagnostic flow DDFTAVE versus time for 1% noise levels, leak size of 30%, leaks at first quarter, midpoint and third quarter of pipeline length, flow decrease transient,  $V_o = 0.30$  m/s,  $R = 0.49$ ,  $V_f = 0.15$  m/s, duration = 5 s, TSV = 0.5.....68

Figure 4-35: Non-dimensional time-averaged diagnostic flow DDFTAVE versus time for 1% noise levels, leak size of 30%, leaks at first quarter, midpoint and third quarter of pipeline length, flow decrease transient,  $V_o = 2$  m/s,  $R = 2.20$ ,  $V_f = 1$  m/s. duration = 5 s, TSV = 0.5.....69

Figure 4-36: Non-dimensional time-averaged diagnostic flow DDFTAVE versus time for 1% noise levels, leak size of 1%, leaks at first quarter, midpoint and third quarter of pipeline length, flow decrease transient,  $V_o = 0.30$  m/s,  $R = 0.49$ ,  $V_f = 0.15$  m/s, duration = 5 s, TSV = 0.5.....69

Figure 4-37: Non-dimensional time-averaged diagnostic flow DDFTAVE versus time for 1% noise levels, leak size of 1%, leaks at first quarter, midpoint and third quarter of pipeline length, flow decrease transient,  $V_o = 2$  m/s,  $R = 2.20$ ,  $V_f = 1$  m/s, duration = 5 s, TSV = 0.5.....70

Figure 4-38: Non-dimensional diagnostic flow DDF versus time for perfect data, leak size of 1%, transient severities of 0.12, 0.33, 0.20 and 0.50, flow increase transient,  $R = 2.20$ ,  $V_o = 2$  m/s, leak at midpoint.....70

Figure 4-39: Non-dimensional diagnostic flow DDF versus time for perfect data, leak size of 1%, transient severities of 0.12 and 0.50, flow decrease transient,  $R = 2.20$ ,  $V_o = 2$  m/s, leak at midpoint.....71

Figure 4-40: Non-dimensional time-averaged diagnostic flow DDFTAVE versus time for 1% noise levels, leak size of 30%, transient severities of 0.12 and 0.50, flow increase transient,  $R = 0.49$ ,  $V_o = 0.3$  m/s, leak at midpoint.....71

Figure 4-41: Non-dimensional time-averaged diagnostic flow DDFTAVE versus time for 1% noise levels, leak size of 1%, transient severities of 0.12 and 0.50, flow increase transient,  $R = 0.49$ ,  $V_o = 0.3$  m/s, leak at midpoint.....72

Figure 4-42: Non-dimensional time-averaged diagnostic flow DDFTAVE versus time for 1% noise levels, leak size of 30%, transient severities of 0.12 and 0.50, flow increase transient,  $R = 2.20$ ,  $V_o = 2$  m/s, leak at midpoint.....72

Figure 4-43: Non-dimensional time-averaged diagnostic flow DDFTAVE versus time for 1% noise levels, leak size of 1%, transient severities of 0.12 and 0.50, flow increase transient,  $R = 2.20$ ,  $V_o = 2$  m/s, leak at midpoint.....73

Figure 4-44: Non-dimensional time-averaged diagnostic flow DDFTAVE versus time for 1% noise levels, leak size of 30%, transient severities of 0.12 and 0.50, flow decrease transient,  $R = 0.49$ ,  $V_o = 0.3$  m/s, leak at midpoint.....73

Figure 4-45: Non-dimensional time-averaged diagnostic flow DDFTAVE versus time for 1% noise levels, leak size of 30%, transient severities of 0.12 and 0.50, flow decrease transient,  $R = 2.20$ ,  $V_o = 2$  m/s, leak at midpoint.....74

Figure 4-46: Non-dimensional time-averaged diagnostic flow DDFTAVE versus time for 1% noise levels, leak size of 1%, transient severities of 0.12 and 0.50, flow decrease transient,  $R = 2.20$ ,  $V_o = 2$  m/s, leak at midpoint.....74

Figure 4-47: Non-dimensional diagnostic flow DDF versus time for perfect data, leak size of 1%, flow conditions of steady state, flow increase and flow decrease transients,  $V_o = 0.3$  m/s,  $R = 0.49$ , leak at midpoint, transient duration = 5 s, TSV = 0.5.....75

Figure 4-48: Non-dimensional diagnostic flow DDF versus time for perfect data, leak size of 1%, flow conditions of steady state, flow increase and flow decrease transients,  $V_o = 2$  m/s,  $R = 2.20$ , leak at midpoint, transient duration = 5 s, TSV = 0.5.....75

Figure 4-49: Non-dimensional time-averaged diagnostic flow DDFTAVE versus time for 1% noise levels, leak size of 30%, flow conditions of steady state, flow increase and flow decrease transients,  $V_o = 0.3$  m/s,  $R = 0.49$ , leak at midpoint.....76

Figure 4-50: Non-dimensional time-averaged diagnostic flow DDFTAVE versus time for 1% noise levels, leak size of 1%, flow conditions of steady state, flow increase and flow decrease transients,  $V_o = 0.3$  m/s,  $R = 0.49$ , leak at midpoint.....76

Figure 4-51: Non-dimensional time-averaged diagnostic flow DDFTAVE versus time for 1% noise levels, leak size of 30%, flow conditions of steady state, flow increase and flow decrease transients,  $V_o = 2$  m/s,  $R = 2.20$ , leak at midpoint.....77

Figure 4-52: Non-dimensional time-averaged diagnostic flow DDFTAVE versus time for 1% noise levels, leak size of 1%, flow conditions of steady state, flow increase and flow decrease transients,  $V_o = 2$  m/s,  $R = 2.20$ , leak at midpoint.....77

Figure 4-53: Non-dimensional time-averaged diagnostic flow DDFTAVE versus time for 1% and 3% noise levels of flow, leak size of 30%, flow increase transient,  $R = 2.20$ ,  $V_o = 2$  m/s,  $V_f = 3$  m/s, leak at midpoint,  $TSV = 0.5$ , duration = 5 s....78

Figure 4-54: Non-dimensional time-averaged diagnostic flow DDFTAVE versus time for 1% and 3% noise levels of flow, leak size of 30%, flow decrease transient,  $R = 2.20$ ,  $V_o = 2$  m/s,  $V_f = 1$  m/s, leak at midpoint,  $TSV = 0.5$ , duration = 5 s.....78

## Chapter 1: Introduction

### 1.1 Background

Pipelines are the most efficient way of transporting large quantities of petroleum fluids as they provide a safe, constant and economical means of transport. Pipelines provide a major contribution to the Canadian economy with 84 billions of dollars exported in 2012 (23% of the total merchandise exports) and the industry employs 500,000 people. The Canadian pipeline network has a great extent and approximately 3 million barrels of crude oil are transported daily (Canadian Energy Pipeline Association – CEPA, 2014). Despite strict regulations at the federal and provincial levels, and pipeline companies implementing many actions to maintain and monitor their pipelines to ensure safe operations, there is always a possibility that a pipeline leak could occur. Over the period 2003-2012, an annual average of 93 release events of oil or gas were reported to the Transportation Safety Board of Canada on the federally-regulated pipeline network of 75,000 kilometres. These events released over 20,000 cubic metres of fluids. Alberta is the origin and hub of many oil pipelines and there were 145 oil pipeline failures between 2006 and 2012 (Alberta Energy Regulator, 2013). Each leak may lead to significant contamination of the affected areas, sanctions by the regulatory authorities, lack of credibility and resistance to the pipeline operators from social groups, costs of remediation actions such as clean up, repair and investigations, and the loss of revenues associated with the loss of fluids and the cost of repairs. For instance, the 2010 liquid pipeline rupture and release in Marshall, Michigan, United States released over 8,000 barrels of crude oil into the Talmadge Creek and the Kalamazoo River. The cleanup cost was estimated to be over \$767 million. Local residents evacuated their homes and 320 people reported symptoms due to crude oil exposure (US National Transportation Safety Board, 2010). The enhancement of current leak detection systems is highly desirable because it may improve the response time to a leak event, thus reducing the environmental and economic losses. This enhancement may also reduce the current resources invested in extensive model tuning, identification and investigation of possible leaks (USDOT, 2007). The enhancement may

provide guidelines for effective design, upgrading and operation of the pipelines (Liou, 1993).

There are a variety of leak detection techniques employed by the energy pipeline industry. Some of these techniques detect a leak based on its local properties such as the escaping substances, the emission of a characteristic noise, or the occurrence of some other signal; other techniques analyze the hydraulic behaviour inside the pipeline. A leak creates a transient event in which pressure waves travel in both directions along the pipeline. The leak results in an abrupt drop in the pressure at its source, a rise of the incoming flow upstream of the leak and a decrease of the pipeline flow downstream of this leak location (USDOT, 2007). Therefore, the presence of a leak can be detected by analyzing the hydraulic behaviour (primarily the pressure and the flow rate) of a pipeline system, both under steady state and transient conditions (e.g. during pipeline start-up and shutdown, and pump and valve operations). The hydraulic state in a pipeline can be predicted by a computer model which solves the partial differential equations of conservation of mass, momentum and energy. This model then compares the calculated state to the actual state derived from field measurement data which is obtained and transmitted through the supervisory control and data acquisition (SCADA) system. The discrepancies between the two states indicate a leak may occur (Alaska Department of Environmental Conservation, ADEC, 1999). The computer model based leak detection technique is broadly used in the energy pipeline industry (e.g. Bustnes et al, 2011; Al-Khomairi, 2008; and Balda, 2012) and is the focus of this research.

## **1.2 Research Impetus**

The ultimate goal of the computer model based leak detection system is to be able to detect leaks of any size as quickly as possible. Small leaks (e.g. 1% leak rate or less) are often hard to detect yet their occurrences are not rare (ADEC, 1999). One typical cause of leaks in oil pipelines is internal corrosion where the water and sediments that are transported along with the oil products accumulate in isolated locations and lead to the formation of small cracks in the pipelines which grow slowly in size (National Association of Corrosion Engineers, 2013).

These small cracks result in small leaks which the pipeline industry strives to detect. In these small leaks where the leak rate is comparable to the instrument noise levels, it is difficult to observe the leaks and accurately estimate the leak rate with use of the computer model based leak detection systems (Liou, 1993). To detect these small leaks the operators of the pipelines set low threshold values which in turn activate alarms for the investigation of possible leaks in the field. The systems with low threshold values have higher chances of activating alarms frequently, and the frequent alarms can lead to the creation of false alarms and ignoring or missing actions to investigate real leaks in the field (USDOT, 2007).

Computer model based leak detection systems face many other challenges in spite of the fact they are widely used by pipeline operators. One of the most significant challenges is that the ability to detect leaks decreases significantly during transient flow conditions, which can be triggered by pipeline operations and accidents. This is a great concern since the probability of a leak occurring during transient conditions is similar to, if not higher than, during steady conditions (USDOT, 2007). Transient operating conditions are frequent on pipelines. It is desirable to identify leaks during transient events and steady state.

Many factors, associated with the different components of the sophisticated computer model based leak detection system, may contribute to the degradation in leak detectability. The uncertainty (error in measurement) of the instruments, the errors in the acquisition and/or transmission of instrument data via the SCADA system, the modeling errors due to inaccuracies in pipeline and fluid properties, the errors of the mathematical model under transient conditions, and coding errors may affect the performance of the computer model based leak detection systems (Liou, 1993; Vitkovsky et al, 2007). Some examples of errors in the SCADA system are the loss of data at specific measurement points due to failure of instruments or of the SCADA components (API 1130, 2002); and communication failures in the acquisition and/or the transmission of measurement data to a control centre.

The presence of column separation phenomenon may degrade leak detection. This phenomenon occurs when the pipeline pressure drops below the vapor pressure causing the liquid to vaporise forming a 'bubble' of vapour in the pipeline. This may result in undesirable operating conditions and physical damage to the pipeline, especially when the 'bubble' collapses. Transporting batches of different fluids, the operation of pumps and valves, and elevation changes can create undesirable low pressures (below the vapor pressure of the liquid) at some locations. When column separation occurs model simulations are not reliable unless the mathematical model accounts for two-phase flow. Instrument noise levels comparable to the leak flow rate in their flow magnitude can mask or delay this leak detection (Liou, 1993). All these factors could have a negative impact on leak detection and be investigated by the research community and the pipeline industry.

To progress towards achieving the ultimate goal of detection of small leaks, this research addresses the specific challenge of the degradation of computer model based leak detection systems in both steady and transient states by identifying the key casual factors of this degradation.

### **1.3 Objective**

The objective of this study is to quantitatively assess the sensitivity of a computer model based leak detection system to key variables related to the physical characteristics of the pipeline, the accuracy of instruments and the pipeline operating conditions. The sensitivity study is to expand the knowledge of the causes and conditions (leak scenarios) in which leaks are harder to detect (i.e. smaller leak detection system outputs). To achieve this, computer simulation tests with use of the leak detection system were conducted.

### **1.4 Thesis Structure**

This thesis is organized in five chapters. Chapter 1 presents the background on pipeline leak detection and the challenges faced by current computer model based leak detection systems. In Chapter 2, the current leak detection techniques and their advantages and limitations are reviewed. Chapter 3

describes the methodology used in this project. The results of the sensitivity study are presented and interpreted in Chapter 4. Lastly, Chapter 5 highlights the conclusions and recommendations of this work.

## Chapter 2: Literature Review of Leak Detection Methods

The great variety of pipeline leak detection methods are grouped in three categories: inspection, external systems and internal systems. Each of these categories employs a defined set of technologies and varies in the temporal and/or the spatial extent of the pipeline being monitored. Every leak detection category has advantages and limitations of cost and of accuracy (Furness and Van Reet, 1998); of reliability, sensitivity, speed of detection, operational flexibility, and ease of operation (US Department of Transportation, DOT, 2007). Many oil pipeline companies test and apply leak detection methods of all the categories (Alaska Department of Environmental Conservation, ADEC, 2012), thus a review of them is first provided. The internal systems, and more specifically the computer model based leak detection methods, are the focus of this research project because of their extensive application in the industry. Therefore, these leak detection methods will be reviewed in more detail. Colombo et al. (2009), Geiger (2006), Balda (2012), USDOT (2007), the American Petroleum Institute (API) (2002) and ADEC (2012, 1999) provide additional discussions and references regarding leak detection methods.

### 2.1 Inspection

The USDOT (2007) defines the physical inspection of pipelines as the simple visual observation or patrolling to detect the presence of leaks. Physical inspection includes looking for evidence of leaks, damage or abnormal conditions such as ponded soil near the leak. This leak detection category is evaluated as reliable to identify actual leaks. However, it does not assure leak detection in a timely manner due to the constraints in the frequency, the temporal and spatial extent, and the level of detail of the search for evidence of lost product (USDOT, 2007). Physical inspection does not continuously monitor data in the domains described above. This category may not be practical for most pipelines, as they are buried underground and can extend over great lengths (Al-Khomairi, 2008). In the United States and Canada, inspection is mandatory according to federal regulations requiring the regular patrolling and monitoring of every pipeline right-

of-way. The USDOT (2007) and the Canadian Standards Association (2011) present a detailed discussion of the inspection methods.

## **2.2 External Systems**

External systems are leak detection methods in which sensors are placed outside of the pipeline to directly detect commodity release (Geiger, 2006; API, 2002). These sensors collect data and their associated SCADA monitors raise leak alarms when the values exceed certain limits. There are several types of external leak detection methods. Acoustic sensors, affixed to the outside of the pipe, detect the unique signal of high frequency oscillations in the pipe wall caused by a leak (Babbitt, 1920; American Water Works Association, AWWA, 1987; Fuchs and Riehle, 1991). Fiber optic sensing cables (installed along the length of the pipeline) detect changes in the temperature of the cable caused by escaping liquid (Grobwig et al., 2001). Vapour sensing tubes placed along the pipeline length detect leaks when substances diffuse into the permeable tubes. Vapour sensors measure the distribution and the magnitude of the concentration of the leaked substance as a function of the pumping time of the gas pushed through the tube (Furness and van Reet, 1998; Black, 1992; Hargesheimer, 1985; Framatome ANP GmbH, 1998). Liquid sensing cables installed beneath or adjacent to the pipeline along its length detect leaks when the surrounding soil becomes saturated by the leaking liquid. This liquid changes the pattern of reflected energy pulses and this deviation from the baseline pulse triggers an alarm (ADEC 1999). These are the most widely used external methods, and their performance is periodically evaluated by the energy pipeline industry and agencies such as C-FER Technologies (2013) in Canada, as well as ADEC (1999, 2012) and USDOT (2007) in the United States. Other external systems are: ground penetrating radar (Eiswirth and Burn, 2001); electromagnetic techniques (Atherton et al., 2000); dielectric sensing cables (API 1130, 2002); pig-based monitoring and on-line surveillance methods (Black, 1992; Weil et al., 1994; Furness and Reet, 1998); remote sensing (Weil et al., 1994); and soil monitoring (Lay-Ekuakille et al., 2010).

Balda (2012), USDOT (2007), Geiger (2006) and ADEC (1999) reported that these external systems usually have high installation and maintenance costs, which in turn limits their usage to localized pipeline sections. Colombo et al. (2009) indicated that some of these systems typically detect leaks within a range of 2 m to 250 m, suggesting the need for a significant amount of equipment to monitor long pipelines. In addition, some of the techniques in this category may have reliability issues. They may have difficulty detecting large leaks because these generate low frequency signals that are beyond the range of the sensors (Colombo et al., 2009). Another issue is the different levels of experience and expertise of the members of the leak detection team. Some personnel may be better at detecting leaks because of their strong knowledge, solid experience and continuous professional development (Echo-logics, 2006). This range of personnel experience is more important to methods such as the acoustic and the infrared thermography, where the ability of the operator to identify background noise and properly operate specialized equipment is critical (Echo-logics, 2006).

### **2.3 Internally Based Computational Pipeline Monitoring Systems**

This research project focuses on the widely-employed computational pipeline monitoring approaches to leak detection. These methods use field sensors installed on the pipeline, as part of a SCADA system, to monitor operating conditions such as pressure and flow rate (API 1130, 2002). The data collected by the sensors are transmitted to a central control location (which is geographically-distant from the pipeline) by the SCADA system. This control location may have a computer simulator for the prediction of model outputs and a screen for display of the field and of the estimated data, primarily (ADEC, 1999; USDOT, 2007). The data is used by the computer model to produce new values via algorithmic computation. If the calculated new values exceed some predefined thresholds the computational pipeline monitoring system generates an alarm that may indicate the occurrence of a leak. A pipeline controller evaluates the alarm and additional information presented by the computational pipeline monitoring system to support their decision of taking appropriate action (API 1130, 2002).

The algorithms used in computational pipeline monitoring system range widely in their level of complexity from balance methods to real-time transient modeling. These are described in the following sections.

### 2.3.1 Balance Methods

Balance methods are based on the principle of mass conservation. That is, that mass is conserved if there is no leak in the pipeline. Three types of balance methods are discussed in this subsection: the line balance method, the volume balance method and the mass balance method.

The simplest computational pipeline monitoring system method, the line balance method, can be done with a simple hand calculation. This method calculates the difference between the incoming and the outgoing volumes of a pipeline section, and compares this difference to an alarm threshold. The method does not account for linefill (the amount of fluid in the pipeline) changes due to pressure, temperature or composition changes (API 1130, 2002; Geiger, 2006). This linefill change is partially taken into account in the volume balance method. The linefill change due to changes in pressure and/or temperature is considered but the effect of density change is not included (API 1130, 2002; Geiger, 2006).

The mass balance method (Liou, 1993; and API 1130, 2002) separates the pipeline into sections defined between two instrument locations. This provides more accurate pressure and temperature to be used for the linefill change calculation than other balance methods. The mass balance methods account directly for the fluid density with the use of densitometers, as opposed to the line balance or volume balance method (ADEC, 1999). The mass balance is calculated over a range of time windows, where a leak may be detected when the imbalance of the amount of fluid injected, delivered, and the change in inventory, exceeds the sum of the uncertainties in the flow measurements and in the linefill change. This uncertainty in linefill change could be calculated using partial derivatives of the scaled linefill with respect to pressure and temperature, plus the uncertainties of pressure and of temperature (Liou, 1993). The results of all the balance procedures can be plotted on a graph of the scaled leak flow rate

versus time for a range of time windows for interpretation (Liou, 1993). The method was originally developed for crude oil and refined petroleum liquids (Liou, 1993), and was expanded to apply to natural gas liquid by Balda (2012). The latter work provides graphs of the scaled leak flow rate over time derived from three dimensionless sensitivity coefficients that account for uncertainties in flow, pressure and temperature. The mass balance method is mainly used for leak detection during steady state flow conditions (ADEC, 2012). For leak detection under transient conditions, a correction is needed to account for the linefill change induced by a transient (Liou, 1993). This can only be done with adding numerous pressure transmitters in the pipe segment (not practical) or with a transient model (Liou, 1993; and discussed in the following section).

Balance methods may give a baseline to assess the feasibility of leak detection systems (Liou, 1993). They might be useful for detect small leaks, but could result in long detection times and in lack of precision in the leak location when they are compared to transient model based methods (ADEC, 1999).

### 2.3.2 Other Methods

In addition to the balance methods and the real-time transient model based methods, there are other methods currently employed and being explored by the pipeline industry and the research community. Pressure/flow monitoring methods may utilize statistical procedures to detect sudden pressure drops produced by leaks, or may use measurements at pressure transducers to calculate the pressure waves caused by leaks (Geiger, 2006).

The frequency response domain methods use of time series data of the measured pressure at one measurement location to identify leaks (Colombo et al., 2009). In these methods a device can create sharp, fast and periodic transient signals, which arrive at the measurement location separate from the pulses due to reflection at the boundaries (Lee et al., 2006). The frequency response domain methods merge the transient equations with equations in which the pressure and the flow have two parts: a steady state average, which depends on the pipeline system; and an oscillatory component, dependant on the device.

These frequency response domain methods collect amplitudes of the pressure head and discharge for a range of frequencies. The application of this group of methods is valid for medium to large pipeline lengths with a sufficient amount of nodes. This way, there is a specific lowest frequency of the transient signal that can be detected, which is higher than the pipeline length frequency. Another transient method explored by the research community is the rarefaction method, which identifies the low pressure wave caused by pipe rupture (Silva et al., 1996; ADEC, 1999; and Misiunas et al., 2005).

### 2.3.3 Real-Time Transient Model Based Methods

The most sophisticated leak detection method is real-time transient modeling, which uses a computer model to solve the partial differential equations of mass, momentum, and energy conservation. It calculates in real time the hydraulic state (primarily pressure and flow rate) along the pipeline and compares these predicted values with the actual hydraulic state as indicated by field measurements. In these real-time transient model based methods, digital computers calculate real time graphs of key dynamic fluid variables for each pipeline segment. These variables typically are flow, pressure, density, and temperature (ADEC, 1999; Geiger, 2006). Real time measurements, either flow or pressure at both ends of the pipeline segment, are used as boundary conditions to drive the hydraulic calculation (USDOT, 2007; Al-Khomairi, 2008; and Balda, 2012). When the flow is measured at one end, the computer model estimates the pressure at this end, and it estimates the flow when the pressure is measured (Al-Khomairi, 2008). Therefore, these real-time transient model based methods produce one set of predicted and one set of measured pressure and flow for the analysis of the results (Balda, 2012). These equations are solved using a numerical algorithm, such as the method of characteristics, finite difference, finite volume or finite element methods (Geiger, 2006). These real-time transient model based methods compare the measured flow variables with the computer model based leak detection system estimates and send an alarm when the magnitude of the discrepancy reaches a defined value (ADEC, 1999; Geiger, 2006). The pattern of this discrepancy facilitates the early detection of leaks (Al-Khomairi, 2008; and Balda, 2012). Real time transient model based

leak detection systems have two components: the real time transient model and the SCADA system (API 1130, 2002).

Five methods of real time transient modeling are reviewed. The main differences of these methods are: (1) the numerical method being utilized to solve the partial differential equations; and (2) the criterion adopted to identify and declare a leak.

In Liou (1993)'s method, the flow and pressure in the pipeline are predicted by solving the water hammer equations (neglecting the convective terms in the equations for pipe flow) with the method of characteristics. The measured inlet flow and pressure are used to drive the model to compute pressure and flow at the outlet; and the measured outlet flow and pressure are used to compute the pressure and flow at the inlet. The model then compares the calculated flow and pressure at each end to their corresponding measured values. The pipeline is assumed to be intact until the discrepancy between the modeled and measured values shows a pattern attributable to a leak. The model declares the onset of a leak, if the following conditions are met: the discrepancy of the measured minus the calculated pressures decreases at both pipe ends, and has a negative sign; the discrepancy of flows increases at the upstream pipe end, with a positive sign; and the discrepancy of flows decreases at the downstream end, having a negative sign (Liou and Tian, 1995). This method provides the basis of many of the commercial leak detection software for pipelines carrying crude oil and refined products.

Liou (1993) observed that the performance of this method under steady state provides higher leak detectability than in flow increase and flow decrease transient events. In the steady state, the method detected the occurrence of very small leaks (leak rate of 1% of the pipeline flow rate) regardless of an uncertainty in the pipeline properties, flow conditions and the spacing of instruments. Leaks that occurred during flow increase transient events had the lowest leak detectability in his tests. The level of this degradation increases as the uncertainty in the pipeline properties and the spacing of instruments increases. In

addition, it was shown that it is easier to detect a leak that occurred near the midpoint of the pipeline compared to when it is closer to either end.

Liou (1993) conducted field tests of this method. The model was run in parallel with an actual pipeline. Pressure and flow data from the actual pipeline were acquired and transmitted to the model via SCADA. Different sizes of leaks were mimicked by diverting flows out of the actual pipeline. Transient conditions were created by pump starts and stops. This leak detection system provided reliable detection for large leaks (approximately 15% of the pipeline flow rate), but was not able to detect smaller leaks (approximately 1% of the pipeline flow rate) due to noise in the measurement system. Liou (1993) recommended that the spacing between pressure and flow instruments be reduced and/or the pipeline flow rate be lowered. With these changes, it is possible to detect the small leaks.

Unlike the method proposed by Liou (1993), the method developed by Al-Khomairi (2008) assumes that a leak is present in the pipeline unless no evidence of a leak is found. Trial leaks were continuously imposed on the real time transient model at different locations. Discrepancies between calculated values and the corresponding measurements were minimized when the assumed leak has the same size, location, and starting time as the leak in the actual system. A range of leak sizes at two locations under steady state, mild transient and severe transient flow conditions were created on a laboratory pipeline to test the response of the proposed method. With his model, Al-Khomairi (2008) observed that leak detectability was comparable during steady state and transient conditions.

Balda (2012) makes use of Liou's method for pipelines transporting oil liquid and expanded the application of the method to natural gas liquid. Two common transient scenarios, a pump start-up and a valve closure, were simulated to demonstrate the capability of the model to detect leaks under these specific transient conditions. It was shown that the time required to detect a leak was independent of the leak size and the transient type but that it was affected by the location of the leak, being shortest when the leak was at the mid-point of the

pipeline. In addition, the estimation of leak location was less accurate when the flow rate was increasing as opposed to decreasing.

The inverse analysis method was first introduced by Pudar and Liggett (1992) for detecting leaks during steady flow conditions in water distribution networks. The leak rate, expressed as an equivalent orifice area, was computed by minimizing the difference between the modeled and measured pressures. Liggett and Chen extended this method to transient flow conditions. Since the model is given more measured data than is required, with the use of the least squares minimization of the difference between the measured and the calculated pressures, the pipe friction factor and the leak can be determined together, thus allowing simultaneous model calibration and leak detection. They found that the calibration was better when the pressure and flow varied widely during a short time period (severe transient) than for steady state conditions. The inverse transient analysis method is mainly used for leak detection in water distribution networks. It has also had limited application in energy pipelines.

Stoner Pipeline Simulator (SPS) is employed in this research project due to its wide application for leak detection in the pipeline industry. This method solves the conservation of mass, momentum and energy of transient flow in pipelines with the use of an implicit finite difference method to estimate the hydraulic state of the pipeline. Similar to the method proposed by Liou (1993), the model assumes that the pipeline is intact until evidence shows otherwise. The main difference is, instead of looking for the specific discrepancy pattern between the measured flow and pressure at the two ends of a pipe segment, SPS attempts to achieve a 'best fit' model solution of all the available measurement data within each pipe segment. The Least-square method is used to minimize the sum of squares of the errors in the parameters used in the model (such as pipe roughness, fluid properties), errors in the measurement, and errors induced by a leak (because the model assumes there is no leak). The errors induced by a leak are accounted for by removing fluid from the modeled pipeline in the form of what SPS calls 'diagnostic flow' (DNV GL, 2012, SPS user manual). A leak is suspected if the diagnostic flow exceeds a threshold.

The real time transient model based methods are recognized as more accurate, more sophisticated and more widely used in practice than many other methods. Real time transient model based methods cover a wide range of operating conditions. These methods are complex because they model pipeline components to a high level of detail, they model fluids, and require large quantities of input data collected at fast rates. These methods typically require significant resources, training and personnel experience in the implementation, the testing, the customization and tuning of each case and the maintenance (USDOT, 2007).

The main challenges of the internal systems including the real time transient methods are that they may:

- be more sensitive to measurement errors and noise;
- require extensive configuration efforts (API 1130, 2002);
- generate high quantities of false alarms for low leak alarm limits, which in turn results in higher risk of real leaks being missed (Balda, 2012);
- require extensive amounts of data and have high data collection and transmission requirements.

The most significant operating conditions that lead to degradation of real time transient model based methods are: transient-state hydraulics, communication failures and instrument failures. These conditions worsen the performance of this leak detection system. The hydraulic theory of these computer model based leak detection systems may be compromised in transient events. For instance, column separation or slack line is a physical phenomenon that can occur during a transient event, characterized by the rapid drop of pressure below the vapor pressure of the liquid and the creation of vapour bubbles at a specific location in a fully filled pipeline. The pressure at this location can increase above the vapor pressure later causing the vapor bubbles to change back into liquid. This phase change may cause the collision of a liquid column with another liquid column or with a pipe end, which can cause the formation of vapour cavities that can implode generating intense shockwaves in the system. These shockwaves may

produce a large rapid pressure rise which can travel along the entire pipeline with the potential to cause the collapse of the pipeline after several repetitions (Bergeron, 1961; Bergant et al, 2006). SPS the computer model based leak detection system employed in this study does not fully represent these two-phase flow conditions and therefore, the leak scenarios tested in this project do not include the presence of column separation.

A SCADA system is the other critical component of the real-time transient model based leak detection system (API 1130, 2002). The SCADA system collects, processes, displays and controls data from field instruments (API 1130, 2002). The SCADA data are collected from the instruments at various locations along the pipeline. The key SCADA data for this project are flow, pressure and time. Each instrument has a specific noise level and accuracy and may or may not experience bias errors. The instruments transmit their readings to other components in the SCADA system.

Subsequently, the SCADA system sends this data to the real time transient model software, which calculates estimates of flow and of pressure. Errors may occur during transmission of data or in the SCADA equipment that affect the input data received in the real time transient model software. For example, in the transmission of data through the SCADA system, the linear analog signal is converted into a stepped digital signal, where the input signal could be truncated in this conversion (Industry partner, 2013, MBS Manual).

Two SCADA variables described here affect the leak detection: the polling time and the time skew (Liou, 1993). The polling time is the period between two consecutive readings of the same instrument. The time skew is defined as the duration between the reading of two consecutive instruments (Liou, 1993; ADEC, 1999; API 1130, 2002). Rapid transients in comparison to the polling times and time skews could degrade leak detection (USDOT, 2007).

Furthermore, typical communication failures (Industry partner, 2013, MBS Manual) are caused by the failure of one or more components of the SCADA system. The severity of this failure depends on the extent of the pipeline affected and the duration. The most representative instrument failures are when an instrument stops its operation or when it provides incorrect data. The severity of an instrument failure varies with the type of instrument and its location, being the most severe at the injection and the delivery flow meters. These failures may also decrease leak detectability. The computer model based leak detection systems could be adjusted to work properly until an instrument is fixed (Industry partner, 2013, MBS Manual).

## Chapter 3: Methodology

The sensitivity study presented herein assessed the impact of each key variable on the computer model leak detection system for various leak scenarios. The key variables are related to the physical characteristics of the pipeline, the accuracy of instruments and the pipeline operating conditions. This sensitivity study was performed using the simulated leak test method, which is described first in this section. The design of the testing scenarios and the selection of output variables for result interpretation are also presented here.

### 3.1 Simulated Leak Test

The observation of the response of a leak detection system when a leak occurs in a real pipeline system is the most practical way to test its ability to detect leaks. This type of test, called a fluid withdrawal test, is performed by withdrawing fluid out of the real pipeline in a controlled manner. The volume of fluid withdrawn is metered and then stored in tanker trucks or storage tanks. This type of test is the best representation of an actual leak as it uses measured data collected during the operation of the pipeline. However, these tests are conducted infrequently because of their complexity and high costs, especially for large diameter pipelines with high flow rates where large storage volumes are required (Vinh, 2012). In contrast, simulated leak tests can be conducted more frequently because they are relatively inexpensive and straightforward to complete. This method makes use of a simulation model to generate a dataset describing a fictitious leak in a virtual pipeline. This simulated dataset is subsequently used to test the response of the computer model based leak detection system. Figure 3-1 illustrates the simulated leak test system and its analogy to the real test system. Simulated leak tests are far less complex and much more flexible than the fluid withdrawal test because they are applicable to all operational scenarios, pipelines, leak sizes and leak locations. The simulated leak test is also hydraulically complete and correct in its representation of the real pipeline (Vinh, 2012).

### 3.1.1 *Simulator* Model Configuration

The *Simulator* program of the Stoner Pipeline Simulator software (SPS) referred to as the Simulator model was employed in this study to create simulated leaks since it has the same hydraulic calculation engine as the leak detection software, which is the *Statefinder* program of SPS. A virtual pipeline was created in the Simulator model and instead of reading measurement data from the actual pipeline system, the Simulator model generated simulated Remote Terminal Unit (RTU) data based on the physical characteristics and specified operating conditions. This RTU data is part of the data acquisition system. The virtual pipeline was designed to mimic a specific real pipeline system and its associated data acquisition system (University of Alberta, 2014). Various sizes of leaks can be simulated at different locations on the virtual pipeline. Pressure, flow rate, temperature and density at different locations matching the locations where monitoring instruments are installed along the pipeline can be written to an RTU data file, which closely reproduces what is generated by the real pipeline data acquisition system. Leaks cause changes in pressure and flow rates and therefore leave a distinctive signal in the RTU data file (University of Alberta, 2014).

An idealized pipeline was used in this study because this allowed an exact solution of the hydraulic state of the pipeline and facilitated investigation of the causal factors that impact the detection of a leak. This idealized pipeline had a simplified configuration with a single pipe size, horizontal to neglect the effects of the vertical alignment and transporting a single liquid product. The simulated leak test method provided flexibility to study a wide range of pipeline operating conditions and leak conditions, of physical characteristics and of instrument variables (as many scenarios as desired) with a more efficient use of resources than the use of the real pipeline. The simulated leak was created by opening a valve on a pipe outlet that connects the main idealized pipeline to a simulated receiving tank in which the leaked fluid was stored. The idealized pipeline system layout is illustrated in Figure 3-2. The pipeline system modeled is independent of

temperature as the isothermal mode was selected, that is a constant liquid temperature was specified.

#### 3.1.1.1 Pump and Valve Simulation

For a typical pipeline configuration, a pump station at the injection location is required to provide enough head to move the fluid and a control valve is installed at the delivery location to control the pressure. Specific information is required by the *Simulator* model to correctly simulate the dynamics of pumps and valves. This information is provided as pump or valve curves by vendors. In this project, the pumps and their control valves were not modeled directly but replaced with transient events, that is, flow increase and flow decrease. In these transient events the flow change and duration were specified. This is a sound practice in leak detection, where the measurements of flow and pressure at the ends of a pipe segment represent the behavior of pumps and valves and produce more accurate model results compared to direct modelling of the equipment (Liou, 1993).

#### 3.1.1.2 Leak Simulation

The tests compared two options for creation of a leak in the *Simulator* model: the orifice method and the fixed leak rate method. In the case of the orifice method, the valve opening position ( $X$ ) is controlled and the Simulator model calculates the leak rate ( $LR$ ) based on the following orifice equation,

$$LR = C_V \left( \frac{\rho}{\rho_b} \right) f(\Delta P) \sqrt{\frac{\Delta P \rho_w}{\rho}} \quad (3-1)$$

where  $C_V$  is the valve coefficient of transmissibility which is a function of the valve opening position ( $X$  ranges from 0 for a fully closed valve to 1 when it is fully open);  $\rho$  is the density of the liquid at flowing conditions;  $\rho_b$  is the liquid density at base or custody conditions;  $f(\Delta P)$  is the valve correction coefficient;  $\Delta P$  is the pressure drop; and  $\rho_w$  is the density of water (SPS manual, DNV GL, 2012).

The orifice method better represents a real leak by mimicking a hole on the pipeline. The leak rate will quickly increase due to the large pressure difference inside and outside of the pipeline; then this will slowly increase to a maximum as

the pressure at the hole equalizes. Figure 3-3 presents plots of the leak rate as a function of time for the orifice and the fixed leak rate methods.

In the fixed leak rate method, the flow rate of the escaping fluid at the leak location is set to a constant value. The responses of the leak detection system to leaks created using these two methods were evaluated and they were found to be comparable. The fixed leak rate method was selected for use in this study because it gives a constant flow rate to compare between different scenarios. In all the tests, the change of flow rate at the control valve located at the leak location was set in the Simulator model to achieve the specified leak flow rate in two seconds in order to mimic a typical leak occurrence.

### 3.1.2 Instrument Noise Generation

The simulated RTU data does not contain any instrument noise. To study the effect of instrument noise, a program was developed using MATLAB software to generate noise. The simulated instrument noise added to the flow and pressure measurements of this project was random and Gaussian as described by O'Haver (2008). The input data for this program was the noise free RTU data. The user defined the noise levels for pressure and flow as a percentage of the Simulator model values at each location along the pipeline. The program output was new RTU data which includes this Gaussian noise.

### 3.1.3 Leak Detection System Response Testing

The SPS leak detection system uses values of flow and pressure at the measurement locations (pipe ends) generated by the *Simulator* model as boundary conditions, to calculate estimates of these variables at key points over the entire pipe length. These estimates are known as the hydraulic state of the pipeline and are derived by solving the partial differential equations of mass, momentum, and energy conservation. The simulated measured flow and pressure data has some redundant information and creates an over-determined mathematical system. To achieve an accurate estimate of the actual hydraulic state of the pipeline system, the SPS leak detection system also adjusts the simulated measurement data and the pipeline friction factor. This adjustment

occurs on every pipeline segment interpolating at every measurement location based on all the available measurement data. The adjustment is constrained within defined limits of operation. The interpolation is performed for each measured value (including the redundant values) to select the most representative values of pressure, flow and pressure drop. Interpolating the pressure drop corrects errors in flow and density measurements, and in the pipe friction factor (DNV GL, SPS Help and Reference Manual, 2012).

In this interpolation, SPS leak detection system makes use of adjustable weights that give more importance to certain data (i.e. a variable and/or an instrument with known low uncertainty). These weights also penalize deviations from the measured data. A penalty is calculated based on the sum of the squares of the product of a weight and the discrepancies between measured and calculated values of a variable. Thus, increasing a weight also increases its corresponding penalty and decreases the magnitude of the deviation in the system solution. The SPS leak detection system uses the Least-square method to minimize the sum of squares of errors in the parameters used in the model, errors in the measurement, and errors induced by a leak because the model assumes there is no leak (DNV GL, SPS Help and Reference Manual, 2012).

This leak detection system calculates ten penalties based on the following equations:

$$P_1 = \sum_i [W_1 * DF_i]^2 \quad (3-2)$$

where  $P_1$  and  $W_1$  are the penalty and the weight for the diagnostic flow, and  $DF_i$  is each calculated value of the diagnostic flow at the model element  $i$ .

$$P_2 = \sum_i \left[ \frac{W_2}{R_i} * (PM_i - PC_i) \right]^2 \quad (3-3)$$

where  $P_2$  and  $W_2$  are the penalty and the weight for the discrepancy between the calculated and the measured pressure,  $R_i$  is the repeatability at the element  $i$ , and  $PM_i$  and  $PC_i$  are the measured and calculated pressure at the element  $i$ , respectively, in psig units.

$$P_3 = \sum_i \left[ \frac{W_3}{1,000 * dt} * (PM_i - PM_{i,prev}) \right]^2 \quad (3-4)$$

where  $P_3$  and  $W_3$  are the penalty and the weight for the rate of change of the model pressure,  $dt$  is the time step, and  $PM_i$  and  $PM_{i,prev}$  are the calculated pressure at the element  $i$  for the current and previous time steps, respectively.

$$P_4 = \sum_i \left[ \frac{W_4}{R_i} * (QM_i - QC_i) \right]^2 \quad (3-5)$$

where  $P_4$  and  $W_4$  are the penalty and the weight for the discrepancy between the calculated and the measured flow,  $R_i$  is the repeatability at the element  $i$ , and  $QM_i$  and  $QC_i$  are the measured and calculated pressure at the element  $i$ , respectively.

$$P_5 = \sum_i \left[ W_5 * \left( P_i^- - P_i^+ - \frac{k_i |Q_i| Q_i}{\rho_i} \right) \right]^2 \quad (3-6)$$

where  $P_5$  and  $W_5$  are the penalty and the weight for the pressure difference at a flow meter that does not match the frictional pressure drop,  $P_i^-$  and  $P_i^+$  are the pressure upstream and downstream of the flow meter at the element  $i$ ,  $k_i$  is the frictional pressure drop constant for the flow meter,  $Q_i$  is the flow through the flow meter, and  $\rho_i$  is the fluid density in the flow meter.

$$P_6 = \sum_i [W_6 * F_i]^2 \quad (3-7)$$

where  $P_6$  and  $W_6$  are the penalty and the weight for the frictional component of the pressure drop correction, and  $F_i$  is the frictional component of the pressure drop correction at the element  $i$ .

$$P_7 = \sum_i [W_7 * (F_i - F_{i,prev})]^2 \quad (3-8)$$

where  $P_7$  and  $W_7$  are the penalty and the weight for the rate of change of the frictional component of the pressure drop correction, and  $F_i$  and  $F_{i,prev}$  are the frictional component of the pressure drop correction at the element  $i$  for the current and previous time steps, respectively.

$$P_8 = \sum_i [W_8 * G_i]^2 \quad (3-9)$$

where  $P_8$  and  $W_8$  are the penalty and the weight for the gravitational component of the pressure drop correction, and  $G_i$  is the gravitational component of the pressure drop correction at the element  $i$ .

$$P_9 = \sum_i [W_9 * (G_i - G_{i,prev})]^2 \quad (3-10)$$

where  $P_9$  and  $W_9$  are the penalty and the weight for the rate of change of the gravitational component of the pressure drop correction, and  $G_i$  and  $G_{i,prev}$  are the gravitational component of the pressure drop correction at the element  $i$  for the current and previous time steps, respectively.

$$P_{10} = \sum_i \left[ W_{10} * \frac{BM_i}{BMC_{i,a}} \right]^2 \quad (3-11)$$

where  $P_{10}$  and  $W_{10}$  are the penalty and the weight for the bulk modulus error,  $BM_i$  is the bulk modulus correction factor at the element  $i$ , and  $BMC_{i,a}$  is the maximum allowed change in bulk modulus per time step of the element  $i$ .

The values of the weights were tuned by comparing the response of the leak detection system for different values of the same weight. The values of the weights used in this project as input data were:  $W_1 = 5$ ,  $W_2 = 1$ ,  $W_3 = 10$ ,  $W_4 = 1$ ,  $W_5 = 10,000$ ,  $W_6 = 10,000$ ,  $W_7 = 500$ ,  $W_8 = 1,000$ ,  $W_9 = 500$ ,  $W_{10} = 1,000$ . If the value of a weight is small, then it is set with an allowance for deviations of the calculated values of a variable from measured values. The weights can be used to increase or decrease the magnitude of the adjustment of the differences between the measured and the calculated values of flow and pressure, the creation of pressure drops, or adjustments to the bulk modulus. In this project, the weights were set such that the discrepancies of pressure and flow data were penalized the least by setting the weights  $W_2$  and  $W_4$  to the lowest value of all weights at 1. The diagnostic flow is slightly more penalized and the remainder of the weights were set with relatively high penalties to prevent (with zero corrections) or limit (with modest corrections) adjustments in pressure drops and bulk modulus. These weight settings allow the pressure and flow to deviate from the measured values based on instrument repeatability. The leak detection

system minimizes the sum of the penalties from all the model elements between consecutive nodes (DNV GL, SPS Help and Reference Manual, 2012).

The user assigns a repeatability value to the measured values of a variable (e.g. pressure). This repeatability is a measure of how consistently a measurement is made. Repeatability specifies the level of instrument noise of a variable at a measurement location. This, is the maximum amount of deviation of a model value of a variable from the measured value, set with a low limit and a high limit (DNV GL, SPS Help and Reference Manual, 2012).

The diagnostic flow (DF) is defined as the estimate of leak flow rate in the leak detection system. It is calculated based on these weights as the adjustment in flow required to match the difference between the Simulator model and the calculated values from the system, when the repeatability does not explain this difference (i.e. a leak occurs). The SPS leak detection system identifies a possible leak when the diagnostic flow becomes negative. The leak is accounted for by removing fluid from the modeled pipeline in the form of this diagnostic flow (DNV GL, SPS Help and Reference Manual, 2012). In this study the diagnostic flow was used to test the sensitivity of the SPS leak detection system to variations in key variables for a number of testing scenarios.

The values of input parameters required by the leak detection system were determined by conducting simulations designed to test the sensitivity of the diagnostic flow to these parameters. The repeatability of flow and pressure was set to zero to simulate perfect data, and to three noise levels to simulate noisy data (1% in pressure, 1% and 3% in flow). In the input code for the leak detection system, the pressure drop forces option was activated because it was required to perform span estimations, where the pipeline is treated as a single element. The error of tolerance in pressure and temperature was set to zero to eliminate this type of error from model calculations. The errors in the elevations of the pipeline were also set to zero. The time error bound which defines the time difference between the use and the measurement of RTU data, was set to zero. The repeatability decay or rate of change in repeatability was set to zero, neglecting

any changes in the Simulator model values after a value is measured in the field since this project deals with simulated data. The maximum limit of the rate of change in flow and pressure, known as the rate bound, was set to 60,000 m<sup>3</sup>/hr/min and 60,000 psig/min, respectively, which did not restrict the creation of transient events. The bounds for friction correction, batch friction correction, and bulk modulus correction were set to zero preventing any adjustments by the leak detection system due to these bounds. All these parameters were specified in this leak detection system using check lists (see Appendix A for a sample check list), which provided quality control of the tests.

## 3.2 Pipeline Testing

### 3.2.1 Similitude Parameters

Due to the wide range of the physical characteristics, the instruments and the operating conditions of the pipelines, conducting a test for each instrument spacing and pipe diameter was not practical and unnecessary. Therefore, based on the dimensional analysis performed by Liou (1993), two similitude parameters were described below and used to reduce the number of numerical experiments required.

#### 3.2.1.1 *R* Factor

The *R* factor is a dimensionless parameter defined by Liou (1993) as,

$$R = \left(\frac{V_0}{2a}\right) * \left(\frac{L*f}{D}\right) \quad (3-12)$$

where *f* is the friction factor, *L* is the pipe length, *D* is the diameter, *V*<sub>0</sub> is the initial velocity and *a* is the wave speed. Pipelines with the same *R* value will behave identically in terms of their hydraulic state. The *R* factors of energy pipelines were found to vary from 0.49 to 3.08 with an average value of 2.20.

A series of tests was conducted to prove this in which the *R* factor was varied by varying the friction factor and initial velocity. In these tests four simulations were run, with a 5% leak size, a 30-inch pipe diameter, a 150-km pipe length, two with *R* = 0.49 and two with *R* = 3.14. The two simulations with *V*<sub>0</sub> = 0.3 m/s and *f* = 0.0220 and *V*<sub>0</sub> = 1.0 m/s and *f* = 0.0066 both have *R* = 0.49. Likewise, the two

simulations with  $V_o = 2.0$  m/s and  $f = 0.021$  and  $V_o = 3.0$  m/s and  $f = 0.014$  both have  $R = 3.14$ .

The dimensionless diagnostic flow ( $DDF$ ) is a key parameter of this project and it is given by,

$$DDF = \left( \frac{DF}{LR} \right) \quad (3-13)$$

where  $DF$  is the diagnostic flow and  $LR$  is the specified leak flow rate.  $DDF$  facilitates the comparison of simulation results and it is presumably a Pi parameter so the use of  $DDF$  can reduce the number of tests required. In Figure 3-4 the dimensionless diagnostic flow,  $DDF$  is plotted as a function of time for these four simulations. It is evident in this figure that simulations with the same  $R$  value produce identical results. That is the two curves for  $R = 0.49$  plot on top of each other as do the two curves for  $R = 3.14$ . This demonstrates that pipelines with the same  $R$  value behave hydraulically and respond to leaks identically.

The similitude analysis by Liou (1993) showed that one pipeline configuration could be employed to conduct the proposed sensitivity study by varying the initial velocity to obtain  $R$  values of 0.49, 1.26, 2.20 and 3.08 with velocities of 0.3 m/s, 1.0 m/s, 2.0 m/s and 3.0 m/s, respectively. As a result, one pipeline was used for the sensitivity study.

The time averaged dimensionless diagnostic flow ( $DDFTAVE$ ) is a key parameter of this project and it is given by,

$$DDFTAVE = \left( \frac{1}{LR} \right) \left( \frac{1}{2 \text{ min.}} \right) \int_t^{t+2 \text{ min.}} DF(\tau) d\tau \quad (3-14)$$

where  $DF$  is the diagnostic flow at time  $\tau$ , which is calculated every second and smoothed by time averaging over two minutes;  $t$  is the specified time and  $LR$  is the specified leak flow rate.

### 3.2.1.2 Transient Severity

The transient severity  $TSV$  quantifies the impact of a transient event on the pipeline system and is given by,

$$TSV = \frac{MAX(|Q_{in} - Q_{out}|)}{Q_{ref}} \quad (3-15)$$

where the numerator is the maximum of the absolute value of the difference between the instantaneous entering ( $Q_{in}$ ) and exiting ( $Q_{out}$ ) flow rate in the main line over the time period of the test, and ( $Q_{ref}$ ) is the initial steady-state flow rate in the main line (Liou 1993). In this study the transient severity was computed using flow rates assuming there was no leak in order to allow systematic comparisons. High values of  $TSV$  such as 0.50, indicate large and/or rapid flow changes. Low values of  $TSV$  such as 0.12, indicate small and/or slow flow changes.

### 3.2.2 Idealized Study Pipeline

The typical specifications of oil pipeline systems were reviewed including their layout, dimensions and operating variables. These specifications were provided by the industry partner for a pipe network comprised of 26,000 km of steel pipe. The outside diameter ranged from 0.219 m to 1.219 m, the wall thickness from 0.00318 m to 0.02062 m, the spacing between pumps stations from 17 km to 220 km, the flow rate from 20 m<sup>3</sup>/hr to 5,860 m<sup>3</sup>/hr, the fluid density from 550 kg/m<sup>3</sup> to 935 kg/m<sup>3</sup>, the fluid viscosity from 0.2 cSt to 302 cSt and the maximum allowable operating pressure up to 2,400 psi. The limits of operating flow rate and pressure were used as reference to validate the tests checking the imposed flow changes were within these limits. The nominal outside diameter that occurred most often (i.e. longest length) was 30 inches and therefore this was selected as the diameter for the idealized study pipeline. A line spacing of 150 km was selected because it is the average line spacing in the network. A wall thickness of 0.375 inches was chosen because it is the median of wall thicknesses of the lines with a 30-inch diameter.

The same fluid Suncor A crude oil (OSA) was used for all the simulations. This fluid was selected because it is a medium class oil product based on the density. This chosen fluid has a density of 858.6 kg/m<sup>3</sup>, and a fluid viscosity of 4.57 cP (centipoise). The wave speed was set to 1,347 m/s and the fluid was modelled as a slightly compressible liquid in SPS. This option assumes that the liquid can be described by a simple quadratic equation of state (DNV GL, SPS Help and Reference Manual, 2012). In all simulations the Colebrook roughness was set to

0.0001 inches as the Simulator model and the leak detection system calculate the friction factor based on this roughness.

### 3.2.3 Discretization

Three options of node spacing were tested: 500 metres, 1,000 metres and 2,000 metres. The leak detection system results for all the three node spacings tested are comparable and equally accurate. Thus, a node spacing of 500 metres was chosen as this spacing provides the most refined grid for appropriate coverage of the studied pipeline length of 150 km.

Different values of the time step were tested until further reductions did not improve the results. As a result, two time steps were used in this project: 3 seconds from 00:00:00 to 03:55:00 and from 04:40:00 to 08:00:00, and 1 second from 03:55:00 to 04:40:00, period in which the transient events have the greatest impact on the leak detection system results because the simulated leaks occurred at 04:00:00. The one second time step is the minimum time interval allowed for the leak detection system outputs and it is smaller than the duration of the full opening of valves or the spin-up or spin-down of pumps. These time steps and node spacing facilitate efficient testing of this leak detection system without compromising the accuracy of the results. The Courant number for these time steps was 8.1 and 2.7, respectively.

### 3.3 Design Testing Scenarios

In this sensitivity study the following key variables were varied in the idealized pipeline: the  $R$  factor, leak location, transient type and severity and flow noise level. These key variables were varied one at a time to investigate their effect on the response of the leak detection system. Leak rates from 1% to 30% of the pipeline flow rate were tested. Conducting tests only for the 1% and the 30% leak rates is considered adequate with noisy data, as these two leak rates represent leak scenarios with different leak detectability: small leaks and large leaks, respectively. These leak rates resulted in main line flow rates that ranged from 234.1 m<sup>3</sup>/hr to 4681.9 m<sup>3</sup>/hr; initial velocities that varied from 0.30 m/s to 3.00 m/s; friction factors for steady conditions (i.e. the initial state of the system for the tests)

that ranged from 0.0137 to 0.0218. Three leak locations were tested at 0.25L, 0.50L and 0.75L, where L is the total length of the pipeline. Steady flow and transient events with increasing and decreasing flow rates referred to as flow increase and flow decrease were tested. Transient severities ranged from 0.12 to 0.50 and two flow noise levels of 1% and 3% of the flow rate in conjunction with a pressure noise level of 1% were tested. Table 3-1 summarizes the values and the flow conditions of the variables tested.

The sensitivity study was conducted in two stages. First, using the perfect data (i.e. noise free) generated by the Simulator model with the goal to identify the major factors impacting leak detection. Second, using the noisy data (i.e. Simulator model data with the added Gaussian noise) in order to evaluate the effect of noise on the leak detection system which is a more realistic representation of actual pipelines.

### 3.3.1 *R* Factor

The range of *R* factors tested in this project was from 0.49 to 3.08 since this range covers the typical range of operation of flow and pressure in typical pipelines. The *R* factor was varied by changing the initial velocity. Four values of the *R* factor were simulated in this project: 0.49, 1.00, 2.20 and 3.08.

### 3.3.2 Transient Type

Two types of transient events were simulated: a flow increase from the upstream end, which is analogous to a pump start in the real pipeline and a flow decrease from the downstream end that represents a valve closure. Two sets of boundary conditions were used in the Simulator model. In the first case the flow was controlled at the supply tank located at the upstream end and the pressure was controlled at the delivery tank located at the downstream end. This set of boundary conditions was used during steady state and flow increase simulations. For the second set of boundary conditions the pressure was controlled at the supply tank and the flow was controlled at the delivery tank. This second set of boundary conditions was used when simulating flow decrease events.

In practice a transient event can occur at any time. Transients imposed at different times relative to the leak start time were tested and led to the selection of the worst case scenario for identifying a leak, when a transient event and the leak start simultaneously. The start time of all transient events and leaks was set at 04:00:00 so that the initial condition of the tests was a steady hydraulic state. Transient events are introduced to simulate the operation of pumps, valves and flow changes that occur in the pipeline system, and to determine whether or not leaks are harder to identify during transient events.

### 3.3.3 Transient Severity

Several transient severities were tested with *TSV* values ranging from 0.001 to 0.5. This range in *TSV* was achieved using flow changes from 20% to 50% and transient durations from 5 seconds to 30 minutes. These values of *TSV* are comparable to transients caused by real pipeline operations (Liou, 1993; Al-Khomairi, 2008). It was found that some of these simulated transient events resulted in column separation caused by negative pressures at the downstream end of the pipeline. This occurred primarily for flow decrease events with a 20% flow change, 30% leak rate, a transient duration greater than 8 minutes, and *TSV* lower than 0.12. In order to avoid column separation, all remaining simulations were carried out with *TSV* of 0.12 or higher and transient durations of 8 minutes or lower.

For flow decrease events, the minimum value of velocity simulated was a change in velocity from 0.3 m/s to 0.15 m/s and the maximum value from 3.0 m/s to 2.0 m/s. For flow increase events, the minimum value was from 0.3 m/s to 0.45 m/s and the maximum value of velocity simulated was a change of velocity from 2.0 m/s to 3.0 m/s.

### 3.3.4 Noise Level

A noise level of 1% for pressure measurements was used in the tests with noisy data, as this level is typical in real pipelines. Flow measurement noise levels were set to 1% or 3% which is representative of real noise levels observed by the industry partner depending on the type of flow meter.

### 3.4 Diagnostic Flow

As described in subsection 3.1.3, the diagnostic flow ( $DF$ ) is an output parameter of the leak detection system which is indicative of whether or not a leak occurs in the pipeline system. In theory, when there is no leak in the pipeline and everything is perfect, the diagnostic flow will be zero. In this case, the hydraulic states predicted by the leak detection system and the Simulator model are virtually identical and no adjustments are made by the leak detection system. In contrast, if a leak occurs the diagnostic flow will drop to a negative value indicating a loss of product or liquid, and the leak detection system will add or subtract the difference between the Simulator model and the leak detection system plus the repeatability.

In this project the values of  $DDF$  were averaged over two minutes creating the parameter designated as the time averaged dimensionless diagnostic flow ( $DDF\_TAVE$ ). The calculation of  $DDF\_TAVE$  was defined in the code of the Simulator and the leak detection system, and this parameter is included in the outputs of this leak detection system model.  $DDF\_TAVE$  was used to smooth the results from simulations using noisy data to facilitate the comparison of times series curves since the fluctuating values of  $DDF$  do not facilitate this comparison. Figure 3-5 compares the plots of  $DDF$  and  $DDF\_TAVE$  versus time showing that the noisy curve makes it difficult to compare the results from different simulations. Instead, this noisy curve was smoothed by time averaging. Appendix B provides the list of the tests with the individual values of the variables tested.

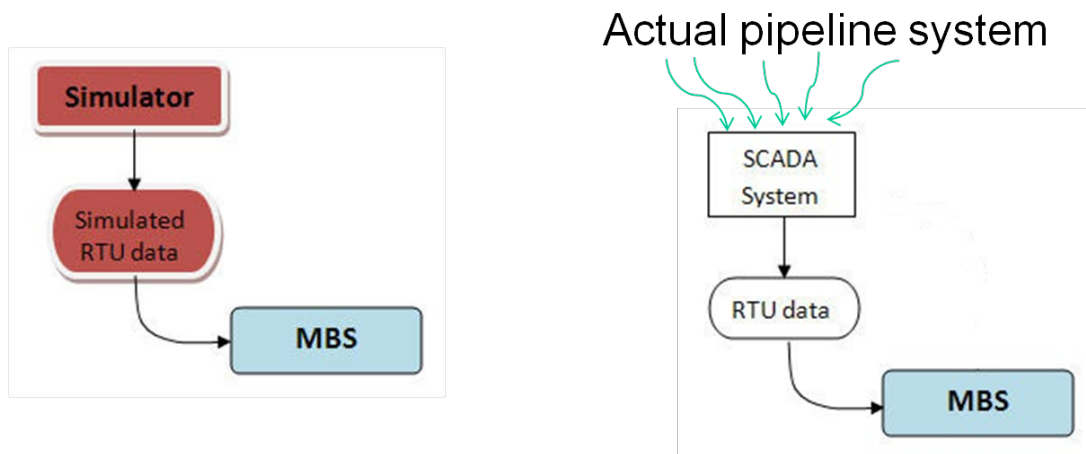


Figure 3-1. Simulated leak test system and its analogy to the real test system (Industry partner, 2013).

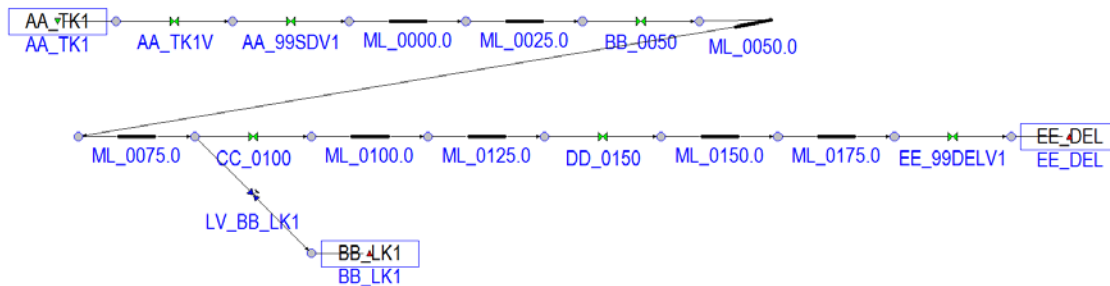


Figure 3-2. Pipeline system layout for the idealized case in the Simulator model. Steel pipeline with a diameter of 30 inches, length of 150 km and Colebrook roughness of 0.0001 inches. Each ML is a point on the pipeline where leak detection system outputs were calculated. The pipeline was divided into eight pipe sections, each 18.75 km in length. Valves are indicated with green and blue

colors. AA\_TK1 is the supply tank; BB\_LK1 is the leak tank in which the leaked volume of fluid is taken out of the main pipeline; and EE\_DEL is the delivery tank.

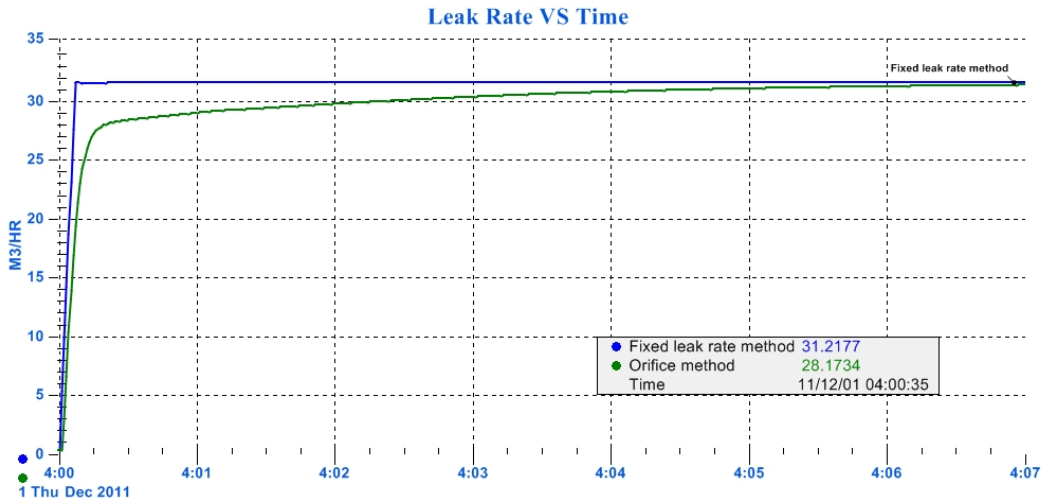


Figure 3-3. Leak rate versus time for the orifice and the fixed leak rate methods. Flow decrease condition, leak size of 1%,  $V_o = 2$  m/s,  $R = 2.20$ ,  $V_f = 1$  m/s, duration = 5 s, TSV = 0.5. Perfect data. Leak starts at 04:00:00.

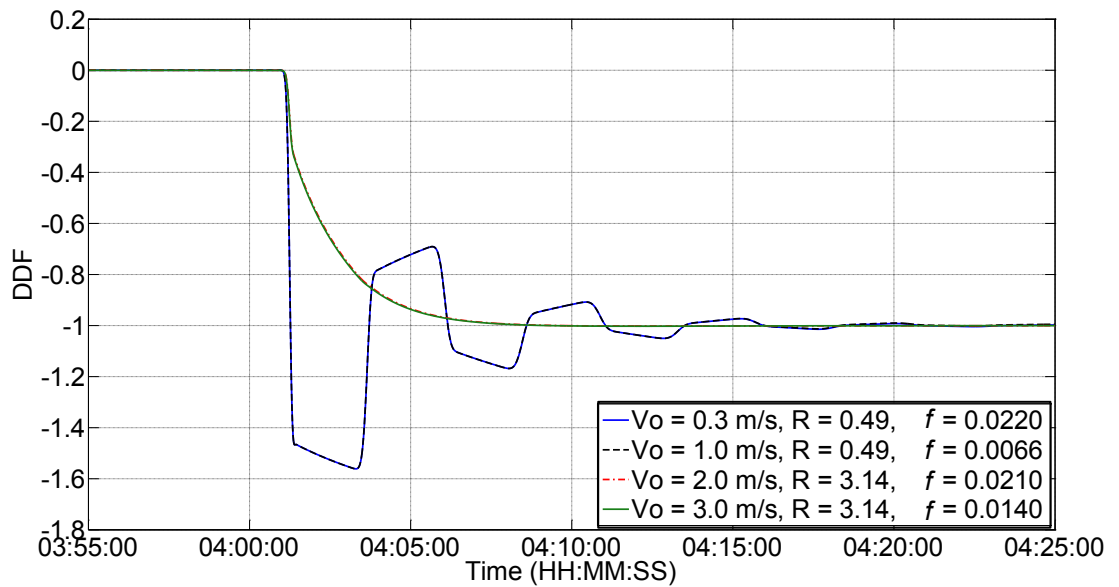


Figure 3-4. Non-dimensional diagnostic flow DDF versus time for different sets of R factors, velocities and friction factors; leak size of 5%, steady state condition, perfect data, leak at midpoint.

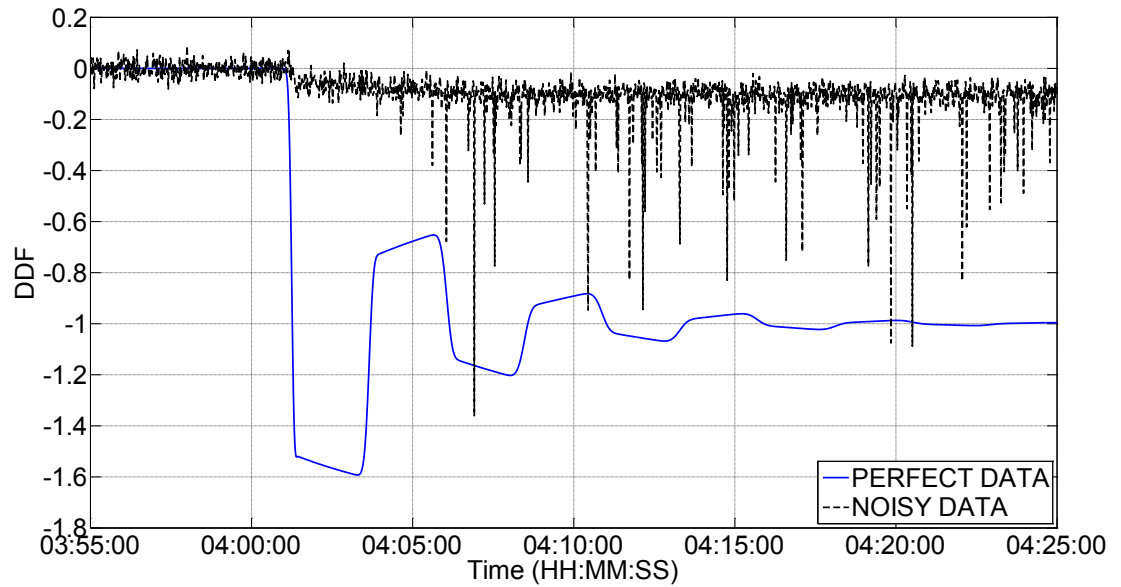


Figure 3-5. Non-dimensional diagnostic flow DDF versus time for perfect data and noisy data, 1% noise levels, leak size of 1%, steady state condition,  $V_o = 0.3$  m/s,  $R = 0.49$ , leak at midpoint, leak starts at 04:00:00.

Variables \ Values				
R factor	0.49	1.26	2.20	3.08
Leak rate (LR)	1%	10%	20%	30%
Leak location (LL)	0.25 L	0.50 L	0.75 L	-
Transient severity for flow increase and flow decrease (TSV)	0.50 (50% flow change in 5 seconds)	0.33 (50% flow change in 8 minutes)	0.20 (20% flow change in 5 seconds)	0.12 (20% flow change in 8 minutes)
Flow state	Steady (ST)	Flow increase (FI)	Flow decrease (FD)	-
Noise level (N)	Pressure = 1%, Flow = 1%	Pressure = 1%, Flow = 3%	-	-

Table 3-1. Values and flow conditions of the tested variables.

## Chapter 4: Discussion of Results

A sensitivity study was carried out on the key input variables for the computer model based leak detection system. The effects of varying the operating conditions and the characteristics of the pipeline and instrumentation were investigated. The sensitivity of leak detectability to each variable is evaluated using perfect data and noisy data.

The performance or leak detectability of the leak detection system is quantified using the dimensionless diagnostic flow  $DDF$  or the time averaged version  $DDFTAVE$  in the noisy data cases. In theory,  $DDF$  is zero when there is no leak in the pipeline and if a leak occurs it would drop to a negative value indicating the loss of product. The absolute values of  $DDF$  indicate the percentage of the leak being detected. The rate of the decrease of  $DDF$  indicates how fast a leak can be detected.

Leaks in real pipelines are detected by setting an alarm threshold based on a variety of criteria. Some thresholds are calculated for each pipeline segment based on the sum of volumetric uncertainties in flow measurements and in linefill change over several time windows, derived from the leak detection methodology for steady state flow (Liou, 1993). In Liou's methodology, these uncertainties are expressed as a fraction of the mainline flow rate. The industry partner uses a volume balance threshold for a specific time window. This volume balance calculates the difference between the incoming and the outgoing volumes of a pipeline section, considers the linefill change due to changes in pressure and/or temperature, and compares this difference to an alarm threshold. Calculated volume balance values are compared to this volume balance threshold. If a threshold is reached, an alarm is created. The alarm notifies a pipeline controller that a leak may exist and an investigation is carried out to confirm whether or not there is an actual leak (Industry partner, 2013).

## 4.1 Sensitivity to Leak Rate

### 4.1.1 Perfect Data

Figure 4-1 presents a plot of *DDF* versus time for four leak events with leak rates (*LR*) ranging from 1% to 30% of the nominal flow rate for steady flow conditions. All the leaks had an imposed start time of 04:00:00. It can be seen from this plot that the magnitude and shape of the four *DDF* curves are comparable over the entire duration. The maximum deviation of the curves occurred at 04:03:00. The largest difference between the curves occurred at the peak of the first oscillation, where the difference in the magnitude of *DDF* between the 30% leak and the 1% leak, is only 0.05. This small difference demonstrates that for perfect data *DDF* is equally sensitive to any leak rate. That is, the system's ability to detect a small or large leak is equal when there is no measurement error (also known as instrument noise) and each input parameter of the computer model based leak detection system is known accurately. These four curves all stabilize at a *DDF* value of -1.0, indicating that the leak detection system eventually captures the leak fully. This finding is valid for the four *R* factors tested and the results are presented in Figures 4-1 to 4-4. This conclusion was also found to be valid when the leak was located at one quarter and three quarters along the pipe length (see Appendix C for these plots).

The same trend described above for steady state also applies to transient operating conditions. Figure 4-5 and Figure 4-6 present the *DDF* curves for the four leak rates simulated under flow increase and flow decrease transient conditions, respectively. Note that these transient events start at 04:00:00. In the flow increase transient events, the upstream flow was increased by 50% within 5 seconds and for the flow decrease events the downstream flow was decreased by 50% within 5 seconds. It can be seen that the four curves in either figure collapse closely together. Therefore, the flow state in the pipeline does not affect leak detectability when there is no error in either measurement data or model input parameters. Conducting tests and interpreting the results based on any one of the leak rates is adequate for tests with perfect data. The results from the 1% leak only are shown hereafter for the perfect data cases.

#### 4.1.2 Noisy Data

The noise levels in both the flow and pressure were set at 1% for the noisy data tests, unless otherwise indicated. In Figure 4-7 *DDFTAVE* computed using steady state noisy data is plotted versus time for leak rates of 1% and 30% and  $R = 0.49$ . It can be seen that unlike in Figure 4-1 there is a large difference between the 30% and 1% leak rate curves. The maximum absolute values of *DDFTAVE* in Figure 4-7 are -1.45 and -0.17 for the 30% and 1% leak rates, respectively. The large difference in the two *DDFTAVE* curves demonstrates that *DDFTAVE* is sensitive to the size of the leak when there is noise in the measured data. This difference in the curves also indicates that as expected it is generally easier to detect large leaks. The time that a leak is detected depends on the specified threshold. A threshold is artificially selected to give an indication of how the detection time compares in these cases. For example, the 1% leak curve reaches the value of -0.13 at 04:10:00 while the 30% leak curve reaches this value at 04:01:30.

The same trend described above for steady state also applies to transient operating conditions. In Figures 4-8 and 4-9 *DDFTAVE* is plotted versus time for 1% and 30% leak rates and an  $R$  factor of 2.20 for flow increase and decrease transients, respectively. The peak value of *DDFTAVE* for a 1% leak rate is -0.01 while for a 30% leak rate it is -0.90 for the flow increase case and the corresponding values for the flow decrease case are -0.43 and -1.03. In Figure 4-9, only a leak with a 30% leak rate can be detected if a threshold is set at -1.0. The threshold can be set at -0.1 to detect a leak with a 1% leak rate; however, such a low threshold is often unpractical in real-world operation. It is worth mentioning about Figures 4-8 and 4-9 is there is a larger *DDF* calculated in the model during flow decrease than during flow increase transient events. This is especially clear for the 1% leak. A larger *DDF* generally indicates a better leak detection. The impact of flow states on leak detectability is further discussed in section 4.6.

Figures 4-10 and 4-11 present the *DDF* curves for steady state and  $R = 0.49$ , with perfect and noisy data for a 1% and a 30% leak rate, respectively. Figure 4-

10 shows that the *DDF* peak negative value for a leak rate of 1% is -1.60 with perfect data while *DDF* slowly decreases to -0.15 with noisy data, indicating that the leak signal is masked by instrument noise and about 10 times smaller than the perfect data signal. Noise has major impact on the system's ability to detect small leak rates. A leak rate can be detected in the computer model based leak detection system only when it overcomes the noise level of the pressure and flow rate data (1% in these tests) in the pipeline. Therefore, the 1% leak rate is almost hidden completely to the leak detection system with the specified noise level whereas this noise level is small compared to the 30% leak rate. The comparison of the *DDF curves* indicates it is easier to detect a leak of the same size with perfect data than with noisy data, however, real pipelines often experience some noise level in their instruments.

## **4.2 Sensitivity to $R$ Factor**

### **4.2.1 Perfect Data**

In Figure 4-12 *DDF* is plotted as a function of time for four  $R$  values of 0.49, 1.26, 2.2 and 3.08, for steady state and a 1% leak rate. It is interesting to notice the different shapes of the *DDF curves*. Despite an initially overlapping sharp drop, the *DDF* pattern is different for low and high  $R$  factors due to the fact that the flow regime is dominated by friction or inertia, respectively. At low  $R$  factors the time series of *DDF* indicates that the system behaves similar to a damped oscillator. This is because at low values of  $R$  the effect of friction is small and the flow is dominated by inertia. At large values of  $R$  the plot indicates that the system is overdamped and the curve decreases smoothly from an initial value of zero to an asymptotic value of -1. Pipeline systems with high  $R$  factors are friction dominated. The transient wave caused by a leak is attenuated rapidly or heavily damped. Figure 4-12 shows that the peak values of *DDF* for a 1% leak rate range from -1.6 for  $R = 0.49$ , -1.25 for  $R = 1.26$ , -1.03 for  $R = 2.20$ , to -1.00 for  $R = 3.08$ . The difference in *DDF* values demonstrates the high sensitivity to  $R$  factor. The comparison of these *DDF curves* indicates that it may be easier to detect a leak in pipelines with smaller  $R$  factors. The different shapes of the *DDF curves* indicate the response of the leak detection system to a leak of a given size is very sensitive to the value of the  $R$  factor. The trends presented in Figure 4-12 for

a 1% leak rate also apply to larger leaks, as *DDF* is equally sensitive to varying leak rates with perfect data.

The *DDF* pattern observed for the steady state is also visible during transients. However, the *R* value of 3.08 is excluded from flow increase transient scenarios, because it was found that a flow increase from an initial velocity of 3 m/s to 4.5 m/s produces a pressure outside typical operating limits. Figure 4-13 shows the *DDF* curves predicted for the three remaining *R* factors for a 1% leak rate during a flow increase transient event. The peak values of *DDF* in Figure 4-13 are -1.47 for the *R* factor of 0.49, -1.12 for the *R* factor of 1.26 and -1.00 for the *R* factor of 2.20, indicating that it may also be easier to detect leaks in pipelines with smaller *R* factors during flow increase transient events. The same is observed for the flow decrease transient cases (Figure 4-14). The peak values of *DDF* are -1.78 for *R* = 0.49, -1.45 for *R* = 1.26, -1.20 for *R* = 2.20, to -1.08 for *R* = 3.08. Therefore, leak detection can be harder in pipeline systems with large *R* factors compared to systems with small *R* factors during all flow states. *R* factor is an important parameter to be considered when exploring measures to improve leak detection on different pipeline systems.

#### 4.2.2 Noisy Data

The *DDFTAVE* curves presented in Figures 4-15 and 4-16 are for the *R* factors of 0.49 and 2.20, steady state flow and noisy data for a 30% and a 1% leak rate, respectively. It can be seen that the maximum absolute values of *DDFTAVE* for a 30% leak rate range from -1.45 for the *R* factor of 0.49, to -0.97 for the *R* factor of 2.20. The maximum absolute values of *DDFTAVE* for a 1% leak rate range from -0.150 for the *R* factor of 0.49, to -0.052 for the *R* factor of 2.20. Same as the perfect data tests showed, leak detection can be easier for small *R* factors when noise is present.

The *DDFTAVE* curves presented in Figures 4-17 and 4-18 are for the *R* factors of 0.49 and 2.20, flow increase transient event and noisy data for a 30% and a 1% leak rate, respectively. The maximum absolute values of *DDFTAVE* for a 30%

leak rate are -1.30 for an  $R$  factor of 0.49 and -0.90 for an  $R$  factor of 2.20, for a 1% leak rate are -0.07 for an  $R$  factor of 0.49 and -0.02 for an  $R$  factor of 2.20.

In Figure 4-19, the  $DDFTAVE$  curves for  $R$  factors of 0.49 and 2.20 are plotted as a function of time for leaks during a flow decrease transient event with noisy data at leak rates of 1% and of 30%. The maximum absolute values of  $DDFTAVE$  are -1.50 for the  $R$  factor of 0.49 and -1.02 for the  $R$  factor of 2.20, when the leak rate is 30%, and -0.62 for the  $R$  factor of 0.49 and -0.42 for the  $R$  factor of 2.20, when the leak rate is 1%.

The difference in the peak values in Figures 4-15 to 4-19 indicates a high sensitivity of the leak detection system to the  $R$  factor. This agrees with what was observed with perfect data. Leak detection is easier for pipelines with lower  $R$  factor also when data noise is present, therefore it is applicable to real pipeline systems where noise is typical.

### 4.3 Sensitivity to Leak Location

Three leak locations are simulated at distances of one quarter (0.25L), halfway (0.50L), and three quarters (0.75L) along the pipeline.

#### 4.3.1 Perfect Data

In Figure 4-20 time series of  $DDF$  corresponding to leaks at the three locations are plotted for an  $R$  factor of 0.49 and a 1% leak rate during steady state conditions. The  $DDF$  presented in Figure 4-21 are of the three leak locations for the  $R$  factor of 2.20 and a 1% leak rate occurring during steady state. Figures 4-22 and 4-23 present the  $DDF$  of the three leak locations for a 1% leak occurring during a flow increase transient event in a pipeline with  $R$  factors of 0.49 and of 2.20, respectively. Figures 4-24 and 4-25 show the  $DDF$  curves of the three leak locations for a 1% leak rate occurred during a flow decrease transient event with  $R$  factors of 0.49 and 2.20, respectively.

In Figures 4-20 to 4-25, the first rapid drop in  $DDF$  when the leak is at  $L/4$  and  $3L/4$  occurred at 04:01:30 but when it was at the midpoint the rapid drop is

delayed 45 seconds and occurred at 4:02:15. The reason for this delay is that measurement instruments are located at the ends of the pipeline. The leak pressure wave must travel a distance of  $L/2$  to reach any one of the instruments at pipe ends if the leak is at the midpoint while only  $L/4$  if it is at the other locations. It is worth noticing the *DDF* for the midpoint leak decreases rapidly to the lowest point after it starts to drop; while in the non-midpoint leak cases, the *DDF* curves have a section of milder slope after the initial sharp drop and then continue to drop to the lowest point. This is more obvious for the low *R* factor cases, where the curves almost plateaued. The duration of this section of slower *DDF* generation equals to the time between the leak signal to travel to the measurement instrument at the nearer pipe end and to the farther end. Therefore, the time that a leak would be detected depends on the threshold specified. If the threshold is above the section of milder slope, e.g. with a threshold value of -0.4, a leak at the midpoint would be detected later than one at non-midpoint locations. Otherwise, a non-midpoint leak would be detected later.

In Figures 4-20, 4-22 and 4-24 the midpoint signals are closer to a square wave than at  $L/4$  and  $3L/4$  but the period of each oscillation is roughly equal for a 1% leak rate and an *R* factor of 0.49. Figures 4-21, 4-23 and 4-25 are very similar in shape for a 1% leak rate and an *R* factor of 2.20. The curves in these figures are not oscillatory as *DDF* decreases smoothly and asymptotically from zero to a value of approximately -1.00. These curves are smooth in pipeline systems with high *R* factors because the flow is dominated by friction and therefore the transient wave caused by the leak is attenuated rapidly or heavily damped.

#### 4.3.2 Noisy Data

Figures 4-26 and 4-27 show the *DDFTAVE* curves for the three leak locations with a 30% leak rate during steady state and *R* factors of 0.49 and 2.20, respectively. The *DDFTAVE* curves in Figures 4-28 and 4-29 present the three leak locations for leaks during steady state with a 1% leak rate and the *R* factors of 0.49 and 2.20, respectively. Figures 4-30 and 4-31 show the *DDFTAVE* curves of the three leak locations for leaks during a flow increase transient event with a 30% leak rate and the *R* factors of 0.49 and 2.20, respectively. Figures 4-32 and

4-33 present the *DDFTAVE* curves of the three leak locations for leaks during a flow increase transient event with a 1% leak rate and the *R* factors of 0.49 and 2.20, respectively. Figures 4-34 and 4-35 present the *DDFTAVE* curves of the three leak locations with a 30% leak rate for leaks during a flow decrease transient event and the *R* factors of 0.49 and 2.20, respectively. Figures 4-36 and 4-37 present the *DDFTAVE* curves of the three leak locations with a 1% leak rate for leaks during a flow decrease transient event and the *R* factors of 0.49 and 2.20, respectively.

The patterns of the curves with noisy data are similar to what was observed with perfect data. The curves in Figures 4-26, 4-30, and 4-34 are damped oscillations, observed for a 30% leak rate and a low *R* factor. The curves in Figures 4-27, 4-31 and 4-35 are not oscillatory as *DDFTAVE* decreases smoothly and asymptotically from zero to a peak value, observed for a 30% leak and a high *R* factor. Same as what the perfect data cases showed, the leak detection model calculated the diagnostic flow for the non-midpoint leak earlier than for the midpoint leak. This trend is less obvious for the 1% leak since noise masked most of the transient signal caused by the small leak, i.e. Figures 4-28, 4-33, and 4-36.

Overall, the results of this section indicated that leak location can affect leak detection. The time at which *DDFTAVE* starts to deviate from zero (i.e. the time when a leak is first evident) depends on the time it takes the transient signal caused by a leak to travel to the nearest measurement location. The time difference of the first rapid decrease in *DDF* between a non-midpoint leak and a midpoint leak depends on the pipeline segment length and the wave speed. Based on the typical range of real pipeline segment lengths from 9 km to 120 km and assuming a wave speed of 1,000 m/s, this time difference would range from 9 seconds to 2 minutes.

#### **4.4 Sensitivity to Transient Severity**

Transient severities (*TSVs*) of 0.12, 0.20, 0.33 and 0.50 were tested to represent mild to severe transient events. The *TSV* of 0.12 is the lowest severity tested, with a transient duration of 8 minutes and a flow change of 20% of the initial flow

rate. The *TSV* of 0.50 is the highest severity tested, with a 5-second duration and a flow change of 50% of the initial flow rate.

#### 4.4.1 Perfect Data

Figure 4-38 presents the *DDF* curves of transient severities of 0.12, 0.20, 0.33 and 0.50 for leaks during flow increase transient events with perfect data, an *R* factor of 2.20 and a 1% leak rate. It can be observed that the three curves with the smaller *TSV* are almost overlapping each other while the curve associated with the most severe transient (*TSV* = 0.5) is separate from the other three. Therefore, only two *TSV* curves are presented in the remaining figures of this subsection. These two transient severities were chosen to cover the limits of the range tested: 0.12 and 0.50.

*DDF* curves for *TSV* of 0.12 and 0.50 are plotted in Figure 4-39 for leaks during a flow decrease transient event with the *R* factor of 2.20, a 1% leak rate, and perfect data. The time that a leak would be detected depends on the specified threshold. For example, the curves for the mild and severe transient both show an initial sharp decrease that overlaps with each other. A leak would be equally easy and fast to detect for mild and severe transients if a threshold for *DDF* is set anywhere between 0 to -0.6. However, a leak during the mild flow decrease transient event would be detected later than during the severe transient if the threshold is set between -0.6 to approximately -1.0, or may not be detected at all (e.g. with a threshold of -1.2).

It is also noticed that, by comparing Figures 4-38 and 4-39, the magnitude of *DDF* is larger for flow decrease transient events than for flow increase transient events. This is because the leak pressure wave attenuates more slowly when flow is decreasing. This is more obvious for the curves of severe transients.

#### 4.4.2 Noisy Data

Figures 4-40 presents the *DDFTAVE* curves for transient severities of 0.12 and 0.50 and an *R* factor of 0.49 during a flow increase transient event for a 30% leak rate. It can be seen that the curve for the mild transient decreases slightly faster

than that for the more severe transient, and has a greater drop as well. After the initial drop, the two curves cross over each other a few times until reaching the equilibrium state. The time that a leak would be detected depends on the threshold specified. If the threshold intercepts the initial decrease of the curves, then a leak would be detected at almost the same time for mild and severe transient events. However, if the threshold was set below the lowest point of the curve for the severe transient, then a leak would only be detected for the mild transient case. Figure 4-41 shows the same curves but for a 1% leak rate. Similarly, despite that the initial sharp decrease is very close between the two curves, the *DDFTAVE* is much lower for the severe transient than that for the mild transient case. Generally speaking, it would be easier to detect a leak during a mild transient under flow increase conditions.

In Figure 4-42 the *DDFTAVE* curves are plotted for transient severities of 0.12 and 0.50, *R* factor of 2.20 and a 30% leak rate for a flow increase transient. Again, the curve of the mild transient decreases faster and has a greater drop. The *DDF* is lower for the mild transient case until both curves reach equilibrium. Therefore, a leak occurred during the severe transient would be detected later than if it was to occur during the mild transient. Depending on how the threshold is set, the difference in detection time may range from seconds to minutes, or only the leak during mild transient can be detected (e.g. a threshold of -0.95). Even though the shape of the curve for a high *R* factor is significantly different than those for a low *R* factor, the conclusion is very similar, i.e. it would likely be easier to detect a leak during a mild transient for flow increase transient events.

Figure 4-43 shows the *DDFTAVE* curves for transient severities of 0.12 and 0.50, an *R* factor of 2.20 and a 1% leak rate during a flow increase transient event. The observation presented in Figure 4-42 for a 30% leak rate is not recognizable here. It can be seen that *DDFTAVE* is comparable in these curves. A leak would be very difficult to detect for both a mild and a severe transient because *DDFTAVE* is small. In addition, the increasing flow as well as the high *R* factor cause greater attenuation of the leak.

Figure 4-44 presents the *DDFTAVE* curves of different transient severity for a 30% leak rate during a flow decrease transient event and the *R* factors of 0.49. Contrary to the previous flow increase transient cases, the curve for the more severe transient decreases slightly faster than that for the mild transient, and has a greater drop as well. After the initial drop, the two curves cross over each other a few times until they reach the equilibrium state. The time that a leak would be detected depends on the specified threshold. If the threshold intercepts the initial decrease of the curves, then a leak would be detected at virtually the same time for mild and severe transient events. However, if the threshold was set below the lowest point of the curve for the mild transient, then a leak would only be detected for the severe transient event. Figure 4-45 presents the *DDFTAVE* curves of different transient severity for a 30% leak rate during a flow decrease transient event with the *R* factor of 2.20. Again, the curve of the severe transient decreases faster and has a greater drop. The *DDFTAVE* is lower for the severe transient case until both curves reach equilibrium. Therefore, a leak occurred during the severe transient would be detected faster than if it occurred during the mild transient. Depending on how the threshold is set, the difference in detection time may range from seconds to minutes, or only a leak during a severe transient can be detected. This observation is also valid for small leaks.

Figure 4-46 presents the *DDFTAVE* curves of different transient severity for leaks during a flow decrease transient event with the *R* factor of 2.20 and a 1% leak rate. The curve for the severe transient is always below the curve for the mild transient even after the *DDFTAVE* starts to decrease. Therefore, it may be easier to detect a leak during severe transient events compared to mild ones. This is in contrast with what was noticed for the flow increase transient, for which it may be easier to detect a leak for mild transient than severe transient events.

## 4.5 Sensitivity to Flow State

### 4.5.1 Perfect Data

Figure 4-47 shows the *DDF* curves of leaks occurred during the three, steady, flow increase and flow decrease flow states for an *R* factor of 0.49, a 1% leak rate and perfect data. It can be observed that all three curves have an initial sharp decrease overlapping each other. A leak would be detected at the same time if the threshold intercepts with this initial decrease. However, the three curves start to separate afterwards. The maximum absolute values of *DDF* are -1.48 for the flow increase transient, -1.59 for the steady state and -1.78 for flow decrease transient.

Figure 4-48 presents the *DDF* curves of the three flow states with the *R* factor of 2.20 and a 1% leak rate. Again all three curves have an initial sharp decrease overlapping each other. There would be no difference in terms of leak detection if a threshold intercepts with this initial decrease. However, the three curves start to separate afterwards. The maximum absolute values of *DDF* are -0.93 for the flow increase transient, -1.03 for the steady state and -1.19 for the flow decrease transient. Thus, a leak would be detected most easily during a flow decrease transient event, compared to steady state or a flow increase transient event, with the latter being the most difficult operating condition for leak detection.

### 4.5.2 Noisy Data

The *DDFTAVE* curves of Figure 4-49 are of leaks occurred during the three flow states with the *R* factor of 0.49 and a 30% leak rate. It can be observed that the three curves all have a sharp initial decrease but are not quite overlapping. The curve for the steady state case is in the middle of the curves for flow decrease and flow increase transient events. The maximum absolute value of *DDFTAVE* for steady state, -1.45, is also in the middle of the other two, with -1.30 for the flow increase event, and -1.50 for the flow decrease event.

Figure 4-50 shows the *DDFTAVE* curves of leaks during the three flow states for an *R* factor of 0.49 and a 1% leak rate. It can be clearly seen that the curve for

steady state is in the middle of the other two curves. The maximum absolute values of *DDFTAVE* are -0.06 for the flow increase transient, -0.12 for the steady state, and -0.62 for the flow decrease transient.

The same trend with regard to flow states observed with a low *R* factor can be seen for the high *R* factor cases. Figure 4-51 presents the *DDFTAVE* curves for steady, flow increase and flow decrease flow states with an *R* factor of 2.20 and a 30% leak rate. It can be observed that the maximum absolute values of *DDFTAVE* are -0.98 for the steady state, -0.92 for the flow increase event, and -1.02 for the flow decrease event. In Figure 4-52 the *DDFTAVE* curves for steady, flow increase and flow decrease flow states with an *R* factor of 2.20 and a 1% leak rate are plotted. It can be observed that the maximum absolute values of *DDFTAVE* are -0.01 for the steady state, -0.05 for the flow increase event, and -0.43 for the flow decrease event.

Based on the results of section 4.5, *DDFTAVE* is small for flow increase leak events compared to steady state and flow decrease transient events with noisy data. Leak detection is easier during flow decrease transient events compared to steady state with the thresholds provided in the figures of this section. A flow increase transient event has the smallest values of *DDFTAVE*. This observation is comparable to the results observed in previous studies: e.g., a leak is more difficult to detect during flow increase transient events than during flow decrease transient events with noisy data (Liou, 1993), and this finding is caused by an increase in the frictional forces (Liou, 1993; Balda, 2012).

In the previous study (Liou, 1993), leak detection was easier during the steady state compared to flow decrease transient events. Liou's observation differs from the results of this study. In this study, it was easier to detect a leak during flow decrease transient events compared to the steady state.

The slope of the initial drop of *DDFTAVE* is comparable for all three flow states with a low *R* factor and the transient events do not have a significant impact on leak detection. The slope of the initial drop of *DDFTAVE* is different for each type

of transient with a high  $R$  factor and the transient events have a significant effect on leak detection. Therefore, a pipeline system with a high  $R$  factor is more prone to transient degradation during flow increase transient events (e.g. a leak would be harder to detect with this high  $R$  factor and a flow increase condition).

#### **4.6 Sensitivity to Noise Level in Flow**

The reference noise level added to the flow and pressure data is 1%. Data with a flow noise level ( $NQ$ ) of 3% and a pressure noise level of 1% is compared to this reference level to evaluate the impact of the noise level in the flow measurement data on the leak detection system during transient events.

In Figures 4-53 and 4-54, the  $DDFTAVE$  curves are plotted for these two flow noise levels with an  $R$  factor of 2.20 and a 30% leak rate for leaks during a flow increase and a flow decrease transient events, respectively. The sensitivity to noise level in flow was only tested for this leak scenario with the  $R$  factor of 2.20 because noise has a bigger impact on systems of large  $R$  factor, as demonstrated in section 4.2.2. Depending on the specified threshold, the time difference a leak may be detected ranges from less than a minute, to a few minutes, or the leak may only be detected when noise level is low. For example, in Figure 4-53, a leak would be only detected with a noise level in flow of 1% for a threshold of -0.9 at 04:10:00. A leak would be detected during the 1% and 3% noise levels for a threshold of -0.6 with detection times of 04:03:00 and 04:04:30, respectively. The difference in the maximum absolute value of  $DDFTAVE$  between these curves is significant and indicates 18% and 10% of the leak rate are being masked by the larger noise for the flow increase and decrease transients, respectively. The higher flow noise masked more of the leak rate and downgrades the identification of this leak. Figures 4-53 and 4-54 show a difference between the flow increase and decrease cases. The space between the two curves in Figure 4-53 is larger than in Figure 4-54, indicating that the effect of the noise is less for flow decrease transients than for flow increase transients. In other words, a flow decrease transient flow condition is more tolerant of data noise than a flow increase condition.

For further details of these results, Appendix C contains the remaining graphs prepared in this project for result interpretation; Appendix D presents the best tuning parameters found for this leak detection system.

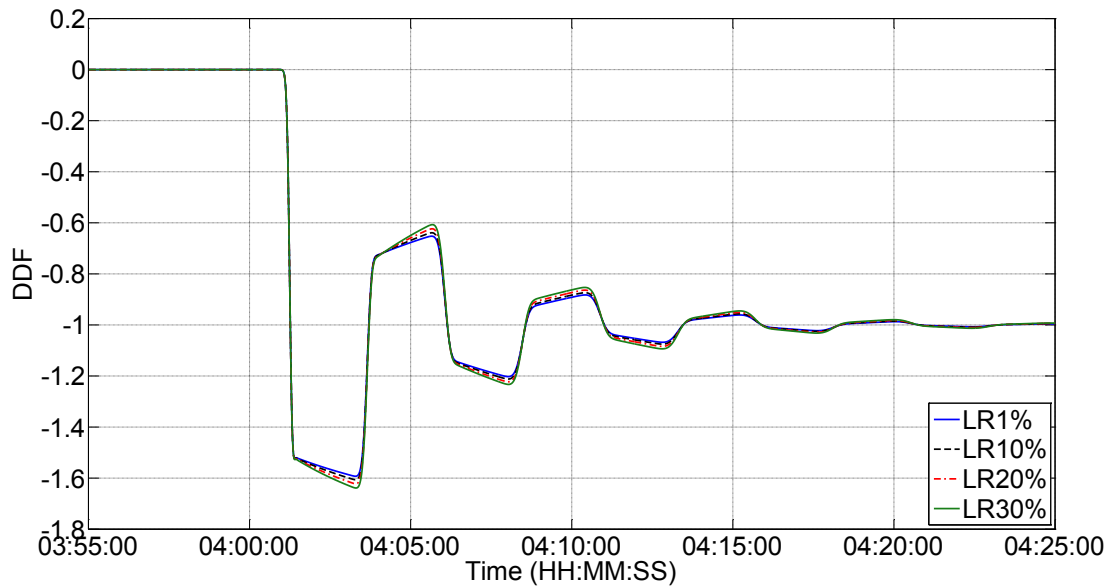


Figure 4-1. Non-dimensional diagnostic flow DDF versus time for perfect data, leak sizes of 1%, 10%, 20% and 30%, steady flow conditions,  $V_o = 0.3 \text{ m/s}$ ,  $R = 0.49$ , leak at midpoint.

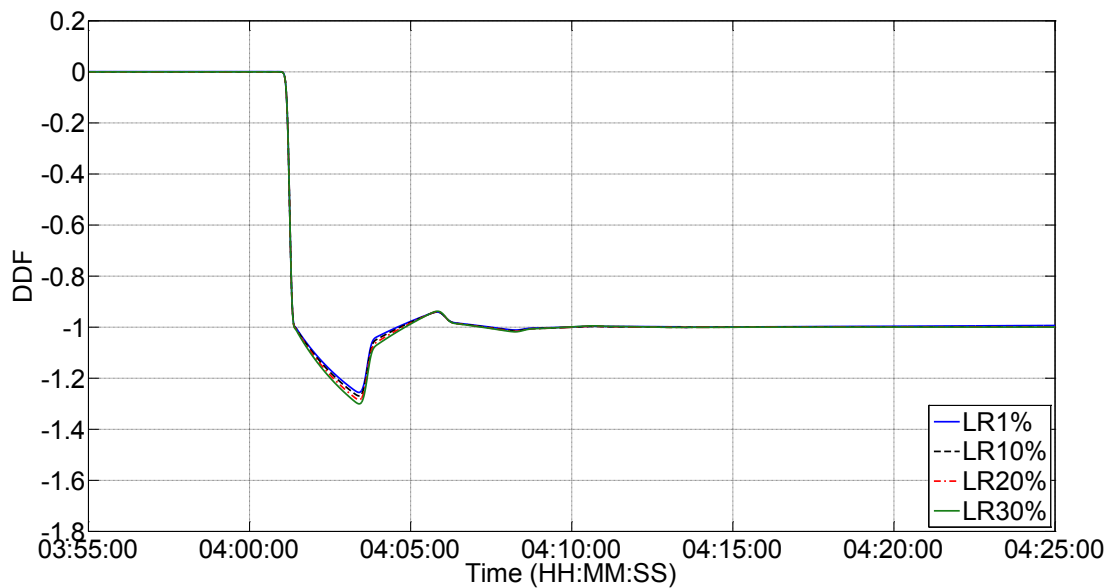


Figure 4-2. Non-dimensional diagnostic flow DDF versus time for perfect data, leak sizes of 1%, 10%, 20% and 30%, steady flow conditions,  $V_o = 1 \text{ m/s}$ ,  $R = 1.26$ , leak at midpoint.

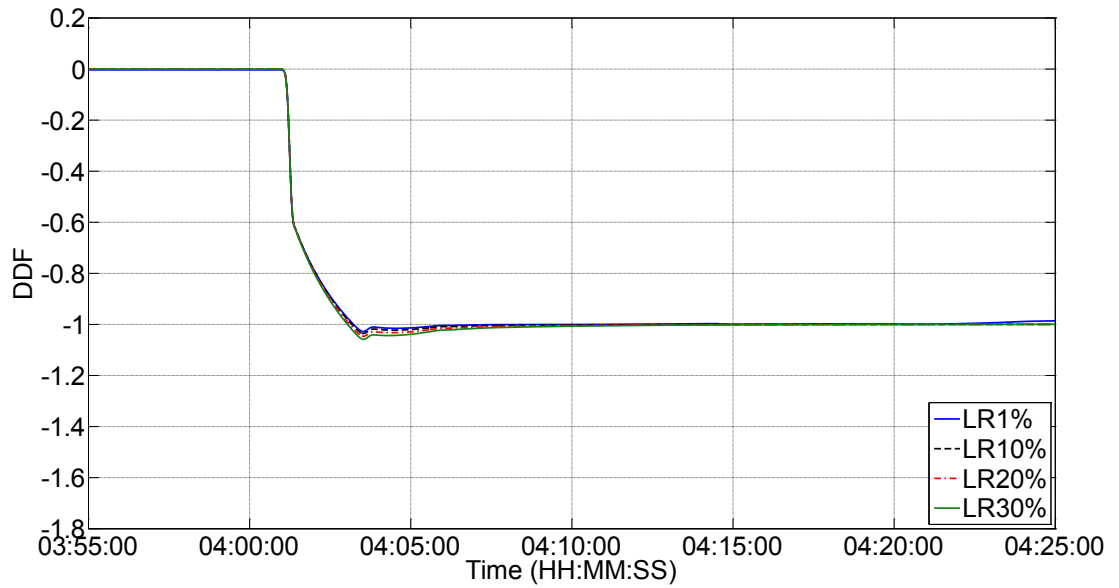


Figure 4-3. Non-dimensional diagnostic flow DDF versus time for perfect data, leak sizes of 1%, 10%, 20% and 30%, steady flow conditions,  $V_o = 2$  m/s,  $R = 2.20$ , leak at midpoint.

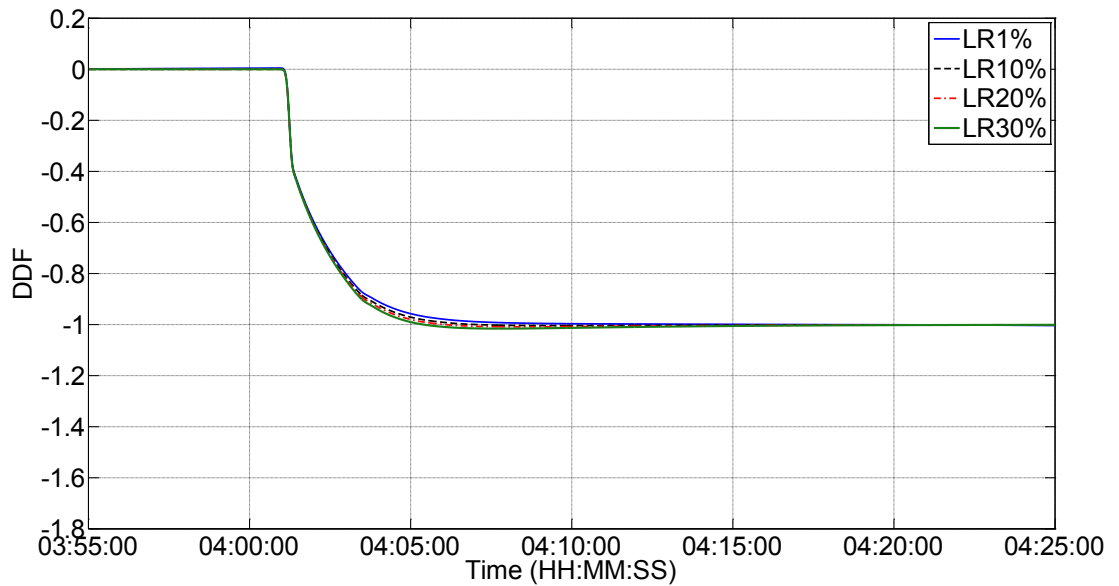


Figure 4-4. Non-dimensional diagnostic flow DDF versus time for perfect data, leak sizes of 1%, 10%, 20% and 30%, steady flow conditions,  $V_o = 3$  m/s,  $R = 3.08$ , leak at midpoint.

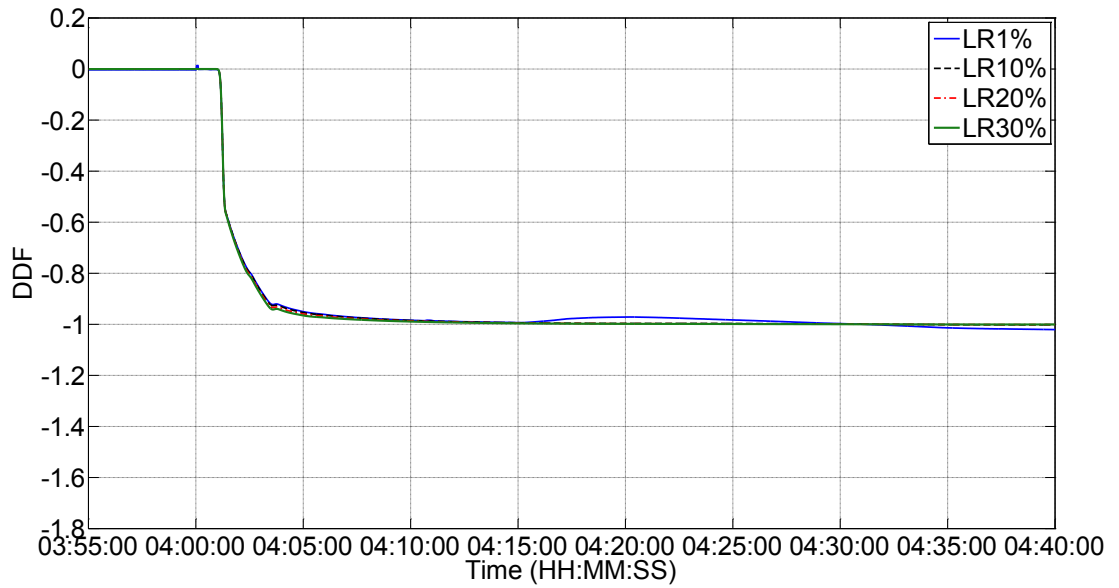


Figure 4-5. Non-dimensional diagnostic flow DDF versus time for perfect data, leak sizes of 1%, 10%, 20% and 30%, flow increase transient,  $V_o = 2$  m/s,  $V_f = 3$  m/s,  $R = 2.20$ ,  $TSV = 0.5$ , duration = 5 s, leak at midpoint.

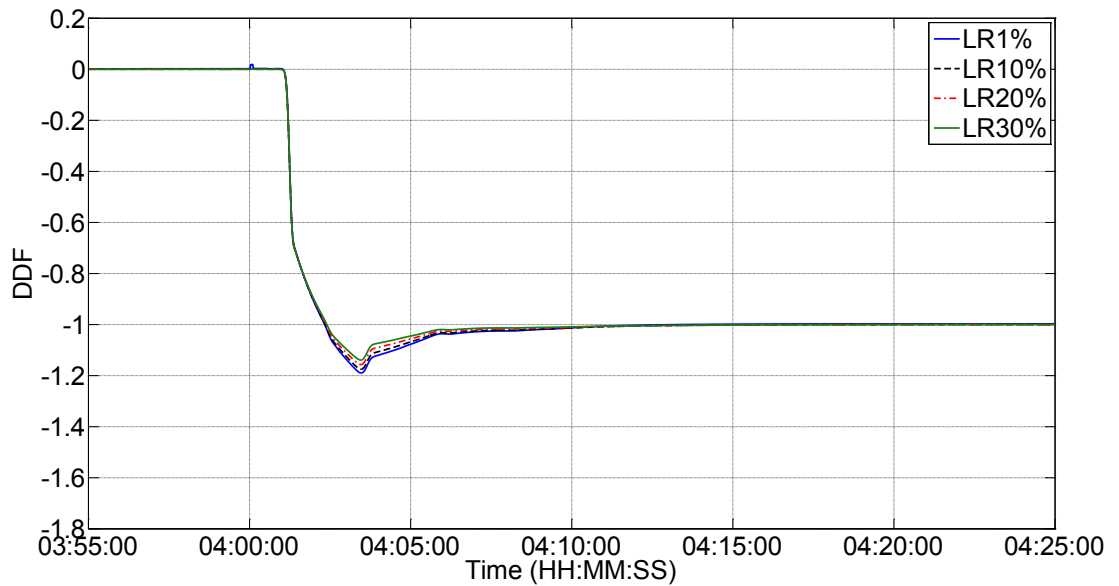


Figure 4-6. Non-dimensional diagnostic flow DDF versus time for perfect data, leak sizes of 1%, 10%, 20% and 30%, flow decrease transient,  $V_o = 2$  m/s,  $V_f = 1$  m/s,  $R = 2.20$ ,  $TSV = 0.5$ , duration = 5 s, leak at midpoint.

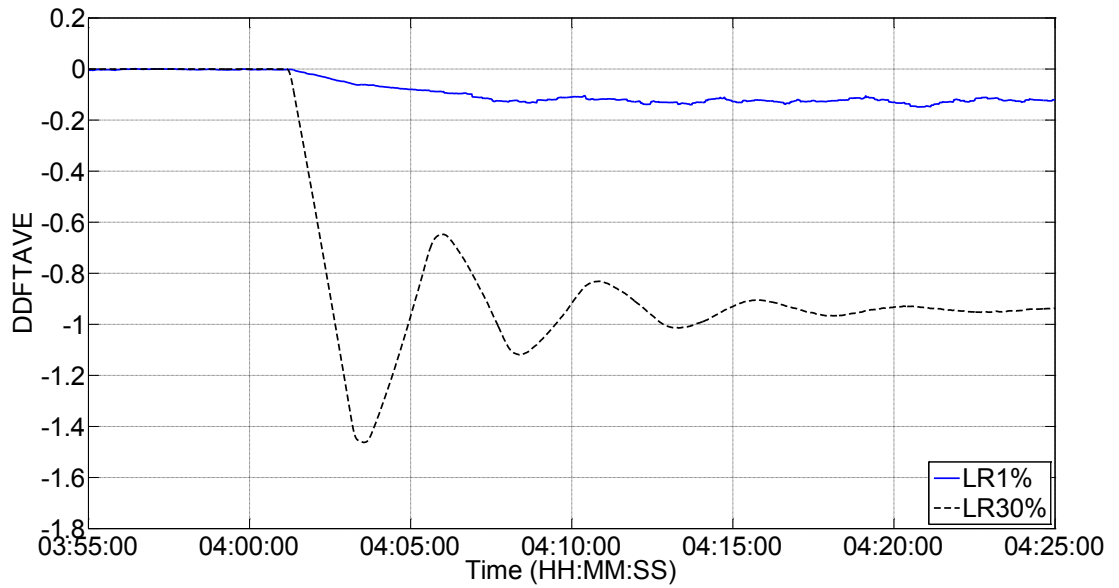


Figure 4-7. Non-dimensional time-averaged diagnostic flow DDFTAVE versus time for 1% noise levels, leak sizes of 1% and 30% and steady flow conditions,  $V_o = 0.3$  m/s,  $R = 0.49$ , leak at midpoint.

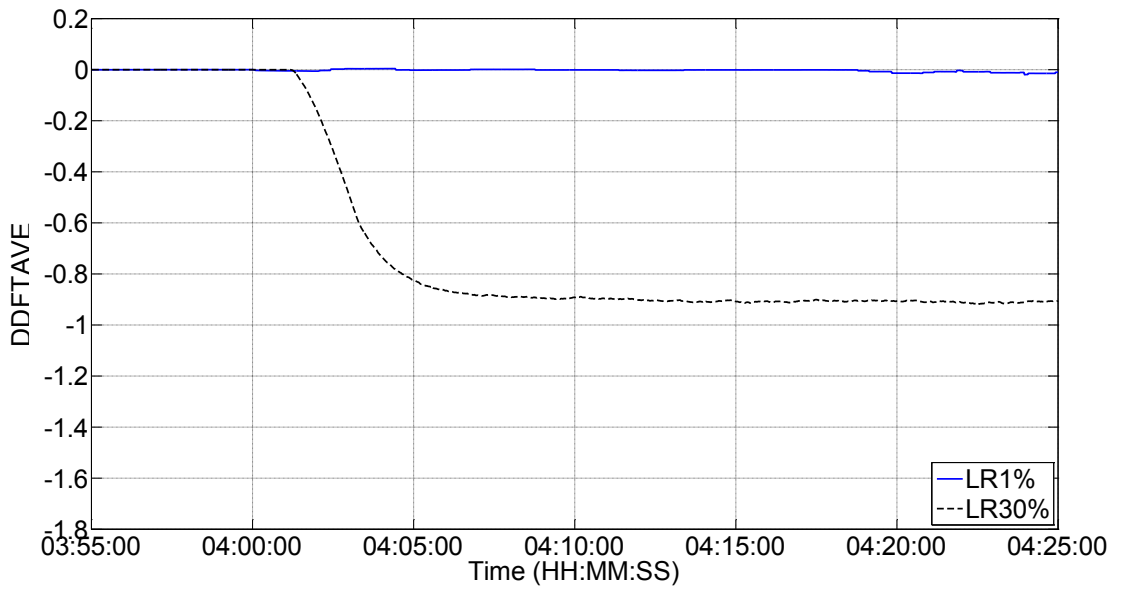


Figure 4-8. Non-dimensional time-averaged diagnostic flow DDFTAVE versus time for 1% noise levels, leak sizes of 1% and 30% and flow increase transient,  $V_o = 2$  m/s,  $V_f = 3$  m/s,  $R = 2.20$ ,  $TSV = 0.5$ , duration = 5 s, leak at midpoint.

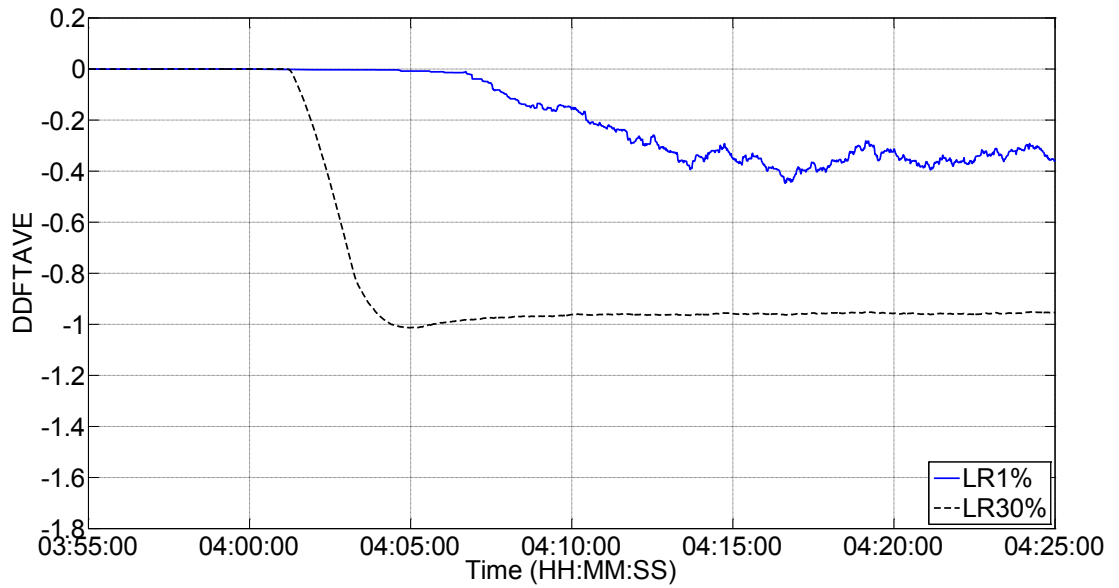


Figure 4-9. Non-dimensional time-averaged diagnostic flow DDFTAVE versus time for 1% noise levels, leak sizes of 1% and 30%, flow decrease transient,  $V_o = 2$  m/s,  $V_f = 1$  m/s,  $R = 2.20$ ,  $TSV = 0.5$ , duration = 5 s, leak at midpoint.

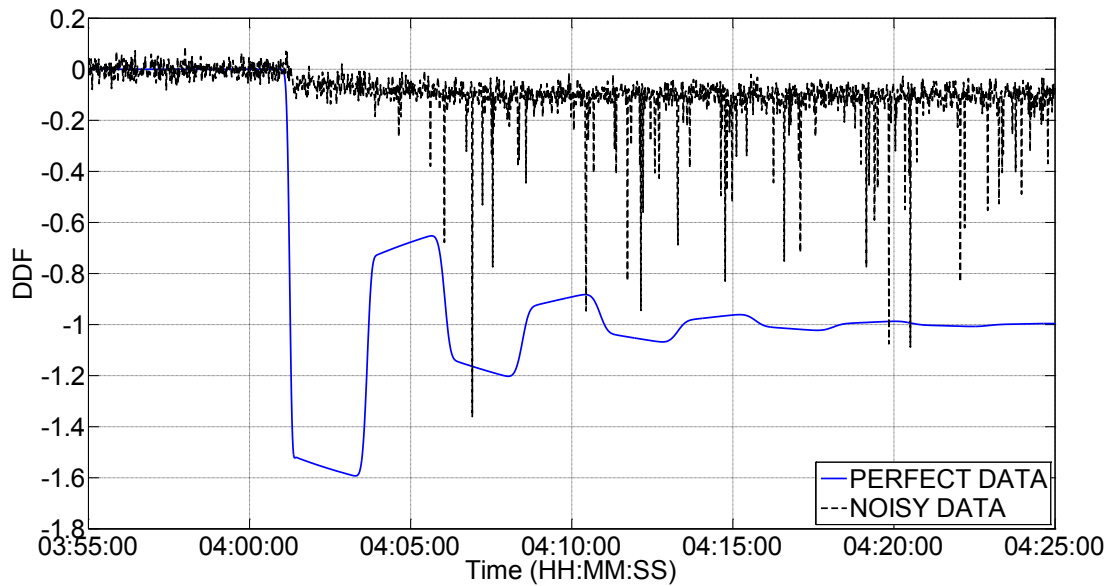


Figure 4-10. Non-dimensional diagnostic flow DDF versus time for perfect data and noisy data, 1% noise levels, leak size of 1%, steady flow conditions,  $V_o = 0.3$  m/s,  $R = 0.49$ , leak at midpoint.

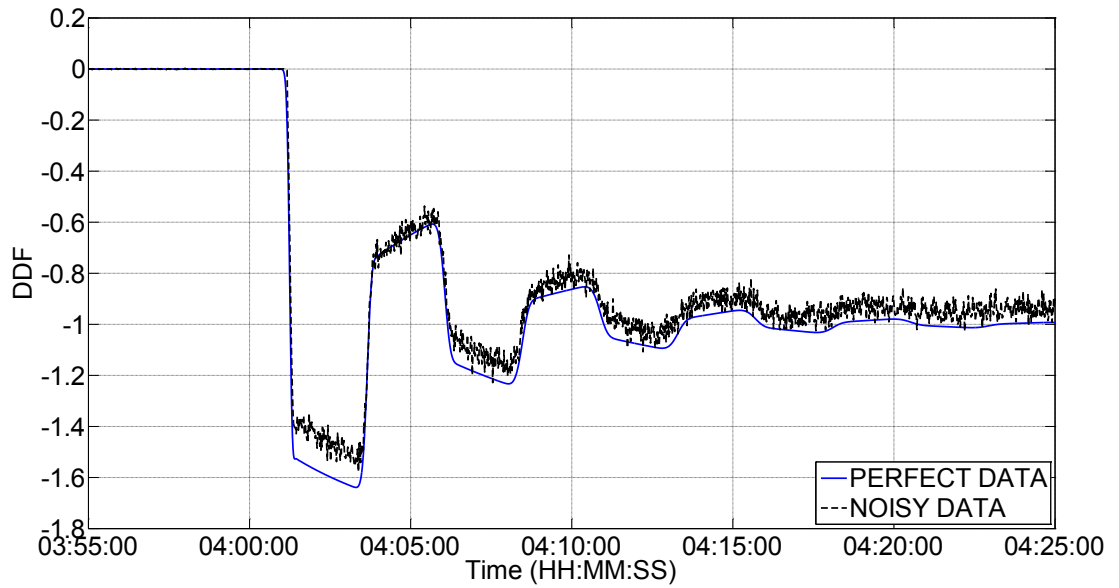


Figure 4-11. Non-dimensional diagnostic flow DDF versus time for perfect data and noisy data, 1% noise levels, leak size of 30%, steady flow conditions,  $V_o = 0.3$  m/s,  $R = 0.49$ , leak at midpoint.

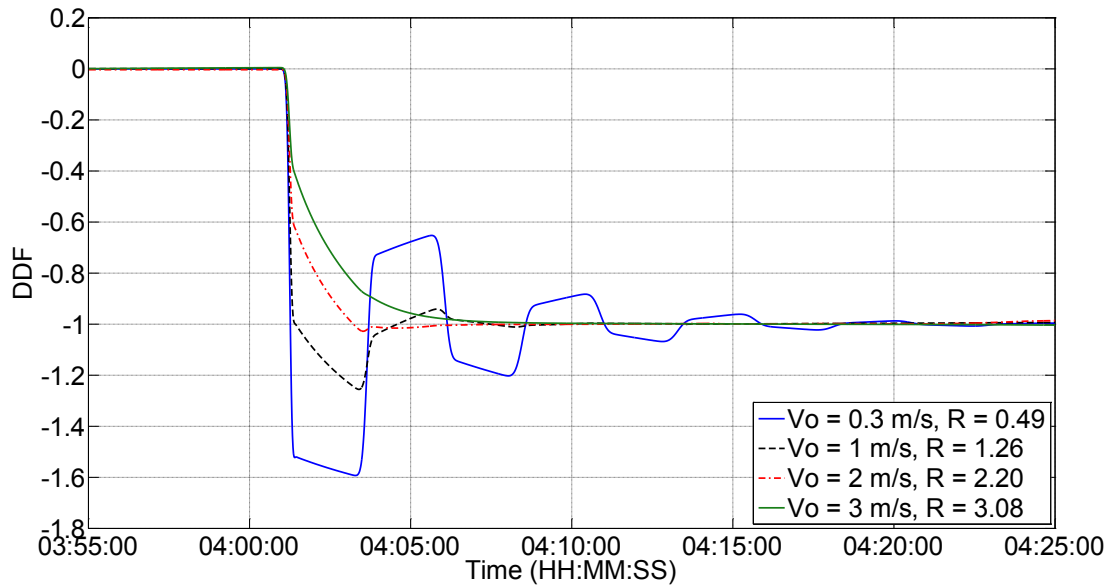


Figure 4-12. Non-dimensional diagnostic flow DDF versus time for perfect data, leak size of 1%, R factors of 0.49, 1.26, 2.20 and 3.08, steady flow conditions, leak at midpoint.

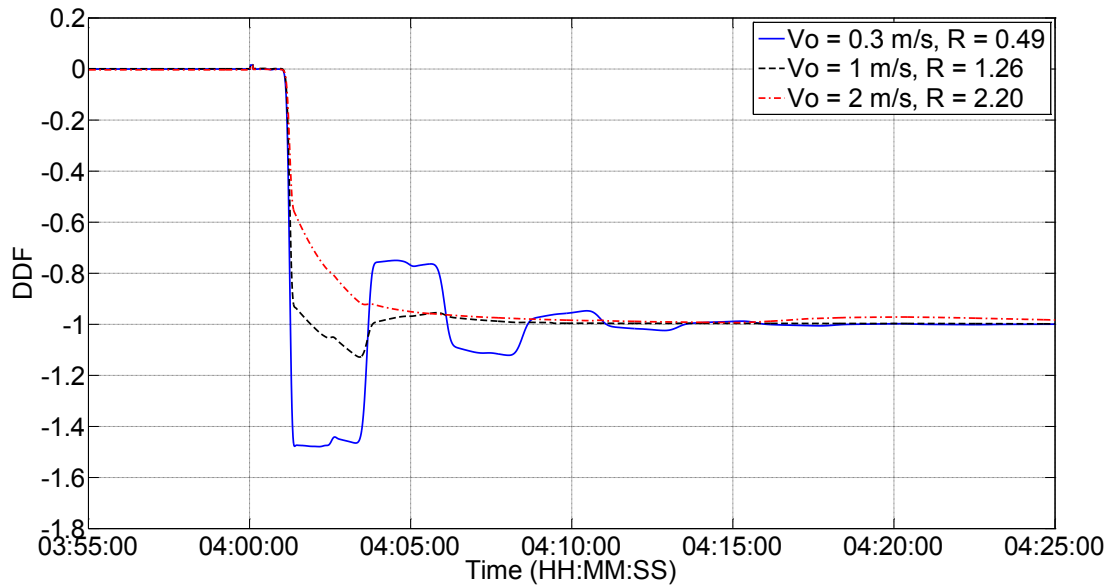


Figure 4-13. Non-dimensional diagnostic flow DDF versus time for perfect data, leak size of 1%, R factors of 0.49, 1.26 and 2.20, flow increase transient, duration = 5 s, leak at midpoint, TSV = 0.5.

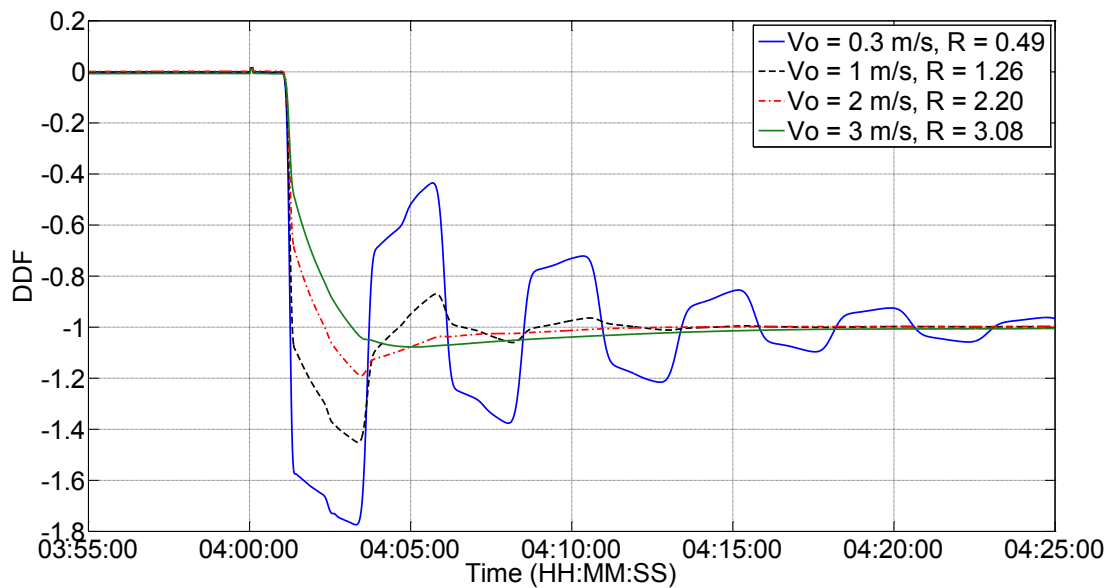


Figure 4-14. Non-dimensional diagnostic flow DDF versus time for perfect data, leak size of 1%, R factors of 0.49, 1.26, 2.20 and 3.08, flow decrease transient, duration = 5 s, leak at midpoint, TSV = 0.5.

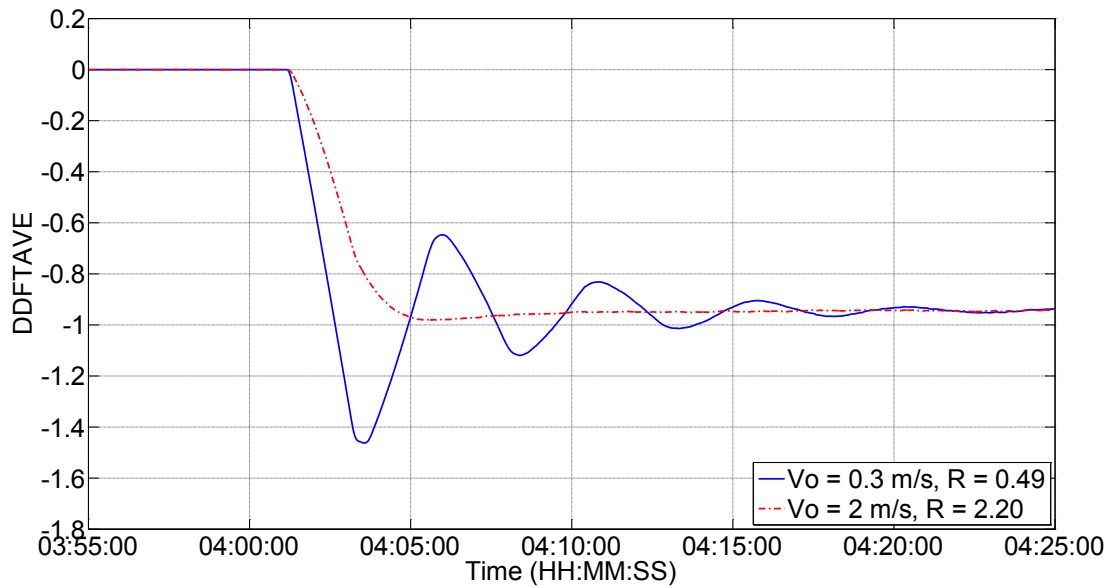


Figure 4-15. Non-dimensional time-averaged diagnostic flow DDFTAVE versus time for 1% noise levels, leak size of 30%, R factors of 0.49 and 2.20, steady flow conditions, leak at midpoint.

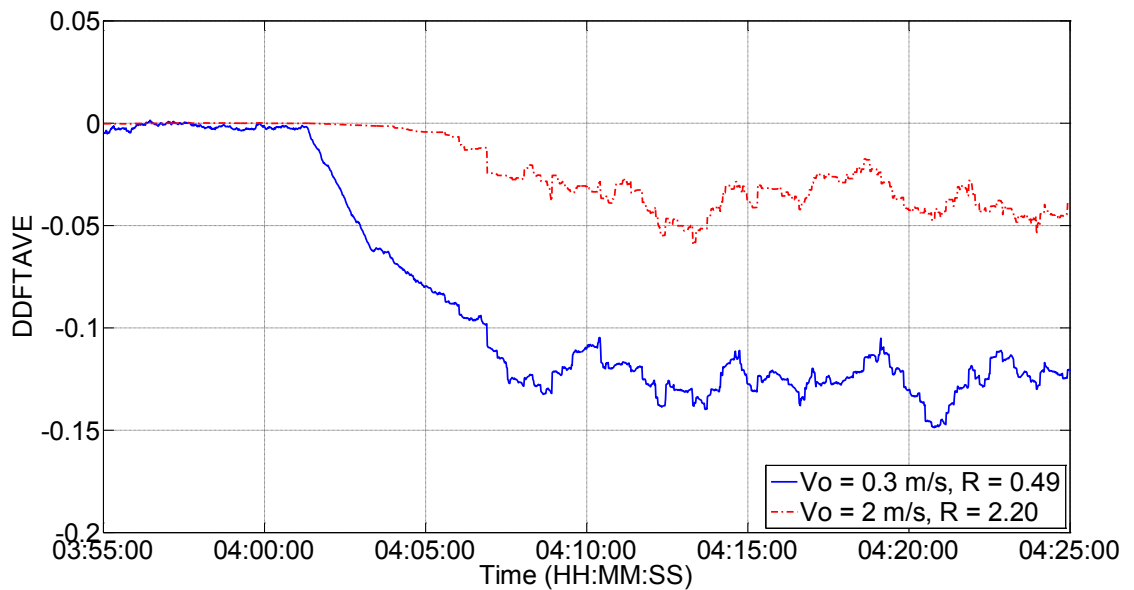


Figure 4-16. Non-dimensional time-averaged diagnostic flow DDFTAVE versus time for 1% noise levels, leak size of 1%, R factors of 0.49 and 2.20, steady flow conditions, leak at midpoint.

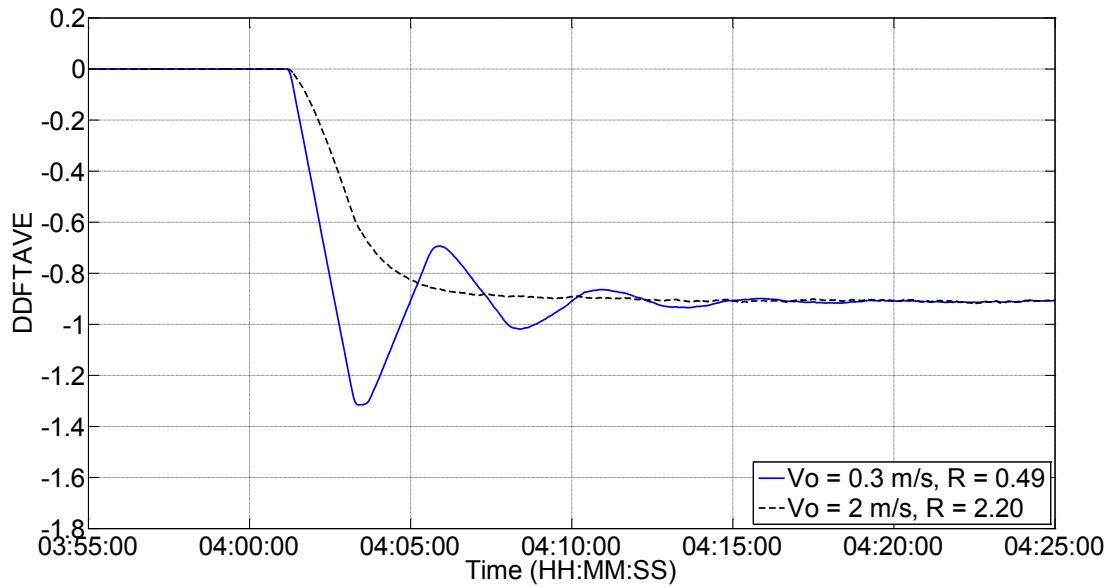


Figure 4-17. Non-dimensional time-averaged diagnostic flow DDFTAVE versus time for 1% noise levels, leak size of 30%, R factors of 0.49 and 2.20, flow increase transient, duration = 5 s, TSV = 0.5, leak at midpoint.

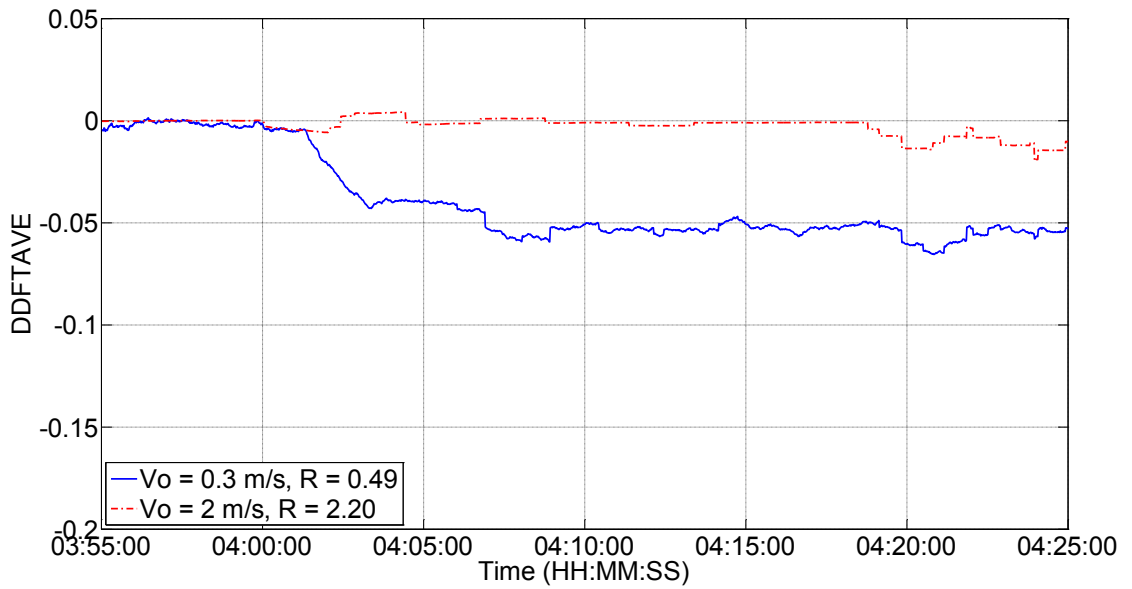


Figure 4-18. Non-dimensional time-averaged diagnostic flow DDFTAVE versus time for 1% noise levels, leak size of 1%, R factors of 0.49 and 2.20, flow increase transient, duration = 5 s, TSV = 0.5, leak at midpoint.

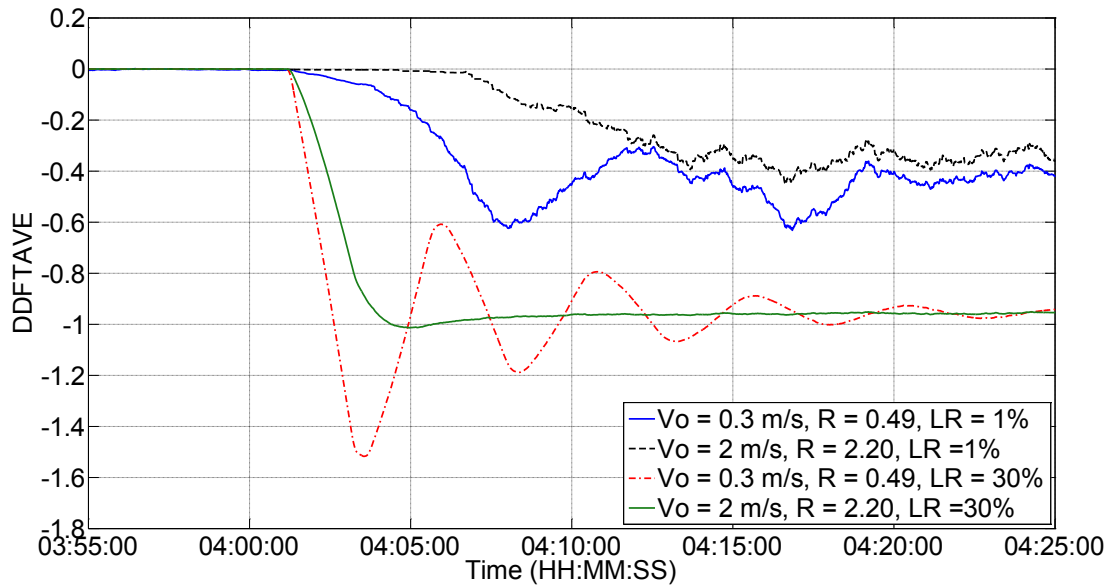


Figure 4-19. Non-dimensional time-averaged diagnostic flow DDFTAVE versus time for 1% noise levels, leak sizes of 1% and 30%, R factors of 0.49 and 2.20, flow decrease transient, duration = 5 s, TSV = 0.5, leak at midpoint.

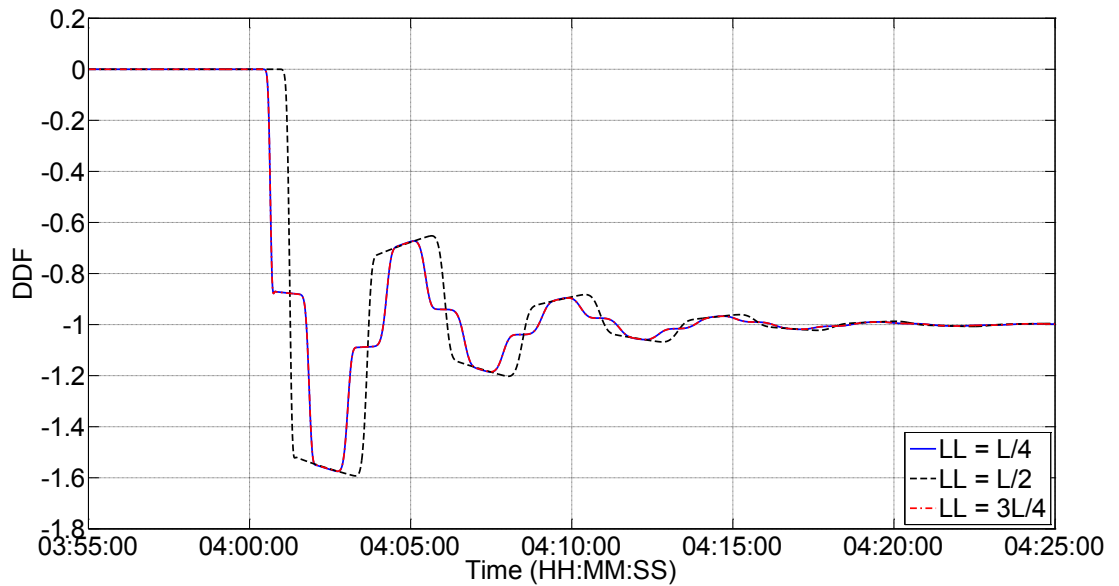


Figure 4-20. Non-dimensional diagnostic flow DDF versus time for perfect data, leak size of 1%, leaks at first quarter, midpoint and third quarter of pipeline length, steady flow conditions,  $V_o = 0.3$  m/s,  $R = 0.49$ .

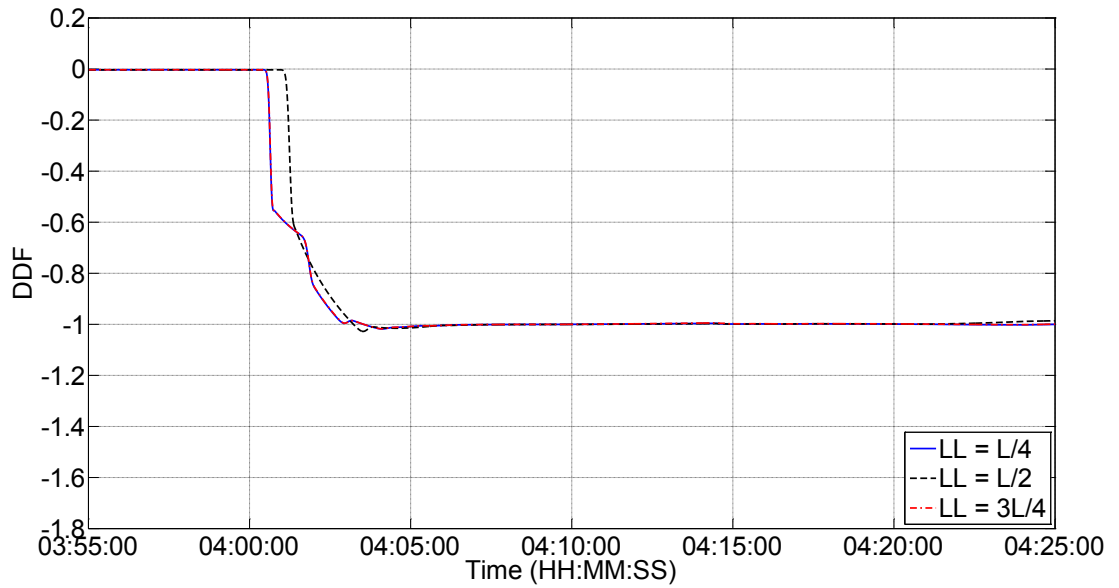


Figure 4-21. Non-dimensional diagnostic flow DDF versus time for perfect data, leak size of 1%, leaks at first quarter, midpoint and third quarter of pipeline length, steady flow conditions,  $V_o = 2$  m/s,  $R = 2.20$ .

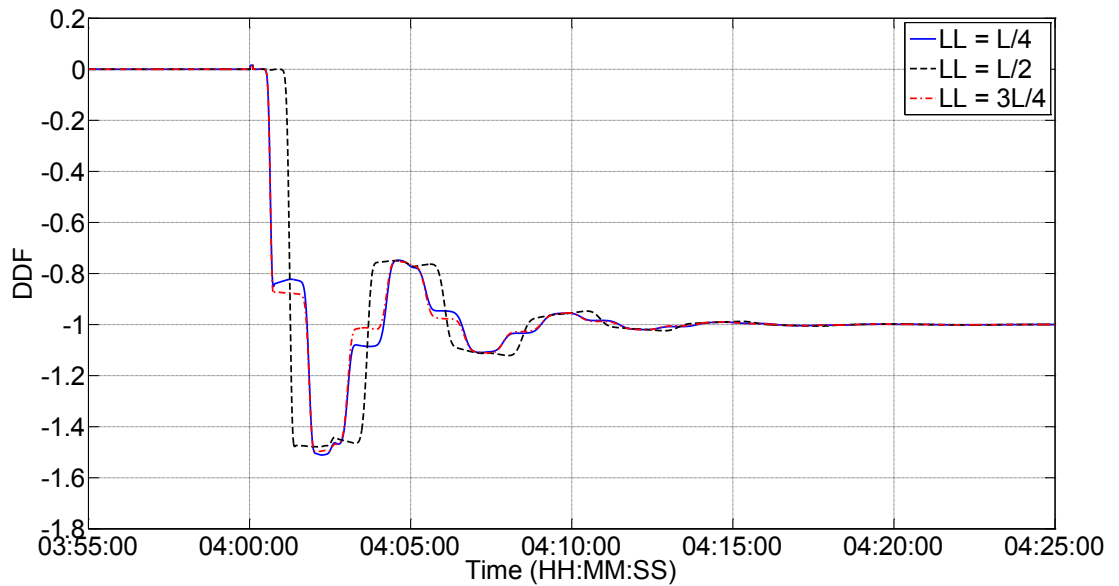


Figure 4-22. Non-dimensional diagnostic flow DDF versus time for perfect data, leak size of 1%, leaks at first quarter, midpoint and third quarter of pipeline length, flow increase transient, duration = 5 s,  $R = 0.49$ ,  $V_o = 0.3$  m/s,  $TSV = 0.5$ .

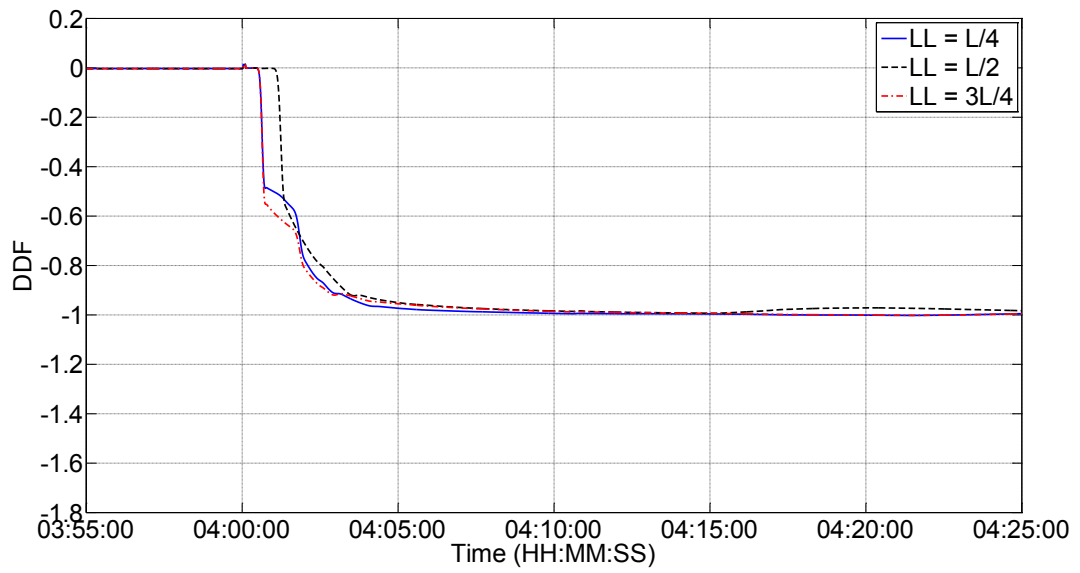


Figure 4-23. Non-dimensional diagnostic flow DDF versus time for perfect data, leak size of 1%, leaks at first quarter, midpoint and third quarter of pipeline length, flow increase transient, duration = 5 s,  $R = 2.20$ ,  $V_0 = 2.0$  m/s,  $TSV = 0.5$ .

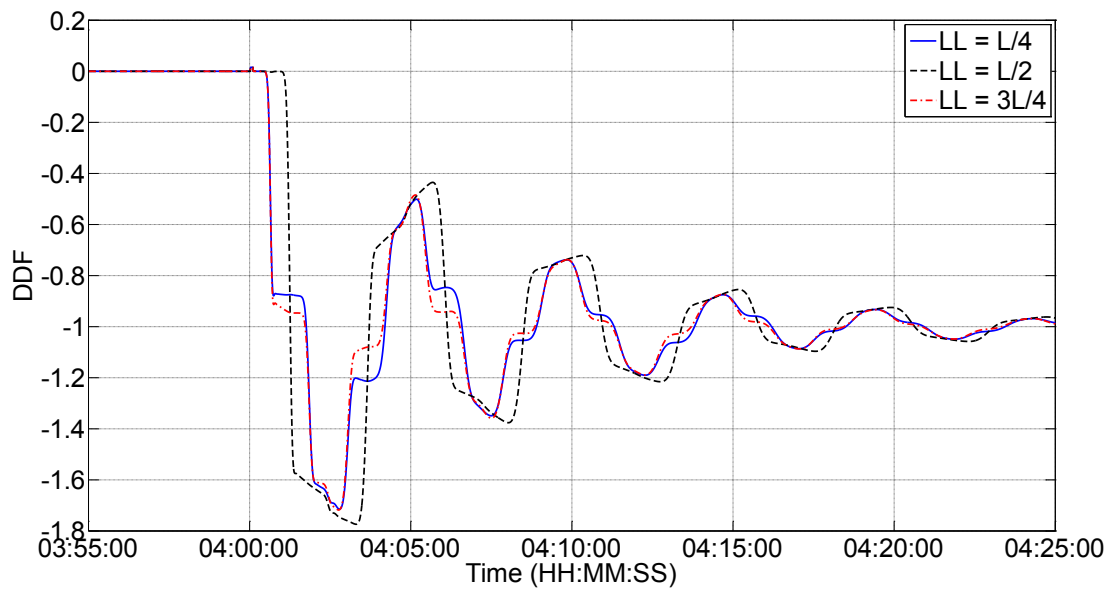


Figure 4-24. Non-dimensional diagnostic flow DDF versus time for perfect data, leak size of 1%, leaks at first quarter, midpoint and third quarter of pipeline length, flow decrease transient, duration = 5 s,  $TSV = 0.5$ ,  $R = 0.49$ ,  $V_0 = 0.3$  m/s.

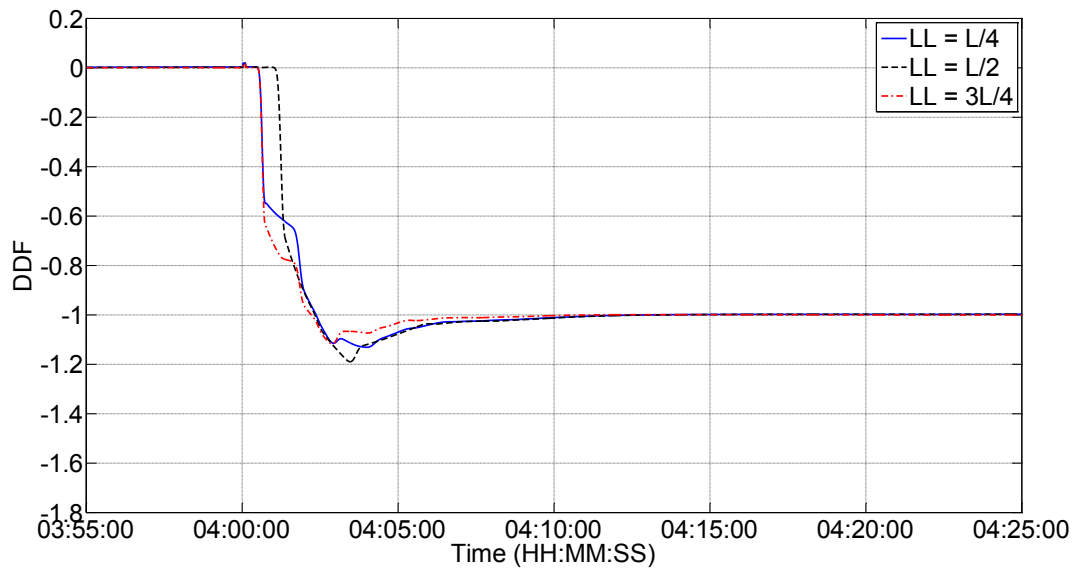


Figure 4-25. Non-dimensional diagnostic flow DDF versus time for perfect data, leak size of 1%, leaks at first quarter, midpoint and third quarter of pipeline length, flow decrease transient, duration = 5 s, TSV = 0.5, R = 2.20,  $V_o = 2.0$  m/s.

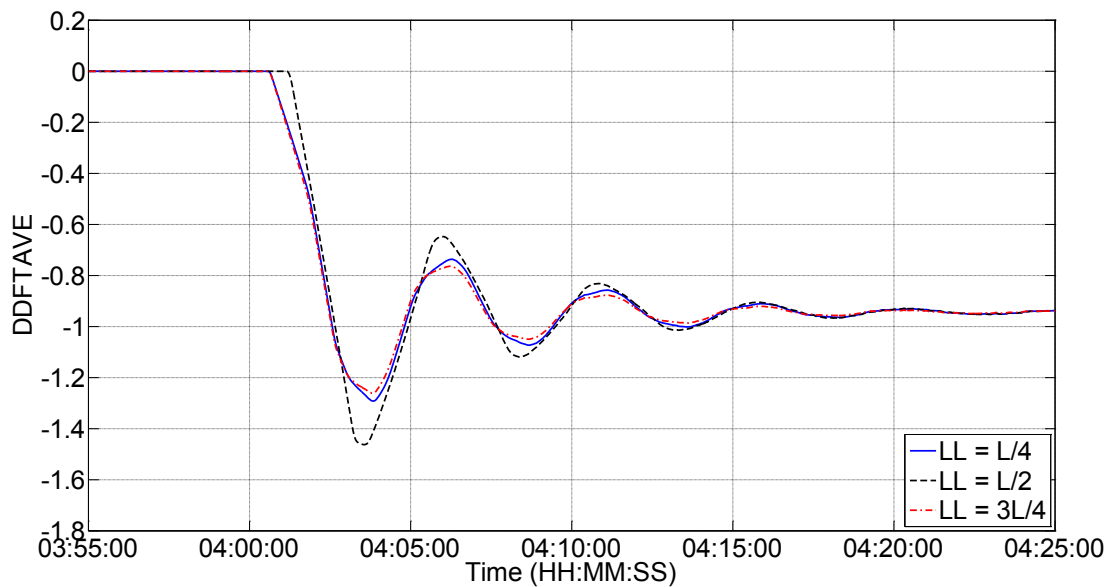


Figure 4-26. Non-dimensional time-averaged diagnostic flow DDFTAVE versus time for 1% noise levels, leak size of 30%, leaks at first quarter, midpoint and third quarter of pipeline length, steady flow conditions,  $V_o = 0.3$  m/s, R = 0.49.

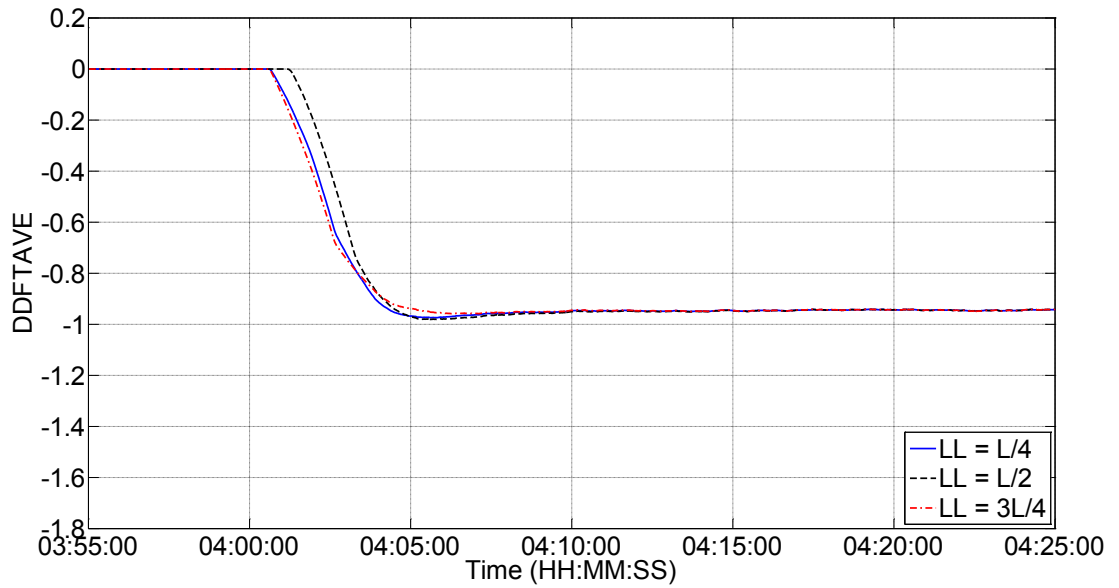


Figure 4-27. Non-dimensional time-averaged diagnostic flow DDFTAVE versus time for 1% noise levels, leak size of 30%, leaks at first quarter, midpoint and third quarter of pipeline length, steady flow conditions,  $V_o = 2 \text{ m/s}$ ,  $R = 2.20$ .

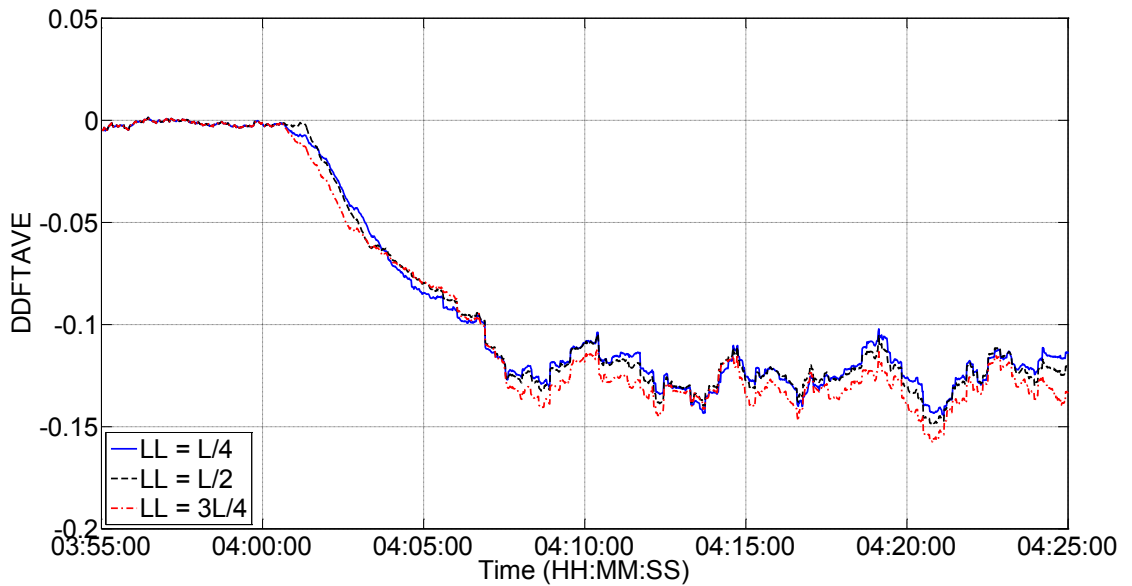


Figure 4-28. Non-dimensional time-averaged diagnostic flow DDFTAVE versus time for 1% noise levels, leak size of 1%, leaks at first quarter, midpoint and third quarter of pipeline length, steady flow conditions,  $V_o = 0.3 \text{ m/s}$ ,  $R = 0.49$ .

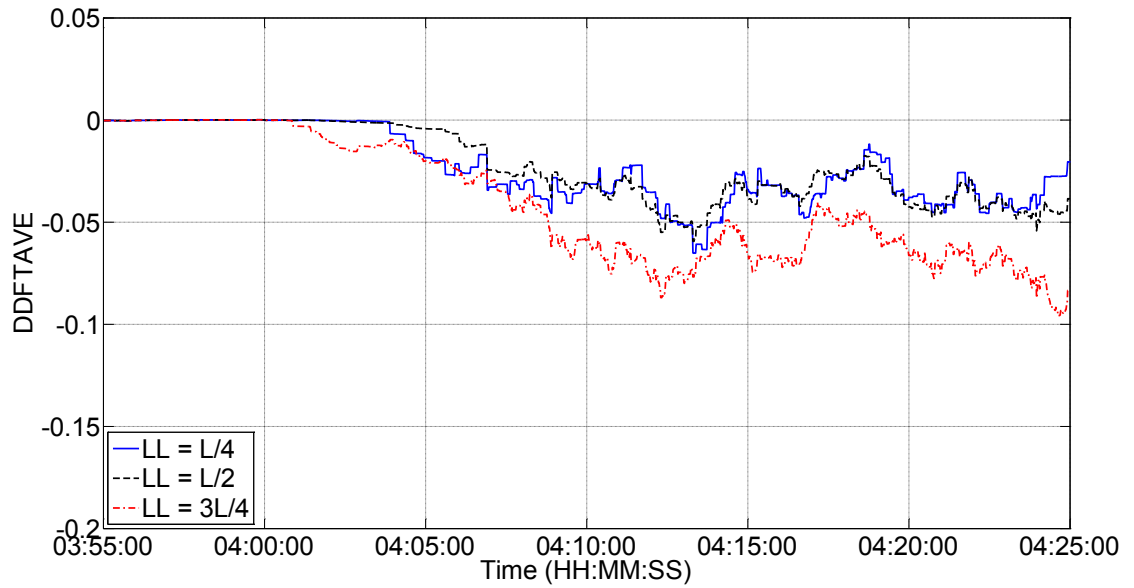


Figure 4-29. Non-dimensional time-averaged diagnostic flow DDFTAVE versus time for 1% noise levels, leak size of 1%, leaks at first quarter, midpoint and third quarter of pipeline length, steady flow conditions,  $V_o = 2$  m/s,  $R = 2.20$ .

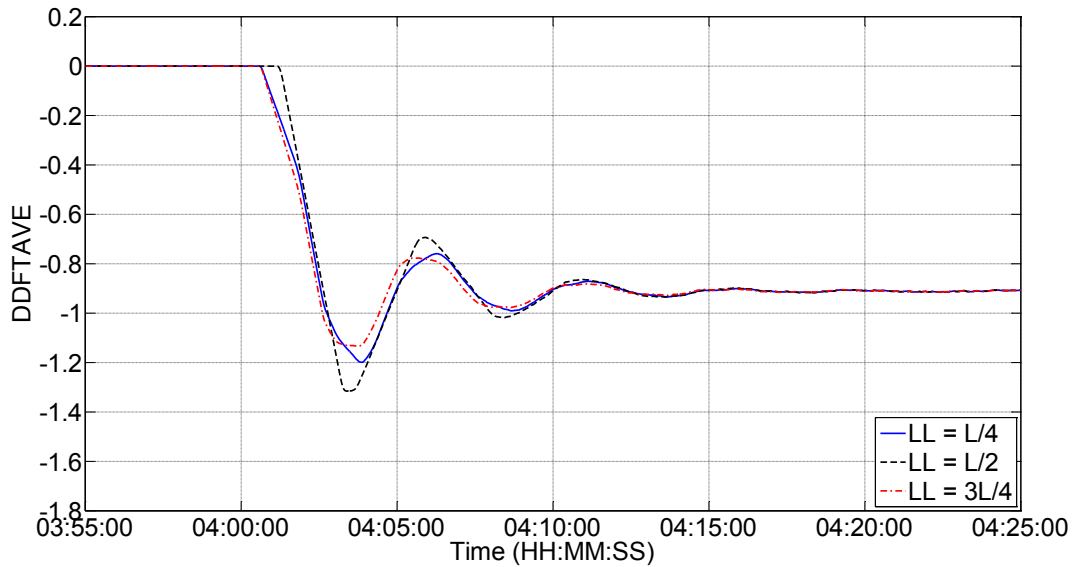


Figure 4-30. Non-dimensional time-averaged diagnostic flow DDFTAVE versus time for 1% noise levels, leak size of 30%, leaks at first quarter, midpoint and third quarter of pipeline length, flow increase transient,  $V_o = 0.30$  m/s,  $R = 0.49$ ,  $V_f = 0.45$  m/s, duration = 5 s, TSV = 0.5.

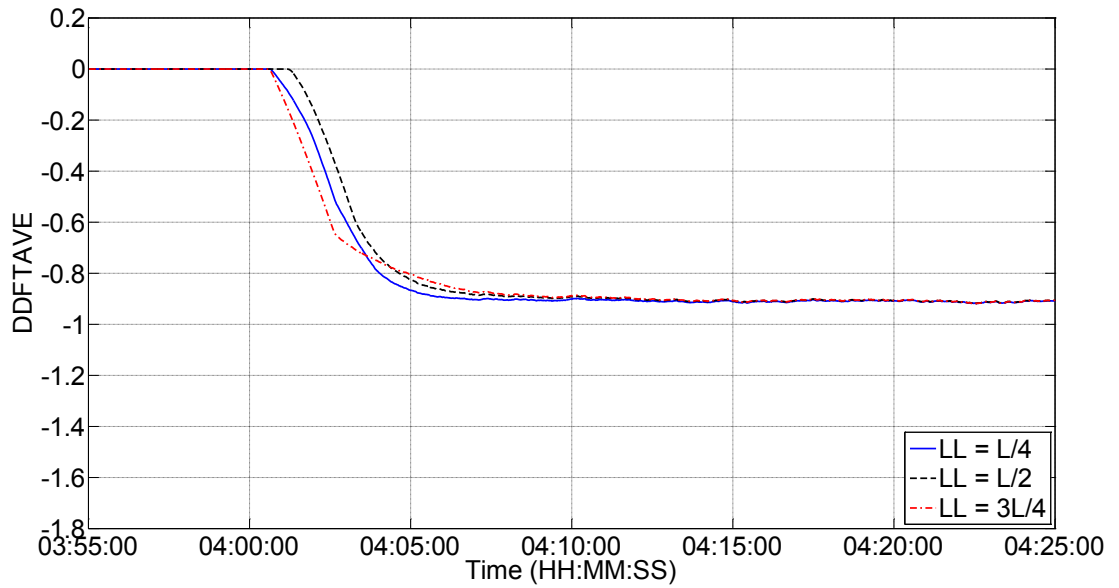


Figure 4-31. Non-dimensional time-averaged diagnostic flow DDFTAVE versus time for 1% noise levels, leak size of 30%, leaks at first quarter, midpoint and third quarter of pipeline length, flow increase transient,  $V_o = 2$  m/s,  $R = 2.20$ ,  $V_f = 3$  m/s, duration = 5s, TSV = 0.5.

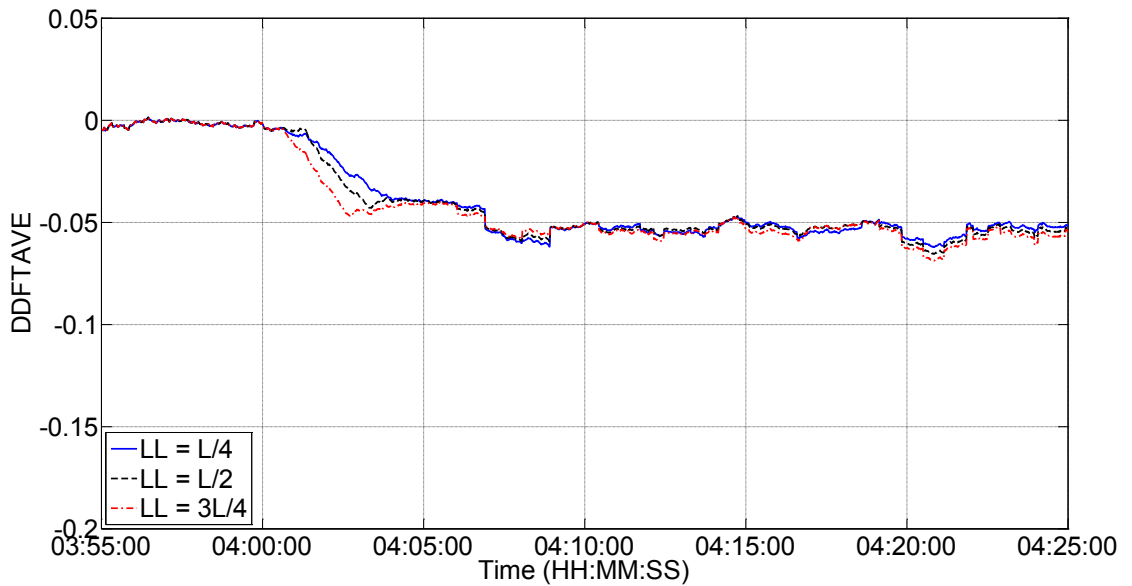


Figure 4-32. Non-dimensional time-averaged diagnostic flow DDFTAVE versus time for 1% noise levels, leak size of 1%, leaks at first quarter, midpoint and third quarter of pipeline length, flow increase transient,  $V_o = 0.30$  m/s,  $R = 0.49$ ,  $V_f = 0.45$  m/s, duration = 5 s, TSV = 0.5.

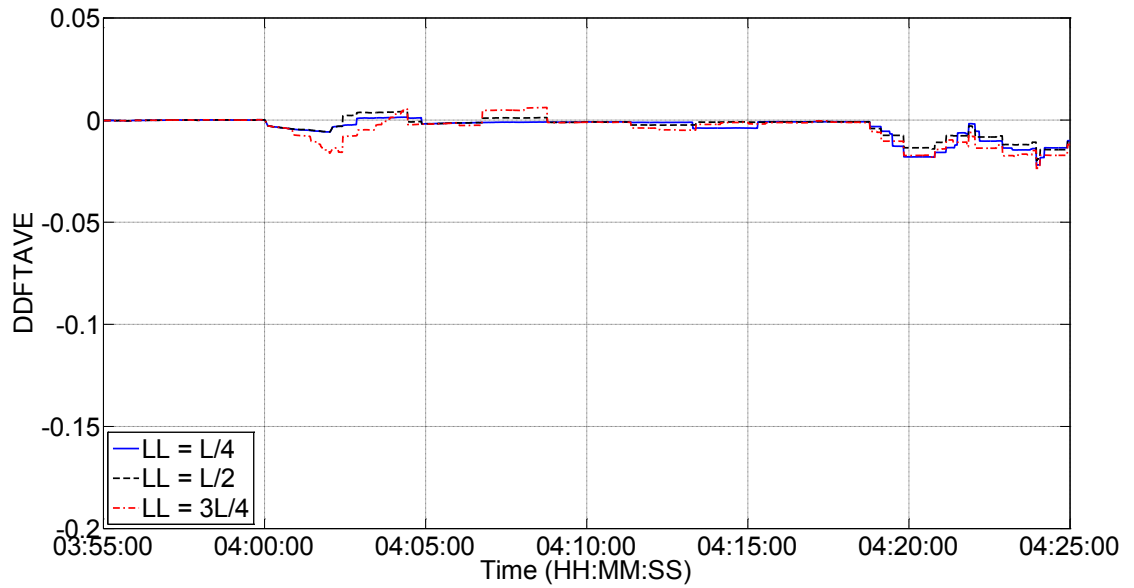


Figure 4-33. Non-dimensional time-averaged diagnostic flow DDFTAVE versus time for 1% noise levels, leak size of 1%, leaks at first quarter, midpoint and third quarter of pipeline length, flow increase transient,  $V_o = 2$  m/s,  $R = 2.20$ ,  $V_f = 3$  m/s, duration = 5 s, TSV = 0.5.

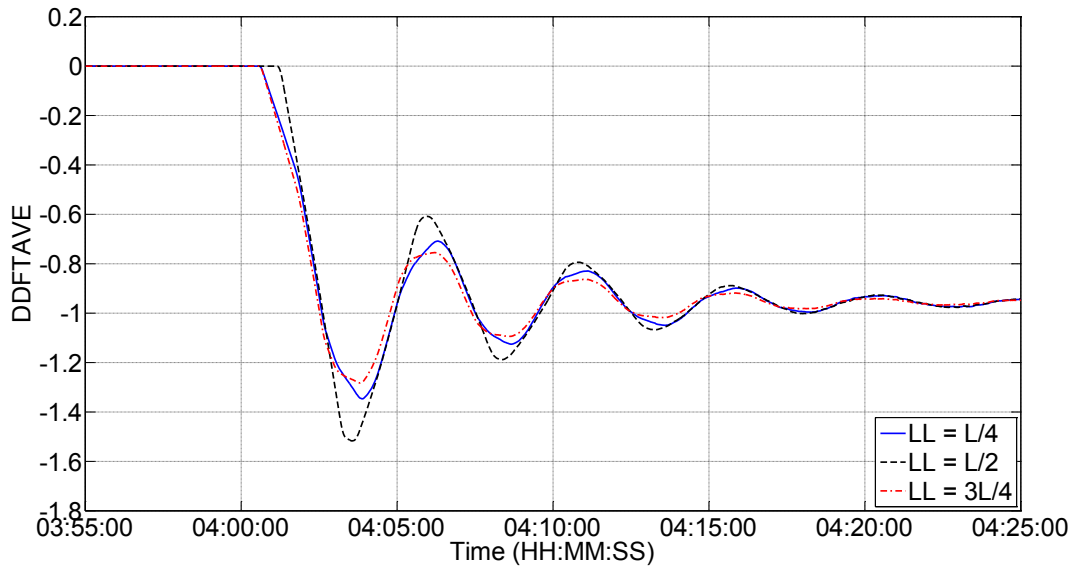


Figure 4-34. Non-dimensional time-averaged diagnostic flow DDFTAVE versus time for 1% noise levels, leak size of 30%, leaks at first quarter, midpoint and third quarter of pipeline length, flow decrease transient,  $V_o = 0.30$  m/s,  $R = 0.49$ ,  $V_f = 0.15$  m/s, duration = 5 s, TSV = 0.5.

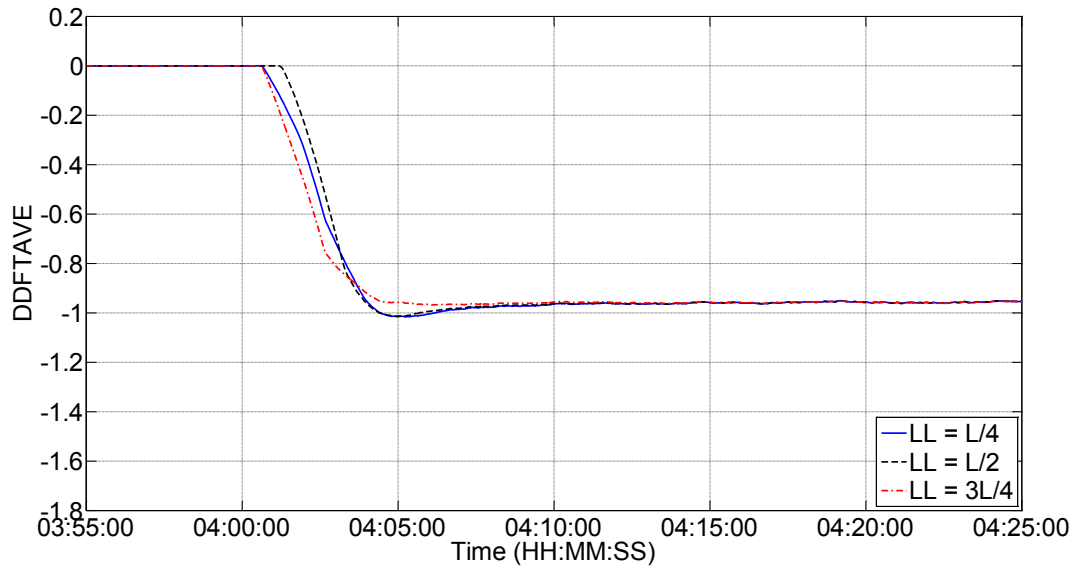


Figure 4-35. Non-dimensional time-averaged diagnostic flow DDFTAVE versus time for 1% noise levels, leak size of 30%, leaks at first quarter, midpoint and third quarter of pipeline length, flow decrease transient,  $V_o = 2$  m/s,  $R = 2.20$ ,  $V_f = 1$  m/s, duration = 5 s, TSV = 0.5.

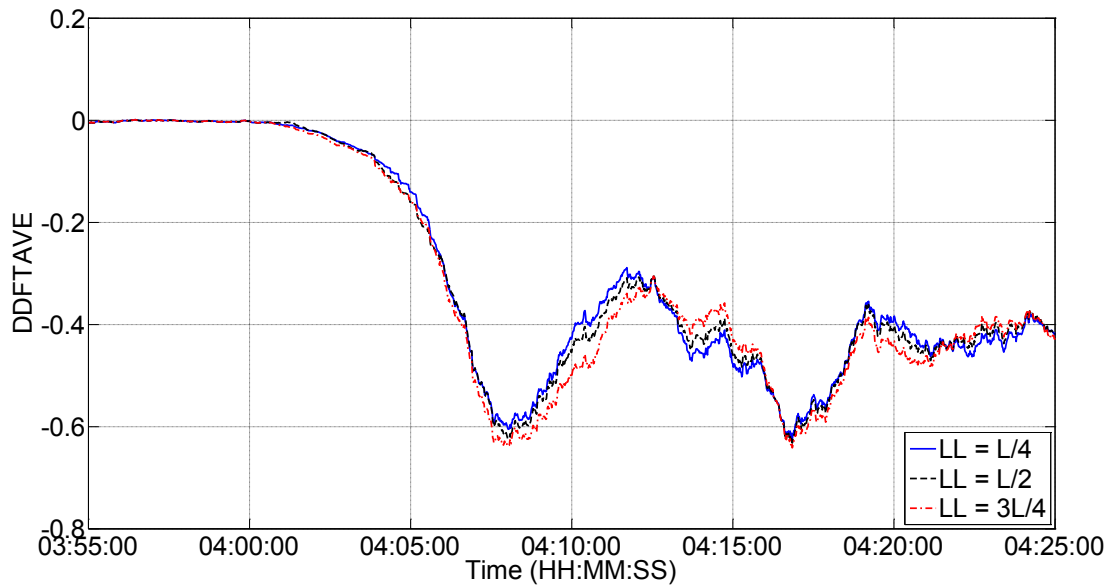


Figure 4-36. Non-dimensional time-averaged diagnostic flow DDFTAVE versus time for 1% noise levels, leak size of 1%, leaks at first quarter, midpoint and third quarter of pipeline length, flow decrease transient,  $V_o = 0.30$  m/s,  $R = 0.49$ ,  $V_f = 0.15$  m/s, duration = 5 s, TSV = 0.5.

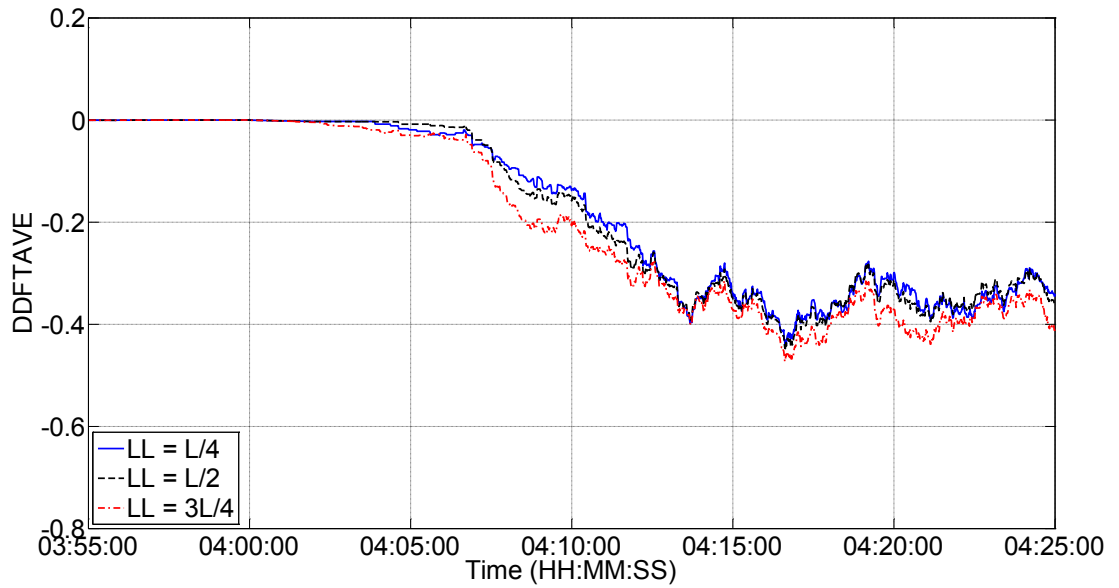


Figure 4-37. Non-dimensional time-averaged diagnostic flow DDFTAVE versus time for 1% noise levels, leak size of 1%, leaks at first quarter, midpoint and third quarter of pipeline length, flow decrease transient,  $V_o = 2$  m/s,  $R = 2.20$ ,  $V_f = 1$  m/s, duration = 5 s, TSV = 0.5.

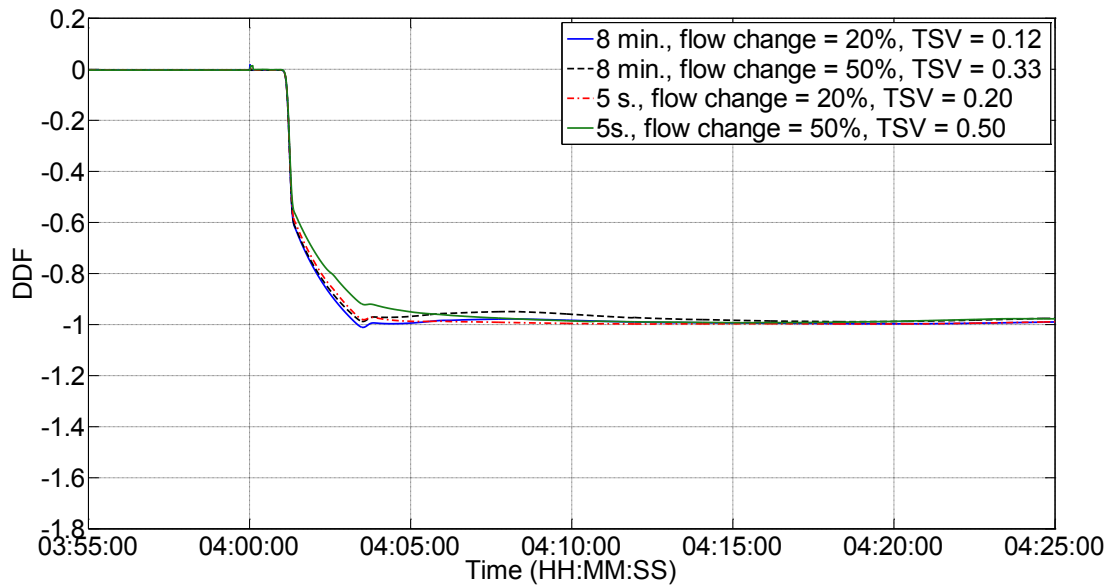


Figure 4-38. Non-dimensional diagnostic flow DDF versus time for perfect data, leak size of 1%, transient severities of 0.12, 0.33, 0.20 and 0.50, flow increase transient,  $R = 2.20$ ,  $V_o = 2$  m/s, leak at midpoint.

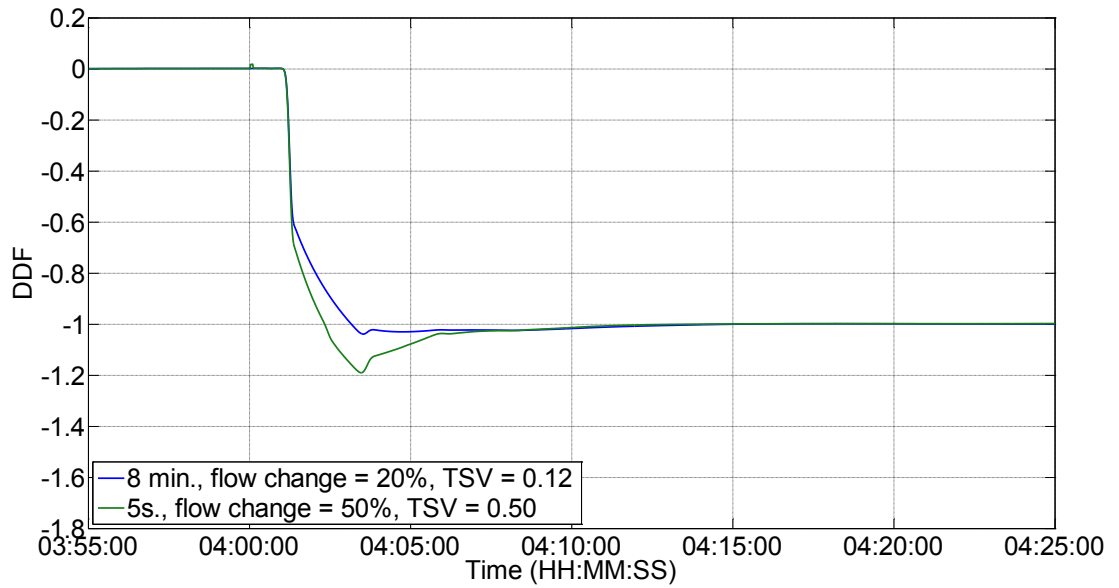


Figure 4-39. Non-dimensional diagnostic flow DDF versus time for perfect data, leak size of 1%, transient severities of 0.12 and 0.50, flow decrease transient,  $R = 2.20$ ,  $V_o = 2$  m/s, leak at midpoint.

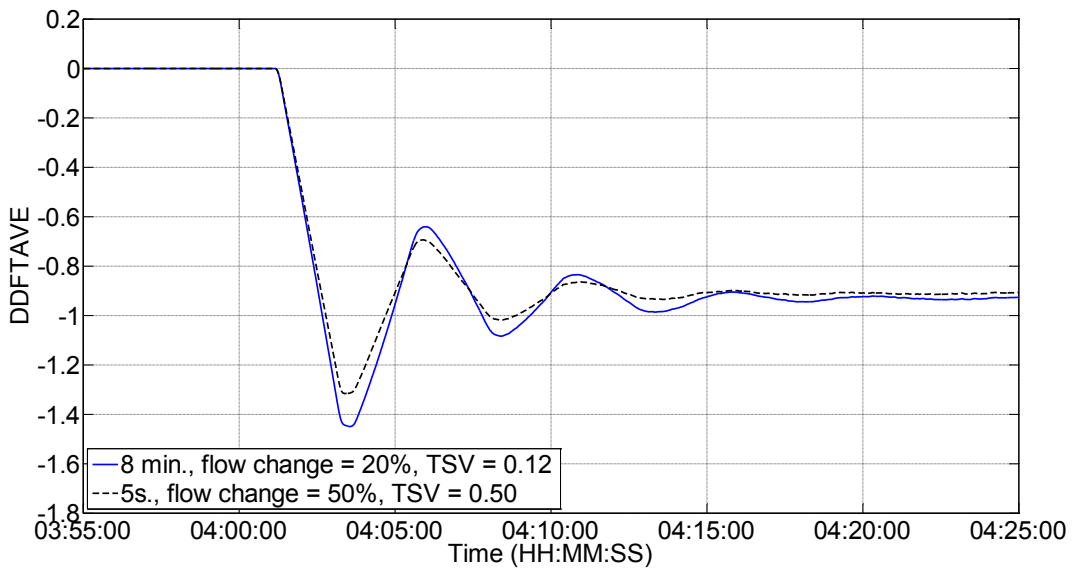


Figure 4-40. Non-dimensional time-averaged diagnostic flow DDFTAVE versus time for 1% noise levels, leak size of 30%, transient severities of 0.12 and 0.50, flow increase transient,  $R = 0.49$ ,  $V_o = 0.3$  m/s.

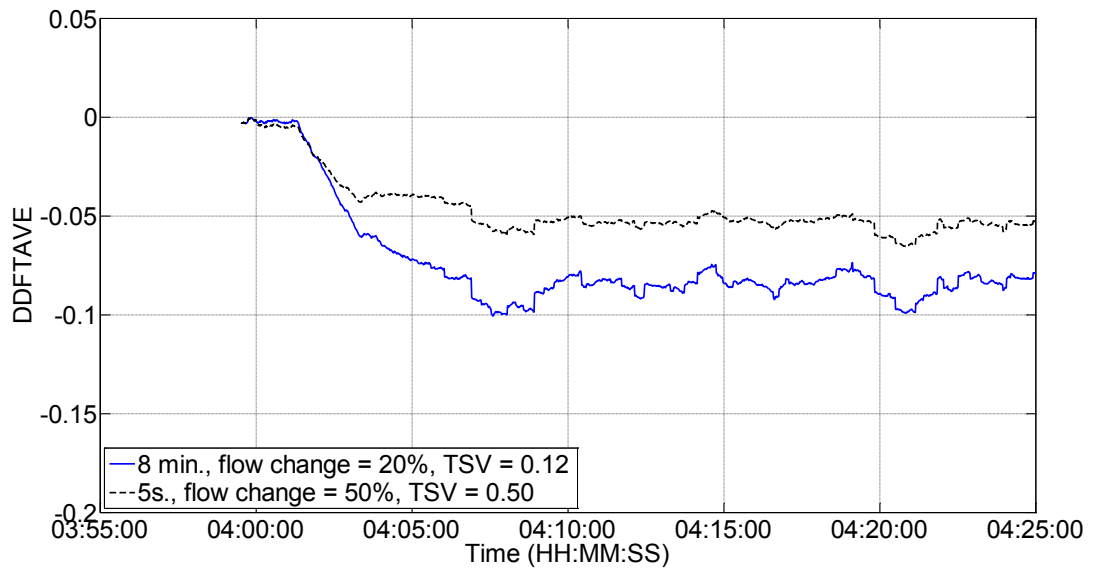


Figure 4-41. Non-dimensional time-averaged diagnostic flow DDFTAVE versus time for 1% noise levels, leak size of 1%, transient severities of 0.12 and 0.50, flow increase transient,  $R = 0.49$ ,  $V_o = 0.3$  m/s, leak at midpoint.

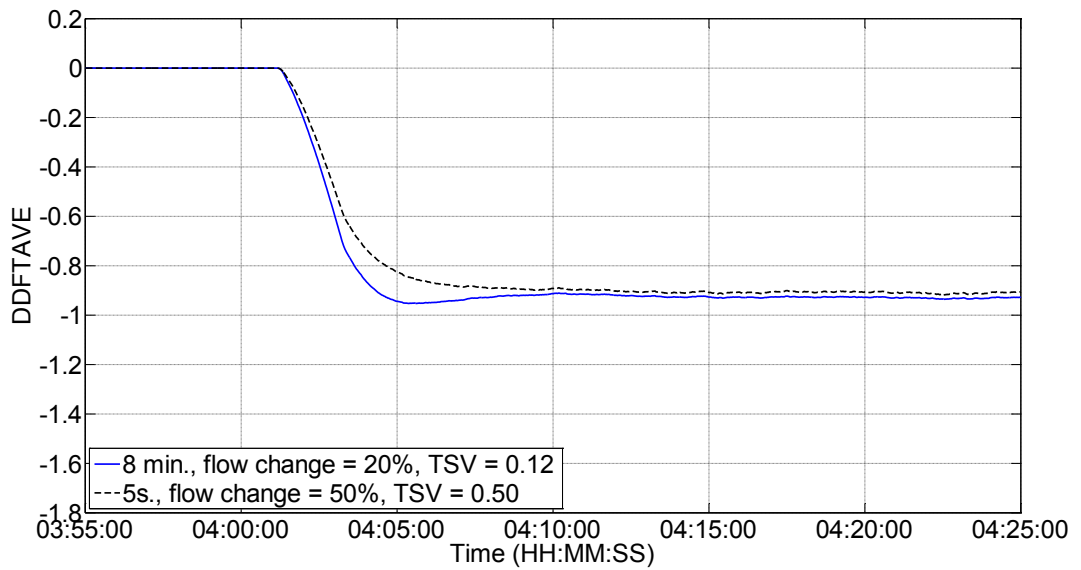


Figure 4-42. Non-dimensional time-averaged diagnostic flow DDFTAVE versus time for 1% noise levels, leak size of 30%, transient severities of 0.12 and 0.50, flow increase transient,  $R = 2.20$ ,  $V_o = 2$  m/s, leak at midpoint.

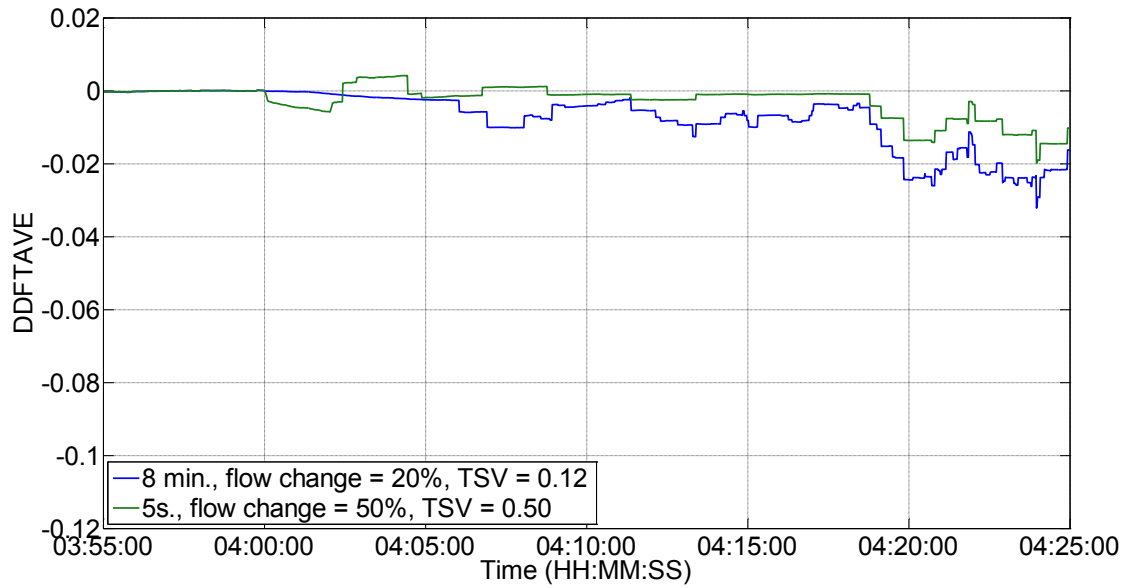


Figure 4-43. Non-dimensional time-averaged diagnostic flow DDFTAVE versus time for 1% noise levels, leak size of 1%, transient severities of 0.12 and 0.50, flow increase transient,  $R = 2.20$ ,  $V_o = 2$  m/s, leak at midpoint.

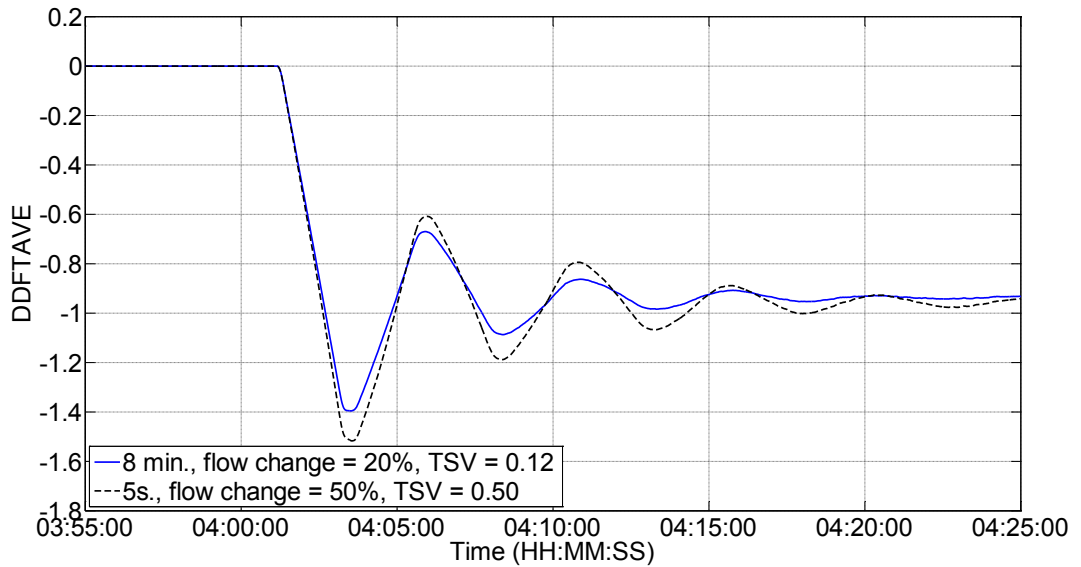


Figure 4-44. Non-dimensional time-averaged diagnostic flow DDFTAVE versus time for 1% noise levels, leak size of 30%, transient severities of 0.12 and 0.50, flow decrease transient,  $R = 0.49$ ,  $V_o = 0.3$  m/s, leak at midpoint.

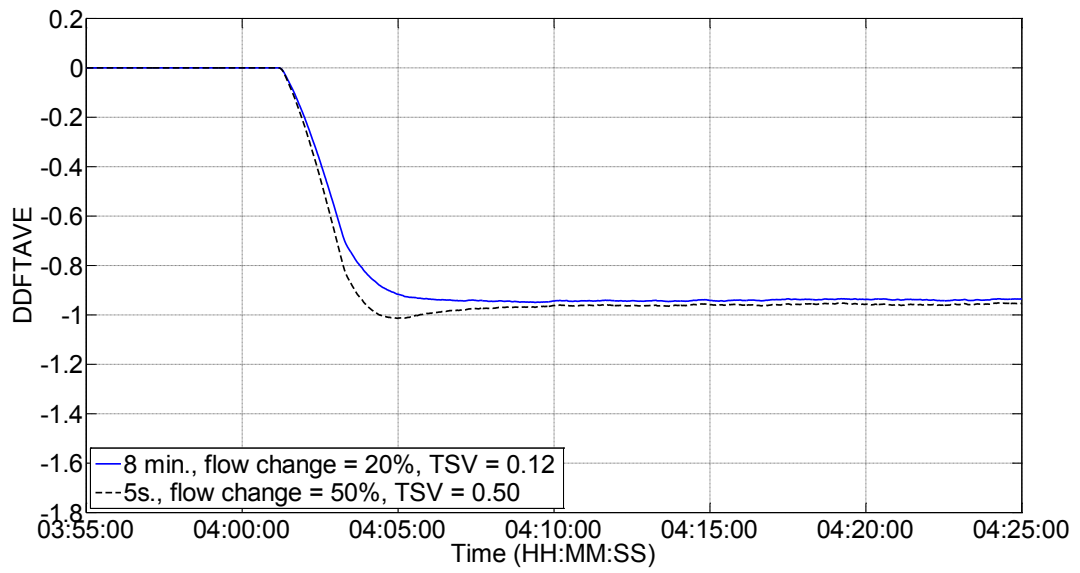


Figure 4-45. Non-dimensional time-averaged diagnostic flow DDFTAVE versus time for 1% noise levels, leak size of 30%, transient severities of 0.12 and 0.50, flow decrease transient,  $R = 2.20$ ,  $V_o = 2$  m/s, leak at midpoint.

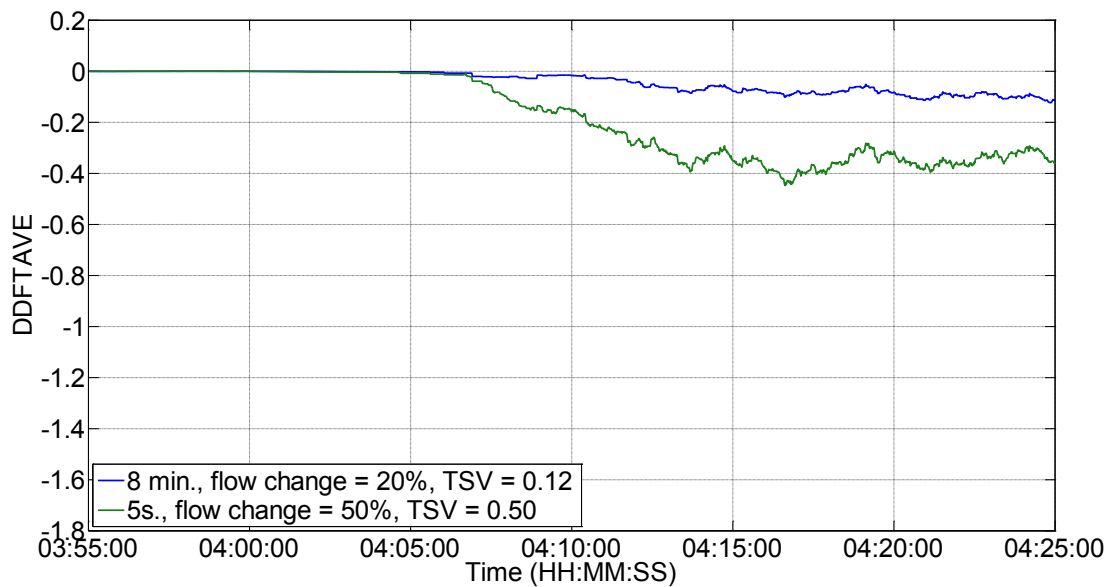


Figure 4-46. Non-dimensional time-averaged diagnostic flow DDFTAVE versus time for 1% noise levels, leak size of 1%, transient severities of 0.12 and 0.50, flow decrease transient,  $R = 2.20$ ,  $V_o = 2$  m/s, leak at midpoint.

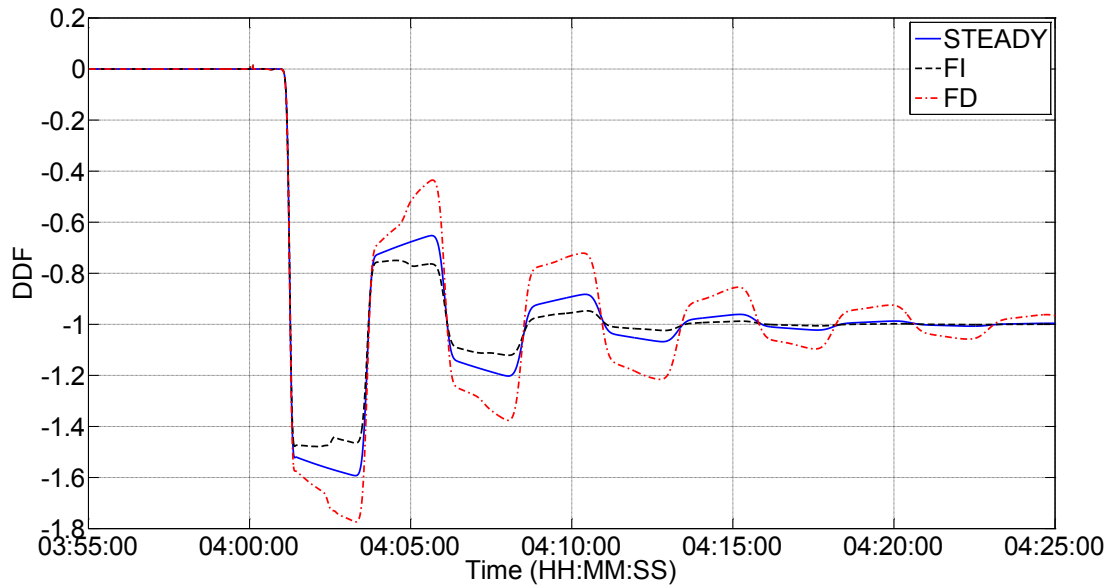


Figure 4-47. Non-dimensional diagnostic flow DDF versus time for perfect data, leak size of 1%, flow conditions of steady state, flow increase and flow decrease transients,  $V_o = 0.3$  m/s,  $R = 0.49$ , leak at midpoint, transient duration = 5 s, TSV = 0.5.

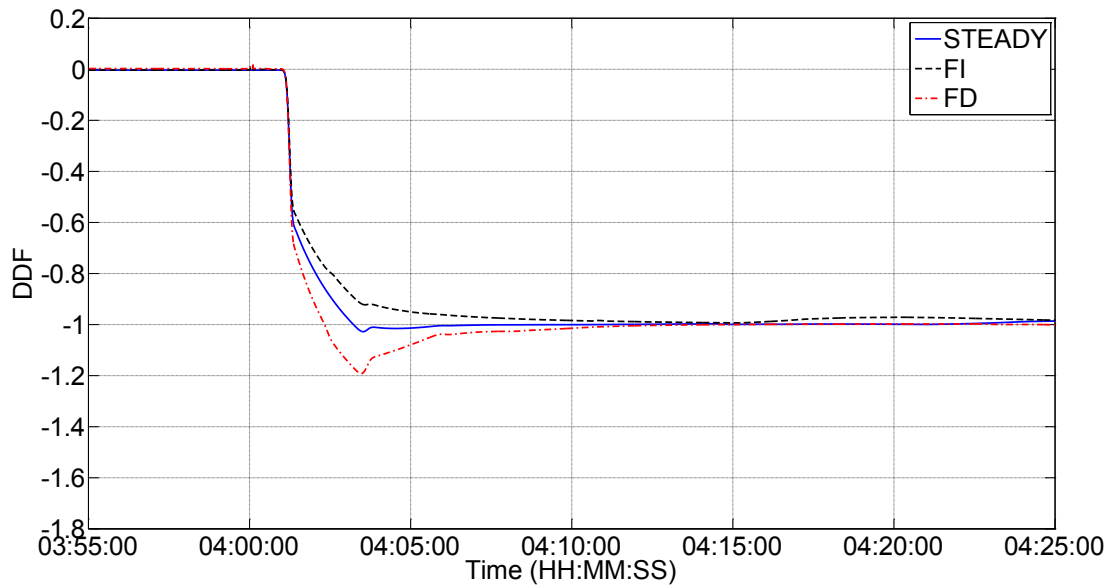


Figure 4-48. Non-dimensional diagnostic flow DDF versus time for perfect data, leak size of 1%, flow conditions of steady state, flow increase and flow decrease transients,  $V_o = 2$  m/s,  $R = 2.20$ , leak at midpoint, transient duration = 5 s, TSV = 0.5.

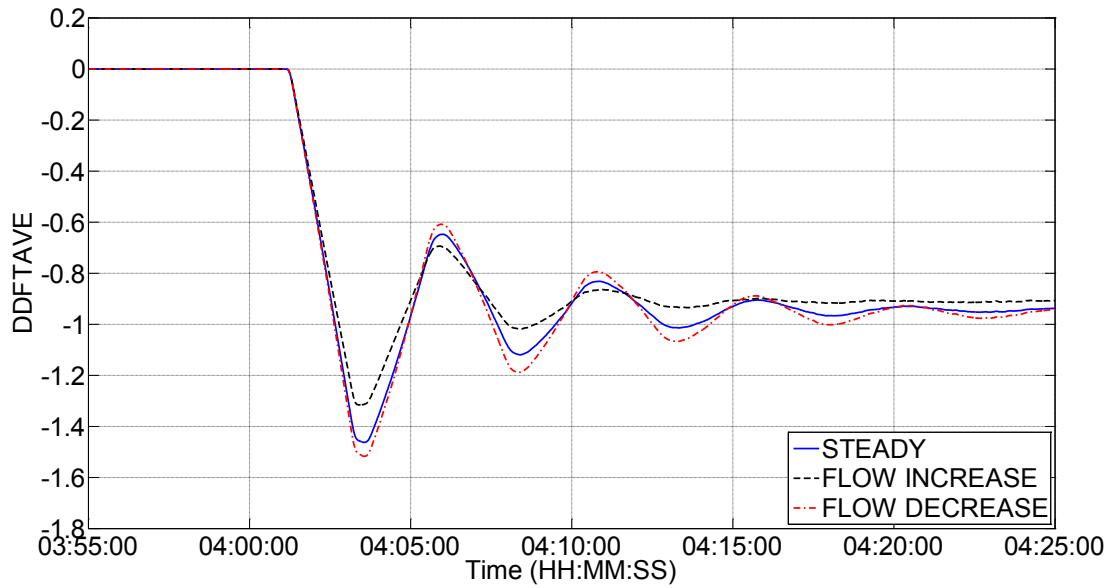


Figure 4-49. Non-dimensional time-averaged diagnostic flow DDFTAVE versus time for 1% noise levels, leak size of 30%, flow conditions of steady state, flow increase and flow decrease transients,  $V_o = 0.3$  m/s,  $R = 0.49$ , leak at midpoint.

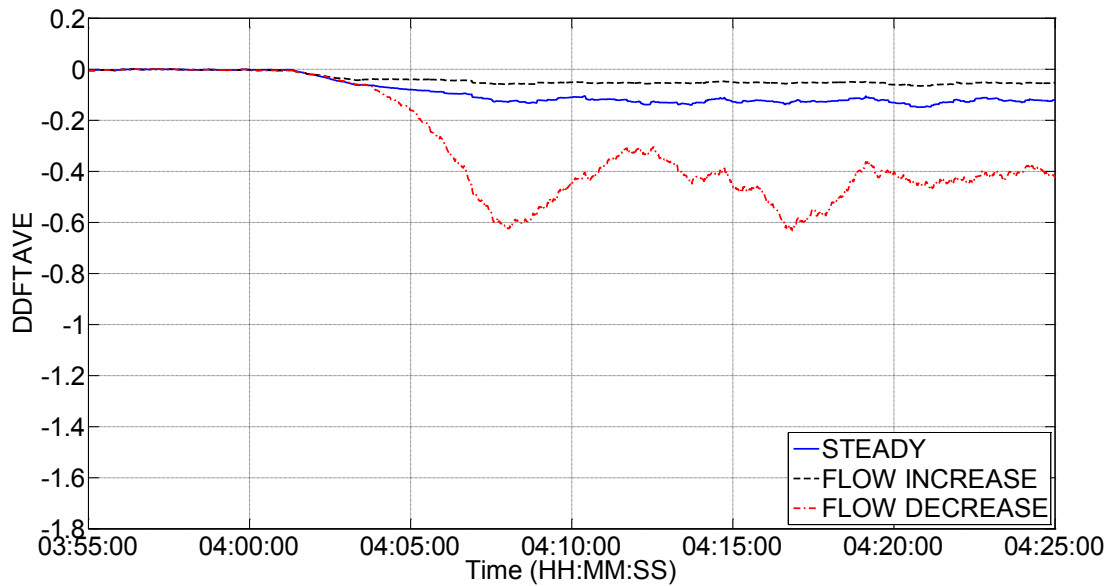


Figure 4-50. Non-dimensional time-averaged diagnostic flow DDFTAVE versus time for 1% noise levels, leak size of 1%, flow conditions of steady state, flow increase and flow decrease transients,  $V_o = 0.3$  m/s,  $R = 0.49$ , leak at midpoint.

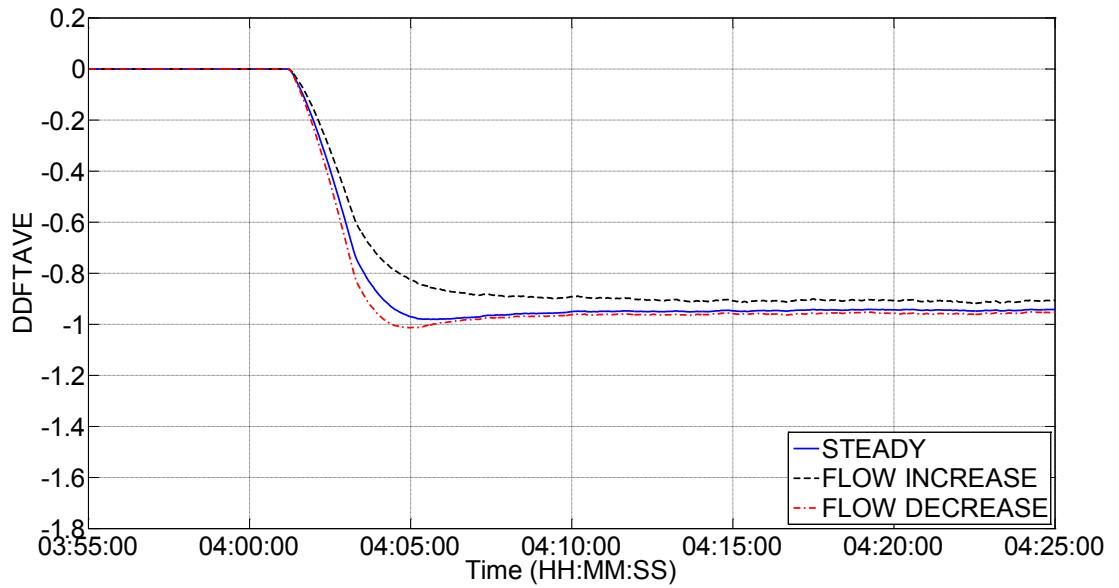


Figure 4-51. Non-dimensional time-averaged diagnostic flow DDFTAVE versus time for 1% noise levels, leak size of 30%, flow conditions of steady state, flow increase and flow decrease transients,  $V_o = 2$  m/s,  $R = 2.20$ , leak at midpoint.

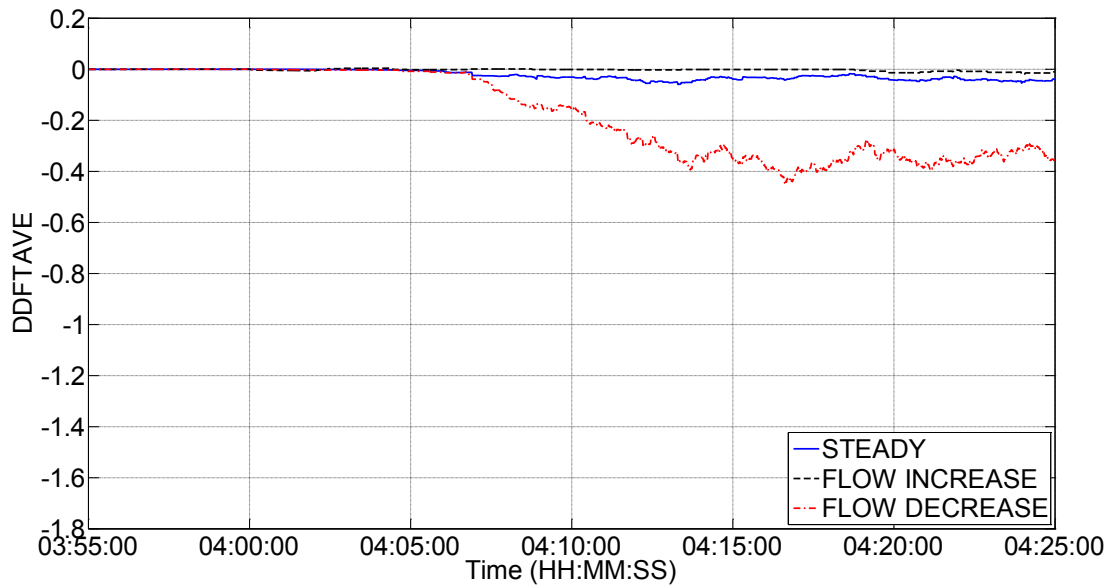


Figure 4-52. Non-dimensional time-averaged diagnostic flow DDFTAVE versus time for 1% noise levels, leak size of 1%, flow conditions of steady state, flow increase and flow decrease transients,  $V_o = 2$  m/s,  $R = 2.20$ , leak at midpoint.

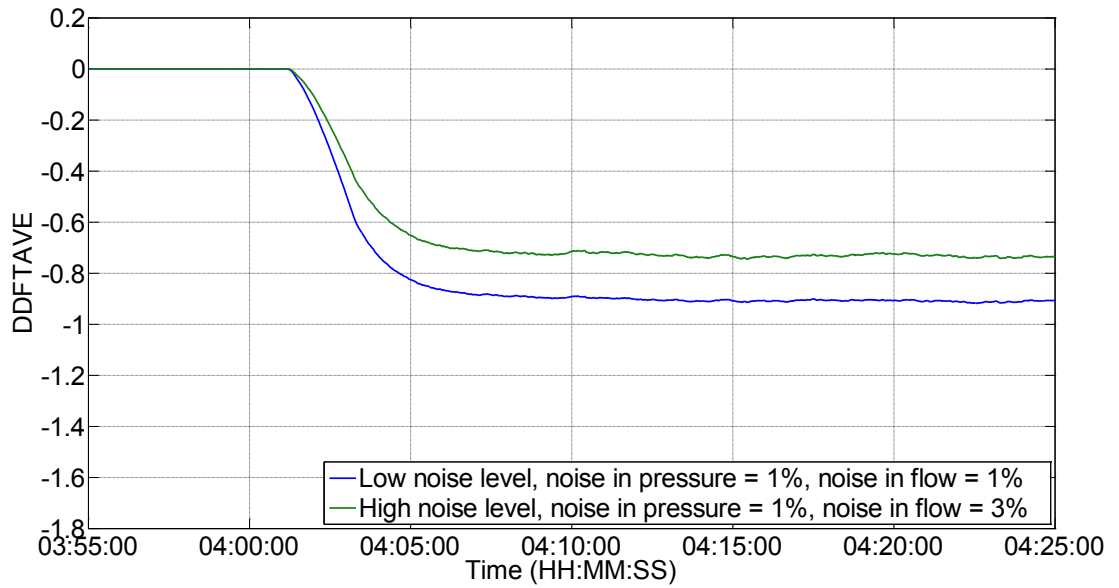


Figure 4-53. Non-dimensional time-averaged diagnostic flow DDFTAVE versus time for 1% and 3% noise levels of flow, leak size of 30%, flow increase transient,  $R = 2.20$ ,  $V_o = 2$  m/s,  $V_f = 3$  m/s, leak at midpoint, TSV = 0.5, duration = 5 s.

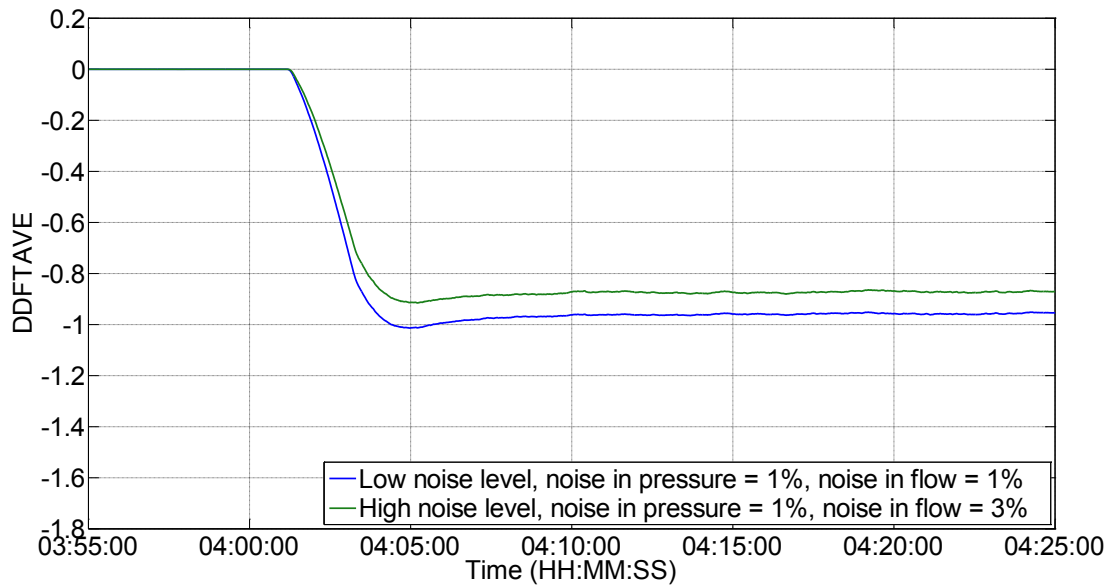


Figure 4-54. Non-dimensional time-averaged diagnostic flow DDFTAVE versus time for 1% and 3% noise levels of flow, leak size of 30%, flow decrease transient,  $R = 2.20$ ,  $V_o = 2$  m/s,  $V_f = 1$  m/s, leak at midpoint, TSV = 0.5, duration = 5 s.

## Chapter 5: Conclusions

Most small leaks (e.g. 1% leak rate or less) in oil pipelines are difficult to detect and yet they occur often (ADEC, 1999). The ability to detect leaks decreases significantly during transient flow conditions, which can sometimes be triggered by pipeline operations. Some errors may contribute to the degradation in leak detection, such as errors in measurements of instruments, acquisition and transmission of instrument data, modeling of pipeline and fluid properties, and the mathematical model during transient conditions. Column separation may also degrade leak detection. The enhancement of current leak detection systems is highly desirable because it may improve the response time to a leak event, thus reducing the environmental and economic losses. This study assessed quantitatively the sensitivity of a computer model based leak detection system to key variables related to the physical characteristics of the pipeline, the accuracy of instruments and the pipeline operating conditions.

This sensitivity study investigated the effect of the leak rate, the  $R$  factor, leak location, transient type and severity and flow noise level on the response of the leak detection system. The sensitivity study was conducted in two stages. First, using perfect data (i.e. noise free) generated by the Simulator model with the goal to identify the major factors impacting leak detection. Second, using noisy data (i.e. Simulator model data with the added Gaussian noise) in order to evaluate the effect of noise on the leak detection system which is a more realistic representation of actual pipelines. The sensitivity study identified the leak scenarios and variables in which leaks are harder to detect (i.e. smaller dimensionless diagnostic flow) in both steady and transient states.

The comparison of the sensitivity of the leak detection system to the key variables leads to the general trends of ranking of the studied variables and they are presented in the order of the highest sensitivity of the leak detection system. The leak detection system is more sensitive to  $R$  factor than to flow state, noise of instruments, and the transient severity. This trend agrees with the work of Liou

(1993), in which he ranked the  $R$  factor with a high importance above other variables. Leak location seems to have a much smaller impact on the leak detection system.

### **5.1 Sensitivity to Leak Rate and Data Noise**

Leak detection is not sensitive to any of the leak rates tested only when using perfect or noise-free data. It is equally easy to detect a leak for leak rates of 1% to 30%. This is valid for the wide range of  $R$  factors from 0.49 to 3.08, the three leak locations and the three flow states tested. However, this is not necessarily indicative of what is being observed with leak detection in a real pipeline system because real pipelines often experience some noise level in their instruments. It is generally harder to detect a leak of the same size when data from measurement instruments is noisy. The effect of the noise is less for flow decrease transient events than for flow increase transient events. A flow decrease transient flow condition is more tolerant of data noise than a flow increase condition. Similarly, a pipeline system with low  $R$  factor is more tolerant of data noise than a system with large  $R$  factor. The tests with noisy data showed that leak detection is sensitive to leak rate. It is easier to detect a large leak with instrument noise. The leak signal is almost masked completely to the leak detection system by instrument noise for leaks of any leak rate. However, for a leak with a 30% leak rate the noise level is small compared to the large leak rate. Higher noise level in the flow measurement data masks more of the leak signal and degrades leak detectability. Leak detection is very sensitive to noise level. The uncertainties in pressure and flow measurements determine the data noise.

### **5.2 Sensitivity to R Factor**

It was found that leak detection is sensitive to  $R$  factor. The range of  $R$  factor tested is from 0.49 to 3.08, which is typical in pipeline operations. At low  $R$  factors the pipeline system behaves similar to a damped oscillator, the flow is inertia dominated, in which the transient wave caused by a leak is attenuated slowly. For pipelines with large values of  $R$ , the flow is friction dominated, thus the transient wave caused by a leak is attenuated more rapidly. Therefore, a leak is generally easier to detect in pipeline systems with a low  $R$  factor than those

with a large  $R$  factor. Five variables are the components of the  $R$  factor: spacing between measurement instruments, pipeline diameter, initial velocity, friction factor and acoustic wave speed. Therefore, leak detection is sensitive to these variables. Pipe diameter, length, wall roughness, temperature, pressure, liquid density, fluid viscosity and flow rate determine the friction factor. Pipe diameter, wall thickness, Young's modulus of the pipe material, Poisson's ratio, operating pressure and temperature, liquid mass density and bulk modulus determine the acoustic wave speed.  $R$  factor is an important parameter to be considered when exploring measures to improve leak detection on different pipeline systems. Measures in pipeline systems with low  $R$  factor improve leak detection.  $R$  factor is also important when assessing the impact of noise and transients on leak detection.

### **5.3 Sensitivity to Flow State and Transient Severity**

Leak detection is sensitive to flow state. Generally speaking, a leak would be detected most easily during a flow decrease transient event, compared to steady state or a flow increase transient event, with the latter being the most difficult operating condition for leak detection. This is because the leak caused transient wave attenuates more slowly when flow is lower. Therefore, leak detection is often degraded when the pipeline is experiencing a transient event which is causing the flow to increase, but not when the flow is decreasing. The flow increase transient degradation is more severe when a leak occurs in a pipeline system with a large  $R$  factor. A pipeline system with a low  $R$  factor can better tolerate a flow increase transient degradation. Leak detection is sensitive to transient severity. It may be easier to detect a leak during a mild transient than a more severe transient (with transient severity of 0.5) for flow increase conditions. It may be easier to detect a leak during severe flow decrease transient events compared to mild events.

### **5.4 Sensitivity to Leak Location**

Leak location can affect leak detection but the impact is not significant. A leak detection system responds to a leak at midpoint and non-midpoint differently because the leak signal can arrive at the measurement instruments located at the

pipe ends at different times. For a leak occurring at a non-midpoint of the pipeline segment, the leak signal arrives at the nearest instrument earlier than a midpoint leak. Thus, the leak detection system will detect the non-midpoint leak earlier and start to respond by deviating diagnostic flow from zero. However, the magnitude of diagnostic flow is only about half of the final detectable leak rate until the transient signal arrives at the other instrument at the far end of the pipeline. For the midpoint leak, two instruments capture the leak signal at the same time. The starting time of diagnostic flow generation is later, but the final detectable leak rate is reached earlier than the non-midpoint leak. If the diagnostic flow generated by one instrument is large enough to exceed the threshold, a leak at a non-midpoint would be detected earlier than one at midpoint locations. Otherwise, a midpoint leak would be detected earlier. Since a leak wave travels at acoustic speed, the time difference discussed above is not significant. Based on the typical range of real pipeline segment lengths from 9 km to 120 km and assuming a wave speed of 1,000 m/s, the time difference between detecting a midpoint leak and a non-midpoint leak would range from 5 seconds to 1 minute.

## **5.5 Significance**

This sensitivity study assesses the leak detection capability of the computer model based leak detection system (i.e. magnitude of the dimensionless diagnostic flow) in response to variations in key variables. Impacts of each variable on the performance of the leak detection system are quantified. This study identifies challenging leak scenarios with system degradation in which the dimensionless diagnostic flow is small (i.e. pipeline with the  $R$  factor of 2.20 or greater noisy data and a small leak rate; flow increase transient events with noisy data and a small leak rate). The study also identifies general trends of the major variables affecting this leak detection system (i.e. the  $R$  factor has a larger impact on the system). These results provide an increased understanding of how future efforts could be focused on three major variables:  $R$  factor, Flow State and Transient Severity (reducing the complexity of analysis by fixing input variables that have no effect on leak detection with a specified value). It also helps prioritizing future improvement on the computer model, instruments, or the SCADA system in pipeline systems with low  $R$  factor. The results of this study

could serve as a guideline to estimate the leak rate values and detection times that could be expected in the real pipelines. In the baseline prepared in this study, the effect of other variables could be tested in future research work: instrument type, location and amount, polling cycle and time skew. The simplifications and assumptions of this study could be progressively reduced in future work, superimposing real pipeline conditions on the baseline (e.g. pipeline with elevation changes).

## References

- Alaska Department of Environmental Conservation, ADEC. 2012. Pipeline Leak Detection Technology 2011 Conference Report.
- Alaska Department of Environmental Conservation, ADEC. 1999. Technical Review of Leak Detection Technologies, Volume I, Crude Oil Transmission Pipelines.
- Alberta Energy Regulator. 2013. Report 2013-B: Pipeline Performance in Alberta, 1990–2012.
- Al-Khomairi, A., 2008. Leak Detection in Long Pipelines Using the Least Squares Method. *Journal of Hydraulic Research*. 46 (3), 392-401.
- American Petroleum Institute, 2002. API 1130: Computational Pipeline Monitoring for Liquid Pipelines, Second Edit. API Publishing Services, Washington, D.C., United States.
- American Water Works Association, 1987. Leaks in Water Distribution Systems: A Technical/Economic Overview. Denver, Colorado, United States.
- Atherton, D., Morton, K., Mergelas, B., 2000. Detecting Breaks in Prestressing Pipe Wire. *Journal of the American Water Works Association, AWWA*. 92 (7), 50-56.
- Babbitt, H.E., 1920. The detection of leaks in underground pipes. *Journal of the American Water Works Association, AWWA*. 7, 589-595.
- Balda, K.V., 2012. An application of the volumetric balance and transient flow modeling for leak detection in liquid pipelines. University of Oklahoma. Norman, Oklahoma, United States.

- Bergant, A., Simpson, A.R., Tijsseling, A.S., 2006. Water Hammer With Column Separation: A Historical Review. *J. Fluids and Structure*. 22, 135.
- Bergeron, L., 1950. *Du Coup de Bélier en Hydraulique - Au Coup de Foudre en Electricité.* (Waterhammer in hydraulics and wave surges in electricity.) Paris: Dunod (in French). English translation by ASME Committee, New York. John Wiley & Sons. 1961.
- Black, P., 1992. A Review of Leak Detection Technologies Pipeline System - Fluid Mechanics of Its Application. Kluwer Academic Publishers, pp. 287-298.
- Bustnes, T.E., Rousselet, M., Berland, S., 2011. Leak detection performance of a commercial Real Time Transient Model for Troll oil pipeline, PSIG 1114, in: Presentation at the Pipeline Simulation Interest Group Annual Meeting. Pipeline Simulation Interest Group. Napa Valley, California, United States. pp. 1-16.
- Canadian Energy Pipeline Association. 2014. About pipelines: Why pipelines are needed; Economic benefits of pipelines.
- Canadian Standards Association. 2011. CAN/CSA-Z662-11, Oil and Gas Pipeline Systems.
- C-FER Technologies, 2013. Evaluation of Leak-Detection Technologies. Pipelines International. June.
- Colombo, A.F., Lee, P., Karney, B.W., 2009. A selected literature review of transient-based leak detection methods. *Journal of Hydro-environment Research*. 2, 212-227.
- DNV GL, 2012. Stoner Pipeline Simulator 9.9.0 Help and Reference Manual. Mechanicsburg, Pennsylvania, United States.

Echo-logics, 2006. Acoustic Leak Detection.

Eiswirth, M., Burn, L.S., 2001. New Methods for Defect Diagnosis of Water Pipelines, In: 4th International Conference on Water Pipeline Systems. York, United Kingdom.

Framatome ANP GmbH, 1998. LEOS – Leak Detection and Location System.

Fuchs, H. and Riehle, R., 1991. Ten Years of Experience With Leak Detection by Acoustic Signal Analysis. Applied Acoustics, 33(1), 1-19. Elsevier Science Publishers Ltd., England. 1991.

Furness, R., van Reet, J., 1998. Pipe Line Rules of Thumb Handbook. Gulf Publishing Company, Houston, Texas, United States.

Geiger, G., 2006. State-of-the-Art in leak detection and localization. Oil Gas European Magazine. 32,4, 193-198.

Grobwig, S. et al, 2001. Distributed Fibre Optical Temperature Sensing Technique – A Variable Tool for Monitoring Tasks, in: Proceedings of the 8<sup>th</sup> International Symposium on Temperature and Thermal Measurements in Industry and Science.

Hargesheimer, E.E., 1985. Identifying Water Main Leaks With Trihalomethane Tracers. Journal of the American Water Works Association. 77 (11), 71-75.

Lay-Ekuakille, A., Vergallo, P., Trotta, A., 2010. Impedance Method for Leak Detection in Zigzag Pipelines. Measurement Science Review, 10 (6), 209-213.

- Lee, P.J., Lambert, M.F., Simpson, A.R., Vitkovsky, J.P., Liggett, J., 2006. Experimental Verification of the Frequency Response Method for Pipeline Leak Detection. *Journal of Hydraulic Research*. 44 (5), 693-707.
- Liggett, J.A., Chen, L.C., 1994. Inverse Transient Analysis in Pipe Networks. *J. Hydraul. Eng.* 120 (8), 934-955.
- Liou, J.C.P., 1993. Pipeline Variable Uncertainties And Their Effects on Leak Detectability. American Petroleum Institute Publication 1149.
- Liou, J.C.P., Tian, J., 1995. Leak Detection – Transient Flow Simulation Approaches. *Journal of Energy Resources Technology, American Society of Mechanical Engineers*. 117, 243-248.
- Misiunas, D., Vitkovsky, J.P., Olsson, G., Simpson, A.R., Lambert, M.F., 2005. Pipeline Break Detection Using Pressure Transient Monitoring. *Journal of Water Resources Planning and Management*, 131 (4), 316-325.
- National Association of Corrosion Engineers. 2013. Managing corrosion of pipelines that transport crude oils. *Pipeline and Gas Journal*. 240 (3).
- O'Haver, T., 2014. e-Page: Signals and Noise. Department of Chemistry and Biochemistry, University of Maryland, United States.
- Pudar, R.S., Liggett, J.A., 1992. Leaks in Pipe Networks. *J. Hydraul. Eng.* 118 (7), 1031-1046.
- Silva, R., Buiatta, C., Cruz, S., Pereira, J., 1996. Pressure Wave Behaviour and Leak Detection in Pipelines. *Computers and Chemical Engineering*. 20, S491-S496.

- University of Alberta, Department of Civil and Environmental Engineering. 2014. e-Page: Undergraduate Research looks at Detecting Pipeline Leaks. Civil Engineering News, August.
- United States Department of Transportation. 2007. Leak Detection Technology Study, For PIPES Act, H.R.5782.
- United States National Transportation Safety Board. 2010. "Pipeline Accident Report, PAR1201, July 25, 2010".
- Vinh, P., 2012. Adding Value to CPM Testing, in: 2012 American Petroleum Institute Pipeline Conference and Cybernetics Symposium.
- Vitkovsky, J.P., Lambert, M.F., Simpson, A.R., Liggett, J.A. 2007. Experimental Observation and Analysis of Inverse Transients for Pipeline Leak Detection. Journal of Water Resources Planning and Management, ASCE, 133 (6), 519-530.
- Weil, G.J., Graf, R.J., Forister, L.M., 1994. Investigations of Hazardous-Waste Sites Using Thermal Air and Ground-Penetrating Radar. Photogrammetric Engineering and Remote Sensing 60 (8), 999-1005.

Appendix A. Sample Check List of Tests.

Run ID: 164-FD-V1to0.5-SS-P-UR30-LL05		Date: April 28, 2014	
Steady / Transient		FD	
V <sub>o</sub>	1 m/s	R factor	1.26
		Leak rate	30 %
V <sub>final</sub>	0.5 m/s	Transient duration	SS
		TSV	0.5
Perfect data / Noise		Perfect data	
Additional comments			
In Simulator:			
<i>Check the following in inprep file</i>			
QRATE of leak external	14 of 5.715 m3/hr/min		
<i>Check the following in intran file</i>			
Upstream boundary	AA_TK1:SQ = — m3/hr	AA_TK1:SP = 261.365	PSIG
Downstream boundary	EE_DEL:SQ = -1560.635 m3/hr	EE_DEL:SP = —	PSIG
Start from archive	steady.ark		
RAMP for transient	RAMP EE_DEL:SQ from -1560.635 m3/hr to -780.3175 m3/hr during 5 seconds		
Transient start time	04:00:00		
scada_rtugen	scada_rtugen.inc		
Leak external	BB_LK1	Leak rate	968.1305 m3/hr
		Start time	04:00:00
RTUDATA	sim1a.dat; rtudata_leak.dat		
MBS:			
<i>Check the following in inprep file</i>			
data.type	Perfect		
SELECT (YES or NO)	PDF	NO	BMC NO SPANS NO
<i>Check the following in intran file</i>			
BEGIN Tolerance	PRES.TOLER = 0	PSIG	TEMP.TOLER = 0
RTU.FILES	sim1a.dat; rtudata_leak.dat		
Start from archive	bal.ark		
Repeatability	FLOW_UNCERT (mbs.inprep) = 0	G.P.REP = 0	PSIG
Time Error Bound	G.Q.TEB = 0	min	G.P.TEB = 0 min
Repeatability decay	G.Q.RDR = 0	m3/hr/min	G.P.RDR = 0 PSIG/min
Rate bound (mbs.inprep)	G.Q.RB = 60,000	m3/hr/min	G.P.RB = 6,000 PSIG/min

Appendix B. List of tests

Steady runs (ST), Flow Increase (FI), Flow Decrease (FD)

Counter	Changed variable and value	Flow state	Velocity Vo [m/s]	Velocity Vf [m/s]	Friction factor	Reynolds number	R factor	Pipe diameter [in]	Pipe length [km]	Vo/2a	Lf/D	LR (%)	LL	TSV	D
1	LR = 1%	ST	0.3	-	0.0218	41865	0.49	30	150	0.0001114	4401	1	0.5	-	-
2	LR = 10%	ST	0.3	-	0.0218	41865	0.49	30	150	0.0001114	4401	10	0.5	-	-
3	LR = 20%	ST	0.3	-	0.0218	41865	0.49	30	150	0.0001114	4401	20	0.5	-	-
4	LR = 30%	ST	0.3	-	0.0218	41865	0.49	30	150	0.0001114	4401	30	0.5	-	-
5	LR = 1%	ST	1.0	-	0.0168	140,000	1.26	30	150	0.0003712	3392	1	0.5	-	-
6	LR = 10%	ST	1.0	-	0.0168	140,000	1.26	30	150	0.0003712	3392	10	0.5	-	-
7	LR = 20%	ST	1.0	-	0.0168	140,000	1.26	30	150	0.0003712	3392	20	0.5	-	-
8	LR = 30%	ST	1.0	-	0.0168	140,000	1.26	30	150	0.0003712	3392	30	0.5	-	-
9	LR = 1%	ST	2.0	-	0.0147	280,000	2.21	30	150	0.0007424	2972	1	0.5	-	-
10	LR = 10%	ST	2.0	-	0.0147	280,000	2.21	30	150	0.0007424	2972	10	0.5	-	-
11	LR = 20%	ST	2.0	-	0.0147	280,000	2.21	30	150	0.0007424	2972	20	0.5	-	-
12	LR = 30%	ST	2.0	-	0.0147	280,000	2.21	30	150	0.0007424	2972	30	0.5	-	-
13	LR = 1%	ST	3.0	-	0.0137	420,000	3.08	30	150	0.0011136	2766	1	0.5	-	-
14	LR = 10%	ST	3.0	-	0.0137	420,000	3.08	30	150	0.0011136	2766	10	0.5	-	-
15	LR = 20%	ST	3.0	-	0.0137	420,000	3.08	30	150	0.0011136	2766	20	0.5	-	-
16	LR = 30%	ST	3.0	-	0.0137	420,000	3.08	30	150	0.0011136	2766	30	0.5	-	-
17	LR = 1%	ST	0.3	-	0.0218	41865	0.49	30	150	0.0001114	4401	1	0.25	-	-
18	LR = 10%	ST	0.3	-	0.0218	41865	0.49	30	150	0.0001114	4401	10	0.25	-	-
19	LR = 20%	ST	0.3	-	0.0218	41865	0.49	30	150	0.0001114	4401	20	0.25	-	-
20	LR = 30%	ST	0.3	-	0.0218	41865	0.49	30	150	0.0001114	4401	30	0.25	-	-
21	LR = 1%	ST	0.3	-	0.0218	41865	0.49	30	150	0.0001114	4401	1	0.75	-	-
22	LR = 10%	ST	0.3	-	0.0218	41865	0.49	30	150	0.0001114	4401	10	0.75	-	-
23	LR = 20%	ST	0.3	-	0.0218	41865	0.49	30	150	0.0001114	4401	20	0.75	-	-

Counter	Changed variable and value	Flow state	Velocity Vo [m/s]	Velocity Vf [m/s]	Friction factor	Reynolds number	R factor	Pipe diameter [in]	Pipe length [km]	Vo/2a	Lf/D	LR (%)	LL	TSV	D
24	LR = 30%	ST	0.3	-	0.0218	41865	0.49	30	150	0.0001114	4401	30	0.75	-	-
25	LR = 1%	ST	1.0	-	0.0168	140,000	1.26	30	150	0.0003712	3392	1	0.25	-	-
26	LR = 10%	ST	1.0	-	0.0168	140,000	1.26	30	150	0.0003712	3392	10	0.25	-	-
27	LR = 20%	ST	1.0	-	0.0168	140,000	1.26	30	150	0.0003712	3392	20	0.25	-	-
28	LR = 30%	ST	1.0	-	0.0168	140,000	1.26	30	150	0.0003712	3392	30	0.25	-	-
29	LR = 1%	ST	1.0	-	0.0168	140,000	1.26	30	150	0.0003712	3392	1	0.75	-	-
30	LR = 10%	ST	1.0	-	0.0168	140,000	1.26	30	150	0.0003712	3392	10	0.75	-	-
31	LR = 20%	ST	1.0	-	0.0168	140,000	1.26	30	150	0.0003712	3392	20	0.75	-	-
32	LR = 30%	ST	1.0	-	0.0168	140,000	1.26	30	150	0.0003712	3392	30	0.75	-	-
33	LR = 1%	ST	2.0	-	0.0147	280,000	2.21	30	150	0.0007424	2972	1	0.25	-	-
34	LR = 10%	ST	2.0	-	0.0147	280,000	2.21	30	150	0.0007424	2972	10	0.25	-	-
35	LR = 20%	ST	2.0	-	0.0147	280,000	2.21	30	150	0.0007424	2972	20	0.25	-	-
36	LR = 30%	ST	2.0	-	0.0147	280,000	2.21	30	150	0.0007424	2972	30	0.25	-	-
37	LR = 1%	ST	2.0	-	0.0147	280,000	2.21	30	150	0.0007424	2972	1	0.75	-	-
38	LR = 10%	ST	2.0	-	0.0147	280,000	2.21	30	150	0.0007424	2972	10	0.75	-	-
39	LR = 20%	ST	2.0	-	0.0147	280,000	2.21	30	150	0.0007424	2972	20	0.75	-	-
40	LR = 30%	ST	2.0	-	0.0147	280,000	2.21	30	150	0.0007424	2972	30	0.75	-	-
41	LR = 1%	ST	3.0	-	0.0137	420,000	3.08	30	150	0.0011136	2766	1	0.25	-	-
42	LR = 30%	ST	3.0	-	0.0137	420,000	3.08	30	150	0.0011136	2766	30	0.25	-	-
43	LR = 1%	ST	3.0	-	0.0137	420,000	3.08	30	150	0.0011136	2766	1	0.75	-	-
44	LR = 30%	ST	3.0	-	0.0137	420,000	3.08	30	150	0.0011136	2766	30	0.75	-	-
45	LR = 1%	FI	0.3	0.45	0.0218	41865	0.49	30	150	0.0001114	4401	1	0.5	0.5	5s
46	LR = 30%	FI	0.3	0.45	0.0218	41865	0.49	30	150	0.0001114	4401	30	0.5	0.5	5s
47	LR = 0%	FI	1.0	1.5	0.0168	140,000	1.26	30	150	0.0003712	3392	-	0.5	0.5	5s
48	LR = 1%	FI	1.0	1.5	0.0168	140,000	1.26	30	150	0.0003712	3392	1	0.5	0.5	5s

Counter	Changed variable and value	Flow state	Velocity Vo [m/s]	Velocity Vf [m/s]	Friction factor	Reynolds number	R factor	Pipe diameter [in]	Pipe length [km]	Vo/2a	Lf/D	LR (%)	LL	TSV	D
49	LR = 30%	FI	1.0	1.5	0.0168	140,000	1.26	30	150	0.0003712	3392	30	0.5	0.5	5s
50	LR = 1%	FI	2.0	3	0.0147	280,000	2.21	30	150	0.0007424	2972	1	0.5	0.5	5s
51	LR = 10%	FI	2.0	3	0.0147	280,000	2.21	30	150	0.0007424	2972	10	0.5	0.5	5s
52	LR = 20%	FI	2.0	3	0.0147	280,000	2.21	30	150	0.0007424	2972	20	0.5	0.5	5s
53	LR = 30%	FI	2.0	3	0.0147	280,000	2.21	30	150	0.0007424	2972	30	0.5	0.5	5s
54	LR = 1%	FI	0.3	0.45	0.0218	41865	0.49	30	150	0.0001114	4401	1	0.25	0.5	5s
55	LR = 30%	FI	0.3	0.45	0.0218	41865	0.49	30	150	0.0001114	4401	30	0.25	0.5	5s
56	LR = 1%	FI	0.3	0.45	0.0218	41865	0.49	30	150	0.0001114	4401	1	0.75	0.5	5s
57	LR = 30%	FI	0.3	0.45	0.0218	41865	0.49	30	150	0.0001114	4401	30	0.75	0.5	5s
58	LR = 1%	FI	2.0	3	0.0147	280,000	2.21	30	150	0.0007424	2972	1	0.25	0.5	5s
59	LR = 30%	FI	2.0	3	0.0147	280,000	2.21	30	150	0.0007424	2972	30	0.25	0.5	5s
60	LR = 1%	FI	2.0	3	0.0147	280,000	2.21	30	150	0.0007424	2972	1	0.75	0.5	5s
61	LR = 30%	FI	2.0	3	0.0147	280,000	2.21	30	150	0.0007424	2972	30	0.75	0.5	5s
62	LR = 1%	FI	2.0	2.4	0.0147	280,000	2.21	30	150	0.0007424	2972	1	0.5	0.2	5s
63	LR = 30%	FI	2.0	2.4	0.0147	280,000	2.21	30	150	0.0007424	2972	30	0.5	0.2	5s
64	LR = 1%	FI	2.0	2.4	0.0147	280,000	2.21	30	150	0.0007424	2972	1	0.5	0.13	8m
65	LR = 30%	FI	2.0	2.4	0.0147	280,000	2.21	30	150	0.0007424	2972	30	0.5	0.13	8m
66	LR = 1%	FI	2.0	3	0.0147	280,000	2.21	30	150	0.0007424	2972	1	0.5	0.33	8m
67	LR = 30%	FI	2.0	3	0.0147	280,000	2.21	30	150	0.0007424	2972	30	0.5	0.33	8m
68	LR = 1%	FD	0.3	0.15	0.0218	41865	0.49	30	150	0.0001114	4401	1	0.5	0.5	5s
69	LR = 30%	FD	0.3	0.15	0.0218	41865	0.49	30	150	0.0001114	4401	30	0.5	0.5	5s
70	LR = 1%	FD	1.0	0.5	0.0168	140,000	1.26	30	150	0.0003712	3392	1	0.5	0.5	5s
71	LR = 30%	FD	1.0	0.5	0.0168	140,000	1.26	30	150	0.0003712	3392	30	0.5	0.5	5s
72	LR = 1%	FD	2.0	1	0.0147	280,000	2.21	30	150	0.0007424	2972	1	0.5	0.5	5s
73	LR = 10%	FD	2.0	1	0.0147	280,000	2.21	30	150	0.0007424	2972	10	0.5	0.5	5s

Counter	Changed variable and value	Flow state	Velocity Vo [m/s]	Velocity Vf [m/s]	Friction factor	Reynolds number	R factor	Pipe diameter [in]	Pipe length [km]	Vo/2a	Lf/D	LR (%)	LL	TSV	D
74	LR = 20%	FD	2.0	1	0.0147	280,000	2.21	30	150	0.0007424	2972	20	0.5	0.5	5s
75	LR = 30%	FD	2.0	1	0.0147	280,000	2.21	30	150	0.0007424	2972	30	0.5	0.5	5s
76	LR = 0%	FD	3.0	1.5	0.0137	420,000	3.08	30	150	0.0011136	2766	-	0.5	0.5	5s
77	LR = 1%	FD	3.0	1.5	0.0137	420,000	3.08	30	150	0.0011136	2766	1	0.5	0.5	5s
78	LR = 30%	FD	3.0	1.5	0.0137	420,000	3.08	30	150	0.0011136	2766	30	0.5	0.5	5s
79	LR = 1%	FD	0.3	0.15	0.0218	41865	0.49	30	150	0.0001114	4401	1	0.25	0.5	5s
80	LR = 30%	FD	0.3	0.15	0.0218	41865	0.49	30	150	0.0001114	4401	30	0.25	0.5	5s
81	LR = 1%	FD	0.3	0.15	0.0218	41865	0.49	30	150	0.0001114	4401	1	0.75	0.5	5s
82	LR = 30%	FD	0.3	0.15	0.0218	41865	0.49	30	150	0.0001114	4401	30	0.75	0.5	5s
83	LR = 1%	FD	2.0	1	0.0147	280,000	2.21	30	150	0.0007424	2972	1	0.25	0.5	5s
84	LR = 30%	FD	2.0	1	0.0147	280,000	2.21	30	150	0.0007424	2972	30	0.25	0.5	5s
85	LR = 1%	FD	2.0	1	0.0147	280,000	2.21	30	150	0.0007424	2972	1	0.75	0.5	5s
86	LR = 30%	FD	2.0	1	0.0147	280,000	2.21	30	150	0.0007424	2972	30	0.75	0.5	5s
87	LR = 1%	FD	2.0	1.6	0.0147	280,000	2.21	30	150	0.0007424	2972	1	0.5	0.2	5s
88	LR = 30%	FD	2.0	1.6	0.0147	280,000	2.21	30	150	0.0007424	2972	30	0.5	0.2	5s
89	LR = 1%	FD	2.0	1.6	0.0147	280,000	2.21	30	150	0.0007424	2972	1	0.5	0.12	8m
90	LR = 30%	FD	2.0	1.6	0.0147	280,000	2.21	30	150	0.0007424	2972	30	0.5	0.12	8m
91	LR = 1%	FD	2.0	1	0.0147	280,000	2.21	30	150	0.0007424	2972	1	0.5	0.3	8m
92	LR = 30%	FD	2.0	1	0.0147	280,000	2.21	30	150	0.0007424	2972	30	0.5	0.3	8m
Noisy data, steady state															
93	LR = 1%	ST	0.3	-	0.0218	41865	0.49	30	150	0.0001114	4401	1	0.5	-	-
94	LR = 30%	ST	0.3	-	0.0218	41865	0.49	30	150	0.0001114	4401	30	0.5	-	-
95	LL = 0.25L	ST	0.3	-	0.0218	41865	0.49	30	150	0.0001114	4401	1	0.25	-	-
96	LL = 0.75L	ST	0.3	-	0.0218	41865	0.49	30	150	0.0001114	4401	1	0.75	-	-
97	LL = 0.50L	ST	0.3	-	0.0218	41865	0.49	30	150	0.0001114	4401	1	0.5	-	-

Counter	Changed variable and value	Flow state	Velocity Vo [m/s]	Velocity Vf [m/s]	Friction factor	Reynolds number	R factor	Pipe diameter [in]	Pipe length [km]	Vo/2a	Lf/D	LR (%)	LL	TSV	D
98	LL = 0.50L	ST	0.3	-	0.0218	41865	0.49	30	150	0.0001114	4401	30	0.5	-	-
99	LL = 0.25L	ST	0.3	-	0.0218	41865	0.49	30	150	0.0001114	4401	1	0.25	-	-
100	LL = 0.75L	ST	0.3	-	0.0218	41865	0.49	30	150	0.0001114	4401	1	0.75	-	-
101	LL = 0.50L	ST	3.0	-	0.0137	420,000	3.08	30	150	0.0011136	2766	1	0.5	-	-
102	LL = 0.50L	ST	3.0	-	0.0137	420,000	3.08	30	150	0.0011136	2766	30	0.5	-	-
103	LL = 0.25L	ST	3.0	-	0.0137	420,000	3.08	30	150	0.0011136	2766	1	0.25	-	-
104	LL = 0.50L	ST	3.0	-	0.0137	420,000	3.08	30	150	0.0011136	2766	1	0.5	-	-
105	LL = 0.25L	ST	3.0	-	0.0137	420,000	3.08	30	150	0.0011136	2766	1	0.25	-	-
106	LL = 0.25L	ST	3.0	-	0.0137	420,000	3.08	30	150	0.0011136	2766	30	0.25	-	-
107	LL = 0.50L	ST	2.0	-	0.0147	280,000	2.21	30	150	0.0007424	2972	1	0.5	-	-
108	LL = 0.50L	ST	2.0	-	0.0147	280,000	2.21	30	150	0.0007424	2972	30	0.5	-	-
Noisy data, transient state															
109	TSV = 0.50	FI	2.0	3	0.0147	280,000	2.21	30	150	0.0007424	2972	1	0.5	0.5	5s
110	TSV = 0.12	FI	2.0	2.4	0.0147	280,000	2.21	30	150	0.0007424	2972	1	0.5	0.12	8m
111	TSV = 0.50	FD	2.0	1	0.0147	280,000	2.21	30	150	0.0007424	2972	1	0.5	0.5	5s
112	TSV = 0.12	FD	2.0	1.6	0.0147	280,000	2.21	30	150	0.0007424	2972	1	0.5	0.12	8m
113	TSV = 0.50	FI	2.0	3	0.0147	280,000	2.21	30	150	0.0007424	2972	30	0.5	0.5	5s
114	TSV = 0.12	FI	2.0	2.4	0.0147	280,000	2.21	30	150	0.0007424	2972	30	0.5	0.12	8m
115	TSV = 0.50	FD	2.0	1	0.0147	280,000	2.21	30	150	0.0007424	2972	30	0.5	0.5	5s
116	TSV = 0.12	FD	2.0	1.6	0.0147	280,000	2.21	30	150	0.0007424	2972	30	0.5	0.12	8m
117	LL = 0.25L	FI	2.0	3	0.0147	280,000	2.21	30	150	0.0007424	2972	1	0.25	0.5	5s
118	LL = 0.75L	FI	2.0	3	0.0147	280,000	2.21	30	150	0.0007424	2972	1	0.75	0.5	5s
119	LL = 0.25L	FD	2.0	1.6	0.0147	280,000	2.21	30	150	0.0007424	2972	1	0.25	0.12	8m
120	LL = 0.75L	FD	2.0	1.6	0.0147	280,000	2.21	30	150	0.0007424	2972	1	0.75	0.12	8m
121	TSV = 0.50	FI	2.0	3	0.0147	280,000	2.21	30	150	0.0007424	2972	1	0.25	0.5	5s

Counter	Changed variable and value	Flow state	Velocity Vo [m/s]	Velocity Vf [m/s]	Friction factor	Reynolds number	R factor	Pipe diameter [in]	Pipe length [km]	Vo/2a	Lf/D	LR (%)	LL	TSV	D
122	TSV = 0.12	FD	2.0	1.6	0.0147	280,000	2.21	30	150	0.0007424	2972	1	0.25	0.12	8m
123	TSV = 0.50	FI	2.0	3	0.0147	280,000	2.21	30	150	0.0007424	2972	1	0.5	0.5	5s
124	TSV = 0.12	FI	2.0	2.4	0.0147	280,000	2.21	30	150	0.0007424	2972	1	0.5	0.12	8m
125	TSV = 0.50	FD	2.0	1	0.0147	280,000	2.21	30	150	0.0007424	2972	1	0.5	0.5	5s
126	TSV = 0.12	FD	2.0	1.6	0.0147	280,000	2.21	30	150	0.0007424	2972	1	0.5	0.12	8m
127	TSV = 0.50	FI	2.0	3	0.0147	280,000	2.21	30	150	0.0007424	2972	30	0.5	0.5	5s
128	TSV = 0.12	FI	2.0	2.4	0.0147	280,000	2.21	30	150	0.0007424	2972	30	0.5	0.12	8m
129	FI	FI	0.3	0.36	0.0218	41865	0.49	30	150	0.0001114	4401	1	0.5	0.12	8m
130	FD	FD	0.3	0.24	0.0218	41865	0.49	30	150	0.0001114	4401	1	0.5	0.12	8m
131	FI	FI	0.3	0.36	0.0218	41865	0.49	30	150	0.0001114	4401	30	0.5	0.12	8m
132	FD	FD	0.3	0.24	0.0218	41865	0.49	30	150	0.0001114	4401	30	0.5	0.12	8m
133	LL = 0.25L	FI	0.3	0.45	0.0218	41865	0.49	30	150	0.0001114	4401	1	0.25	0.5	5s
134	LL = 0.75L	FI	0.3	0.45	0.0218	41865	0.49	30	150	0.0001114	4401	1	0.75	0.5	5s
135	TSV = 0.50	FI	0.3	0.45	0.0218	41865	0.49	30	150	0.0001114	4401	1	0.5	0.5	5s
136	TSV = 0.12	FI	0.3	0.36	0.0218	41865	0.49	30	150	0.0001114	4401	1	0.5	0.12	8m
137	TSV = 0.50	FD	0.3	0.15	0.0218	41865	0.49	30	150	0.0001114	4401	1	0.5	0.5	5s
138	TSV = 0.12	FD	0.3	0.24	0.0218	41865	0.49	30	150	0.0001114	4401	1	0.5	0.12	8m
139	TSV = 0.50	FI	0.3	0.45	0.0218	41865	0.49	30	150	0.0001114	4401	30	0.5	0.5	5s
140	TSV = 0.12	FI	0.3	0.36	0.0218	41865	0.49	30	150	0.0001114	4401	30	0.5	0.12	8m
141	TSV = 0.50	FD	0.3	0.15	0.0218	41865	0.49	30	150	0.0001114	4401	30	0.5	0.5	5s
142	TSV = 0.12	FD	0.3	0.24	0.0218	41865	0.49	30	150	0.0001114	4401	30	0.5	0.12	8m
143	LL = 0.25L	FI	0.3	0.45	0.0218	41865	0.49	30	150	0.0001114	4401	1	0.25	0.5	5s
144	LL = 0.75L	FI	0.3	0.45	0.0218	41865	0.49	30	150	0.0001114	4401	1	0.75	0.5	5s
145	TSV = 0.50	FI	0.3	0.45	0.0218	41865	0.49	30	150	0.0001114	4401	1	0.5	0.5	5s
146	TSV = 0.12	FI	0.3	0.36	0.0218	41865	0.49	30	150	0.0001114	4401	1	0.5	0.12	8m

Counter	Changed variable and value	Flow state	Velocity Vo [m/s]	Velocity Vf [m/s]	Friction factor	Reynolds number	R factor	Pipe diameter [in]	Pipe length [km]	Vo/2a	Lf/D	LR (%)	LL	TSV	D
147	LL = 0.25L	FD	2.0	1.6	0.0147	280,000	2.21	30	150	0.0007424	2972	1	0.25	0.12	8m
148	LL = 0.75L	FD	2.0	1.6	0.0147	280,000	2.21	30	150	0.0007424	2972	1	0.75	0.12	8m
149	Perfect data	FI	2.0	3	0.0147	280,000	2.21	30	150	0.0007424	2972	2	0.5	0.5	5s
150	Noisy data	FI	2.0	3	0.0147	280,000	2.21	30	150	0.0007424	2972	2	0.5	0.5	5s
151	Perfect data	FI	2.0	3	0.0147	280,000	2.21	30	150	0.0007424	2972	3	0.5	0.5	5s
152	Noisy data	FI	2.0	3	0.0147	280,000	2.21	30	150	0.0007424	2972	3	0.5	0.5	5s
153	LL = 0.25L	FI	2.0	3	0.0147	280,000	2.21	30	150	0.0007424	2972	30	0.25	0.5	5s
154	LL = 0.75L	FI	2.0	3	0.0147	280,000	2.21	30	150	0.0007424	2972	30	0.75	0.5	5s
155	LL = 0.25L	FI	2.0	3	0.0147	280,000	2.21	30	150	0.0007424	2972	30	0.25	0.5	5s
156	LL = 0.75L	FI	2.0	3	0.0147	280,000	2.21	30	150	0.0007424	2972	30	0.75	0.5	5s
157	LL = 0.25L	FI	0.3	0.45	0.0218	41,865	0.49	30	150	0.0001114	4401	30	0.25	0.5	5s
158	LL = 0.75L	FI	0.3	0.45	0.0218	41,865	0.49	30	150	0.0001114	4401	30	0.75	0.5	5s
159	LL = 0.25L	FD	0.3	0.15	0.0218	41,865	0.49	30	150	0.0001114	4401	1	0.25	0.5	5s
160	LL = 0.75L	FD	0.3	0.15	0.0218	41,865	0.49	30	150	0.0001114	4401	1	0.75	0.5	5s
161	LL = 0.25L	FD	2.0	1	0.0147	280,000	2.21	30	150	0.0007424	2972	30	0.25	0.5	5s
162	LL = 0.75L	FD	2.0	1	0.0147	280,000	2.21	30	150	0.0007424	2972	30	0.75	0.5	5s
163	LL = 0.25L	FD	0.3	0.15	0.0218	41,865	0.49	30	150	0.0001114	4401	30	0.25	0.5	5s
164	LL = 0.75L	FD	0.3	0.15	0.0218	41,865	0.49	30	150	0.0001114	4401	30	0.75	0.5	5s
165	NQ = 3%	FD	0.3	0.15	0.0218	41,865	0.49	30	150	0.0001114	4401	30	0.5	0.5	5s
166	NQ = 3%	FD	2.0	1	0.0147	280,000	2.21	30	150	0.0007424	2972	30	0.5	0.5	5s
167	FF = 0.0220	ST	0.3	-	0.0218	41,865	0.49	30	150	0.0001114	4401	5	0.5	-	-
168	FF = 0.0066	ST	1.0	-	0.0168	140,000	1.26	30	150	0.0003712	3392	5	0.5	-	-
169	FF = 0.0221	ST	2.0	-	0.0147	280,000	2.21	30	150	0.0007424	2972	5	0.5	-	-
170	FF = 0.0140	ST	3.0	-	0.0137	420,000	3.08	30	150	0.0011136	2766	5	0.5	-	-

Counter	Changed variable and value	Flow state	Velocity Vo [m/s]	Velocity Vf [m/s]	Friction factor	Reynolds number	R factor	Pipe diameter [in]	Pipe length [km]	Vo/2a	Lf/D	LR (%)	LL	TSV	D
171	LL = 0.25L	ST	0.3	-	0.0218	41,865	0.49	30	150	0.0001114	4401	30	0.25	-	-
172	LL = 0.75L	ST	0.3	-	0.0218	41,865	0.49	30	150	0.0001114	4401	30	0.75	-	-
173	LL = 0.25L	ST	2.0	-	0.0147	280,000	2.21	30	150	0.0007424	2972	1	0.25	-	-
174	LL = 0.75L	ST	2.0	-	0.0147	280,000	2.21	30	150	0.0007424	2972	1	0.75	-	-
175	LL = 0.25L	ST	2.0	-	0.0147	280,000	2.21	30	150	0.0007424	2972	30	0.25	-	-
176	LL = 0.75L	ST	2.0	-	0.0147	280,000	2.21	30	150	0.0007424	2972	30	0.75	-	-
177	LL = 0.25L	FD	2.0	1	0.0147	280,000	2.21	30	150	0.0007424	2972	1	0.25	0.5	5s
178	LL = 0.75L	FD	2.0	1	0.0147	280,000	2.21	30	150	0.0007424	2972	1	0.25	0.5	5s

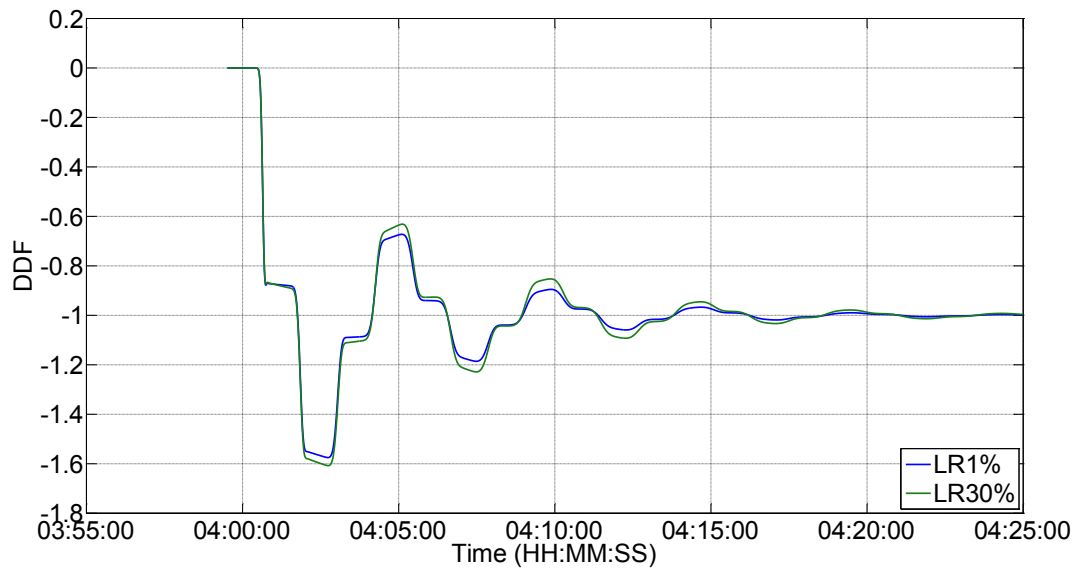


Figure C.1. Non-dimensional diagnostic flow over time for different leak sizes, Perfect data, steady state condition,  $V_o = 0.3$  m/s,  $R = 0.49$ , leak at  $L/4$ .

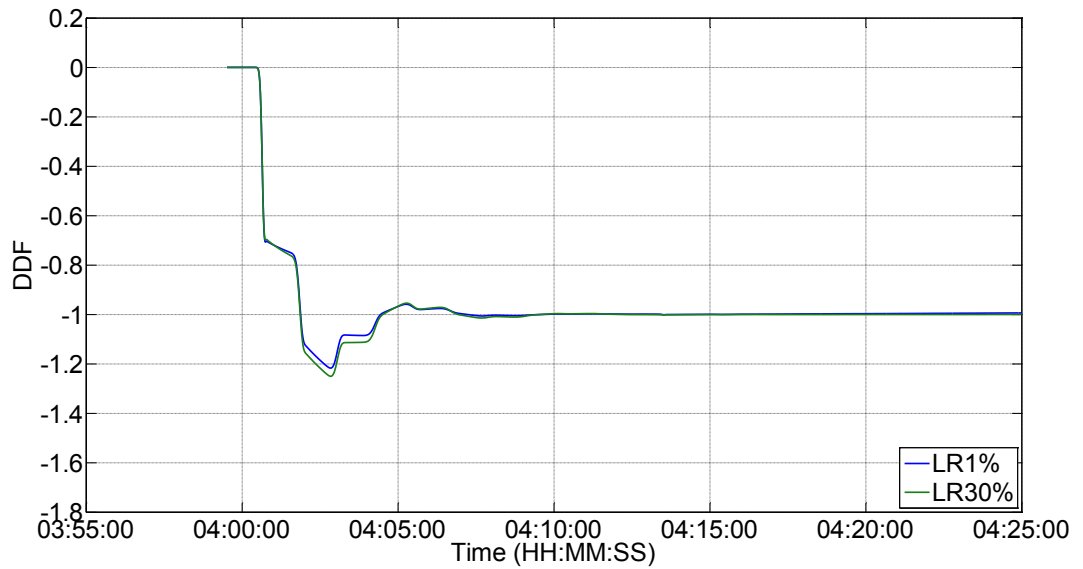


Figure C.2. Non-dimensional diagnostic flow over time for different leak sizes, Perfect data, steady state condition,  $V_o = 1$  m/s,  $R = 1.26$ , leak at  $L/4$ .

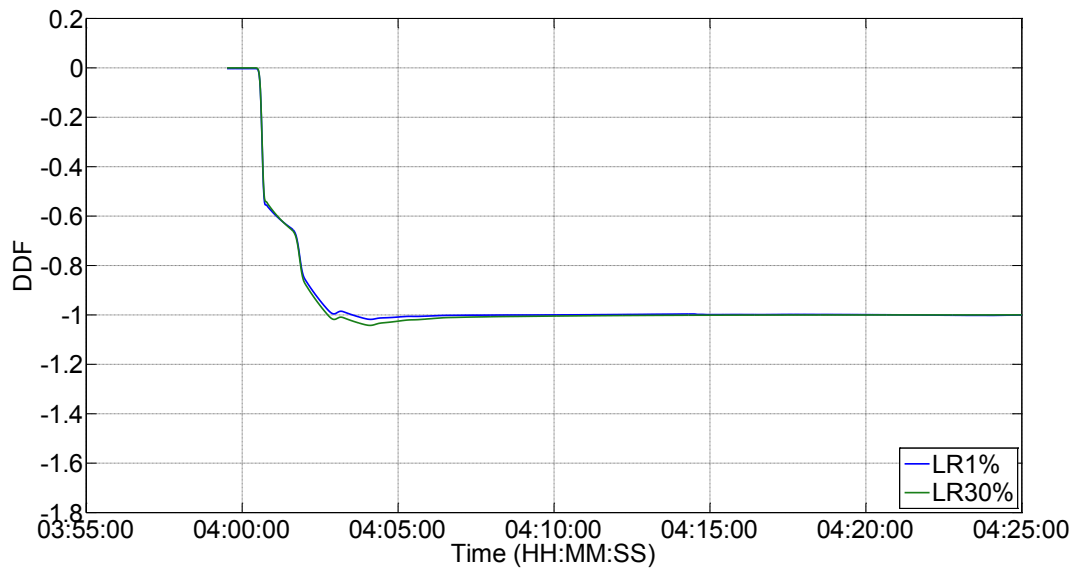


Figure C.3. Non-dimensional diagnostic flow over time for different leak sizes, Perfect data, steady state condition,  $V_o = 2$  m/s,  $R = 2.20$ , leak at  $L/4$ .

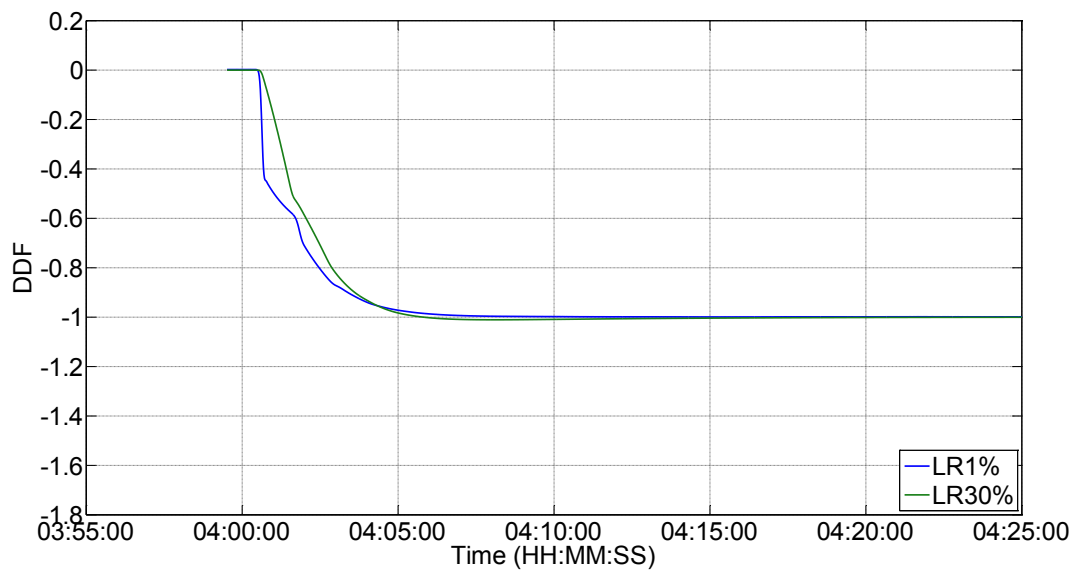


Figure C.4. Non-dimensional diagnostic flow over time for different leak sizes, Perfect data, steady state condition,  $V_o = 3$  m/s,  $R = 3.08$ , leak at  $L/4$ .

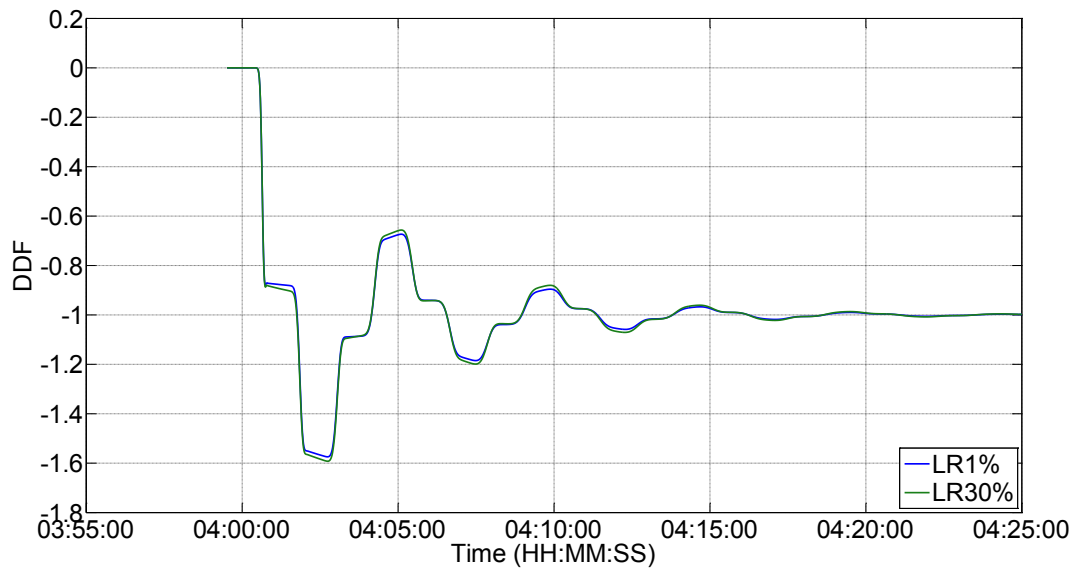


Figure C.5. Non-dimensional diagnostic flow over time for different leak sizes, Perfect data, steady state condition,  $V_o = 0.3$  m/s,  $R = 0.49$ , leak at  $3L/4$ .

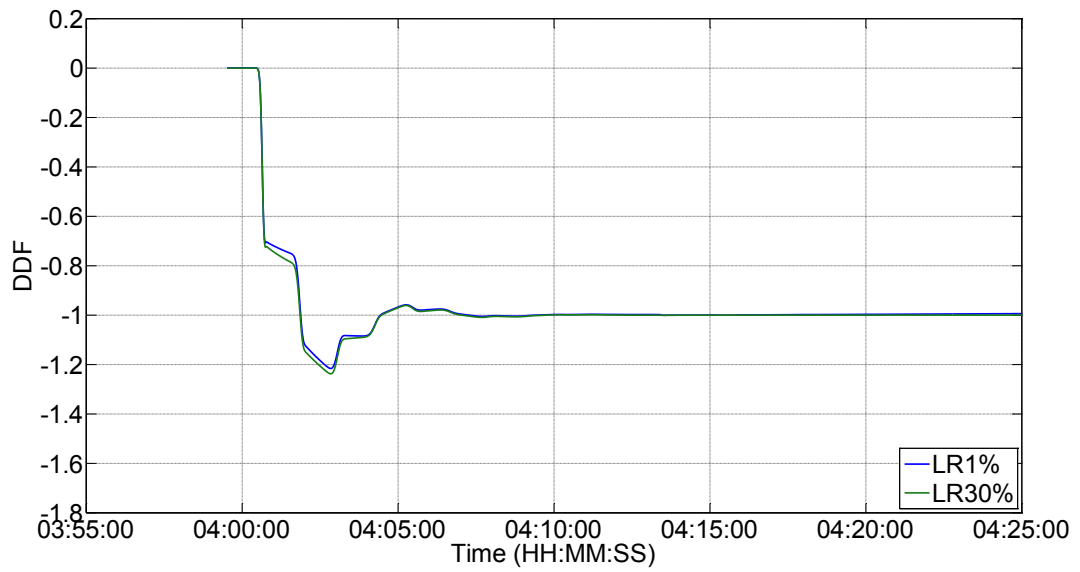


Figure C.6. Non-dimensional diagnostic flow over time for different leak sizes, Perfect data, steady state condition,  $V_o = 1$  m/s,  $R = 1.26$ , leak at  $3L/4$ .

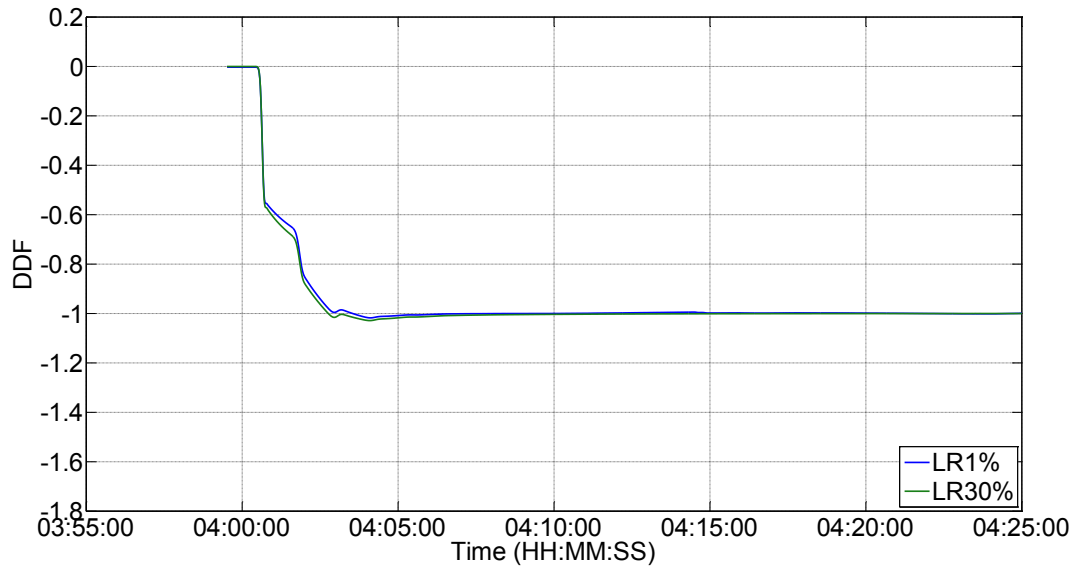


Figure C.7. Non-dimensional diagnostic flow over time for different leak sizes, Perfect data, steady state condition,  $V_o = 2$  m/s,  $R = 2.20$ , leak at  $3L/4$ .

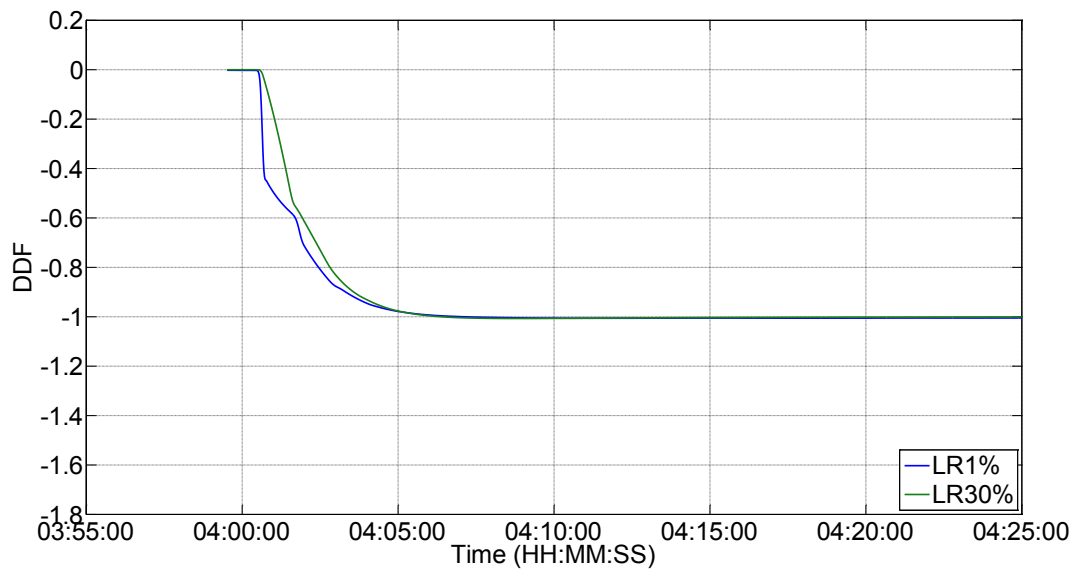


Figure C.8. Non-dimensional diagnostic flow over time for different leak sizes, Perfect data, steady state condition,  $V_o = 3$  m/s,  $R = 3.08$ , leak at  $3L/4$ .

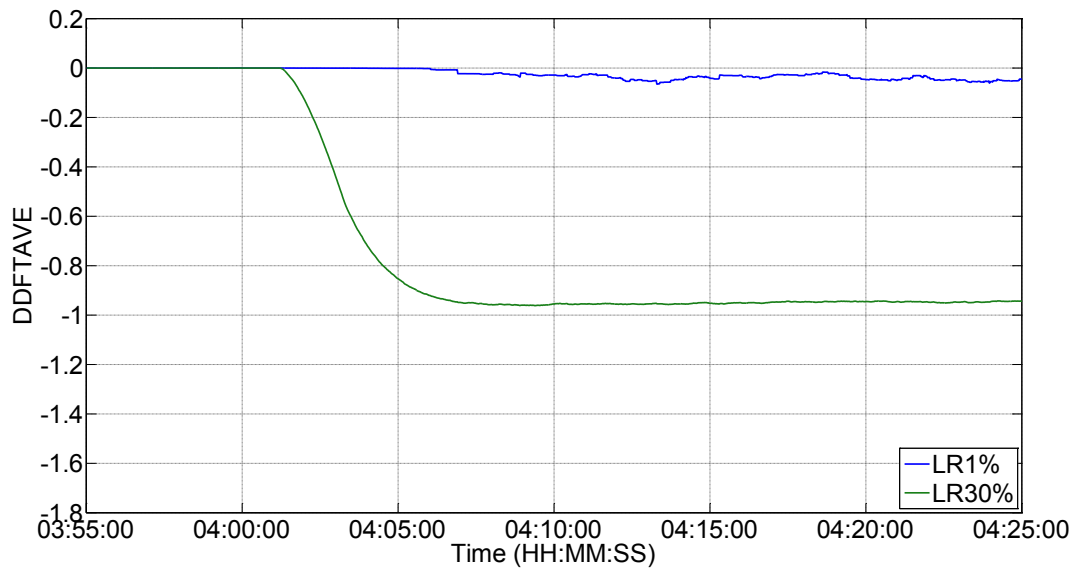


Figure C.9. Non-dimensional time-averaged diagnostic flow over time for different leak rates, steady state condition,  $V_o = 3$  m/s,  $R = 3.08$ , leak at midpoint. Noisy data, Noise in pressure and flow of 1%.

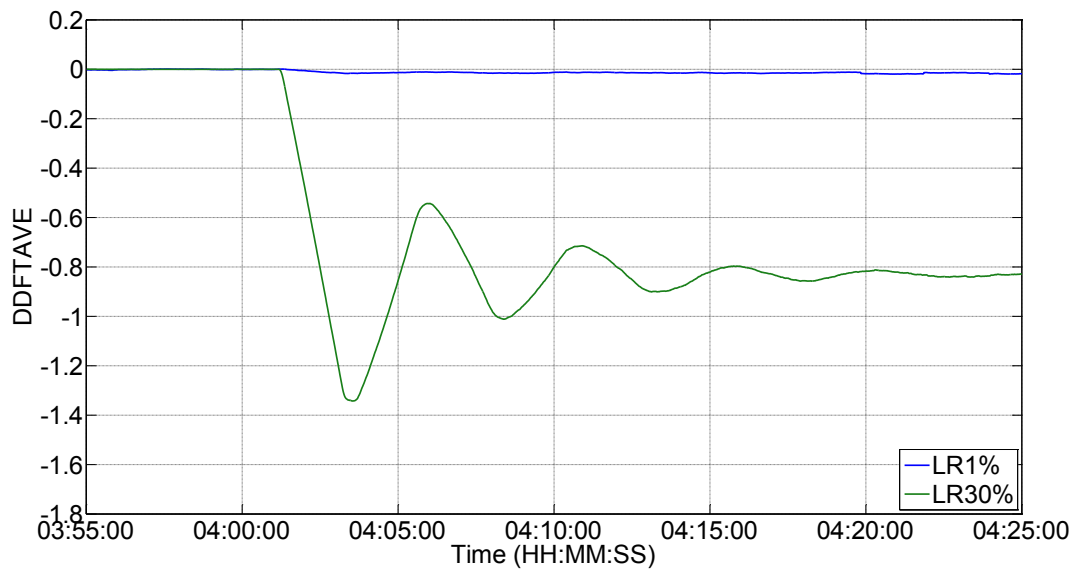


Figure C.10. Non-dimensional time-averaged diagnostic flow over time for different leak sizes, steady state condition,  $V_o = 0.3$  m/s,  $R = 0.49$ , leak at midpoint. Noisy data, Noise in pressure of 1%, noise in flow of 3%.

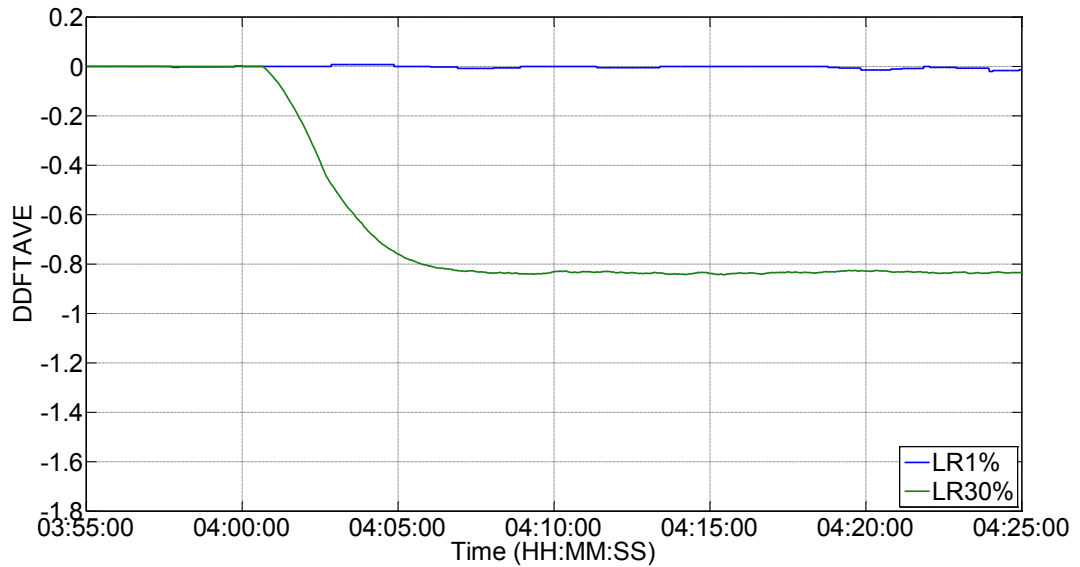


Figure C.11. Non-dimensional time-averaged diagnostic flow over time for different leak sizes, steady state condition,  $V_o = 3$  m/s,  $R = 3.08$ , leak at  $L/4$ . Noisy data, Noise in pressure of 1%, noise in flow of 3%.

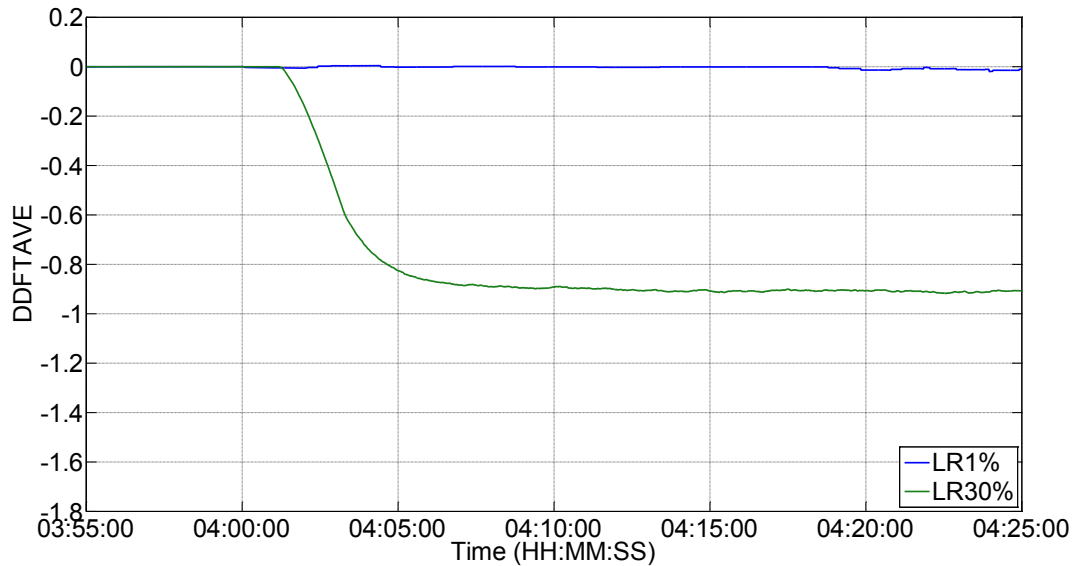


Figure C.12. Non-dimensional time-averaged diagnostic flow over time for different leak sizes, Noisy data. Flow increase condition, duration = 5 s, leak at midpoint,  $TSV = 0.5$ ,  $V_o = 2$  m/s,  $V_f = 3$  m/s, Noise in pressure = 1%, noise in flow = 1%.

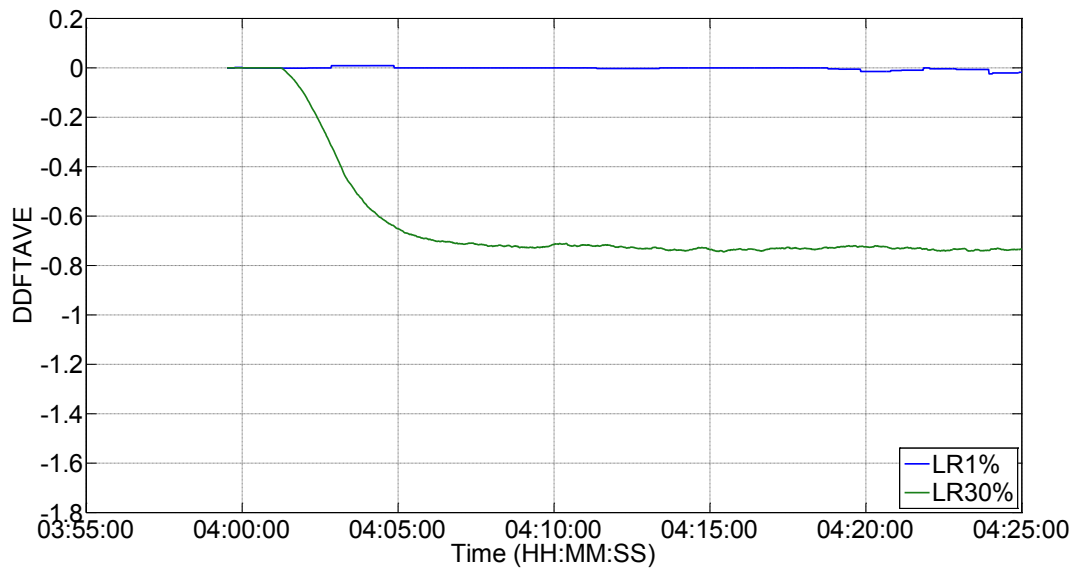


Figure C.13. Non-dimensional time-averaged diagnostic flow over time for different leak sizes, Noisy data. Flow increase condition, duration = 5 s, leak at midpoint, TSV = 0.5,  $V_o = 2$  m/s,  $V_f = 3$  m/s, Noise in pressure = 1%, noise in flow = 3%.

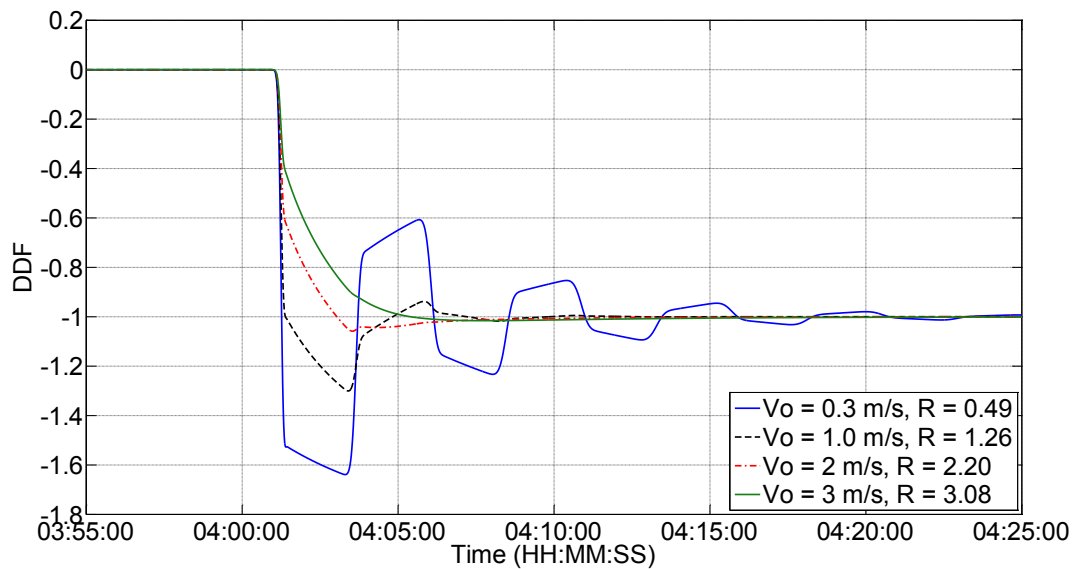


Figure C.14. Non-dimensional diagnostic flow over time for different R factors, Perfect data, steady state condition, LR = 30%, leak at midpoint.

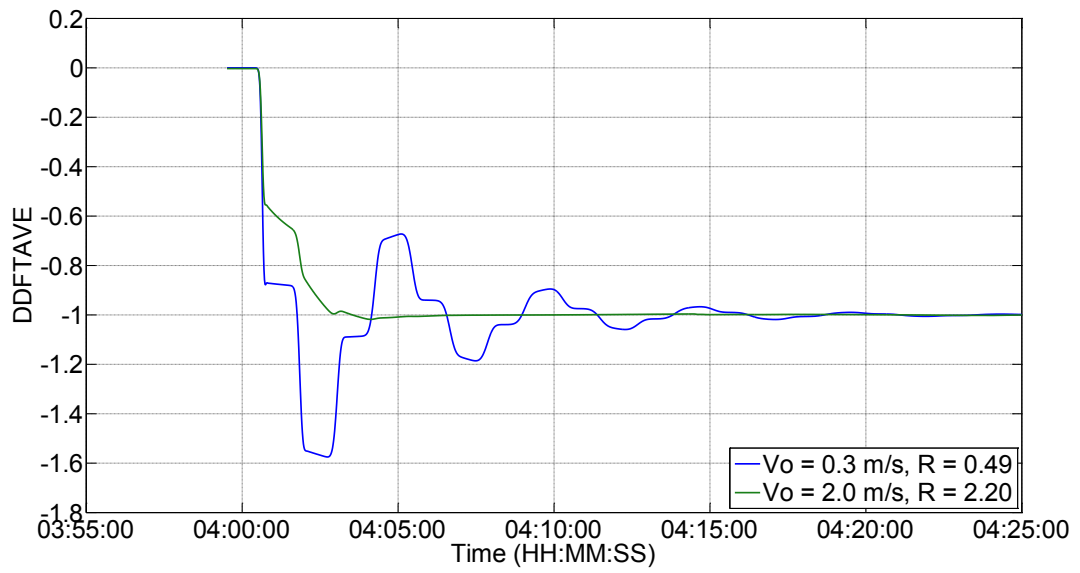


Figure C.15. Non-dimensional diagnostic flow over time for different R factors, Perfect data, steady state condition, LR = 1%, leak at L/4.

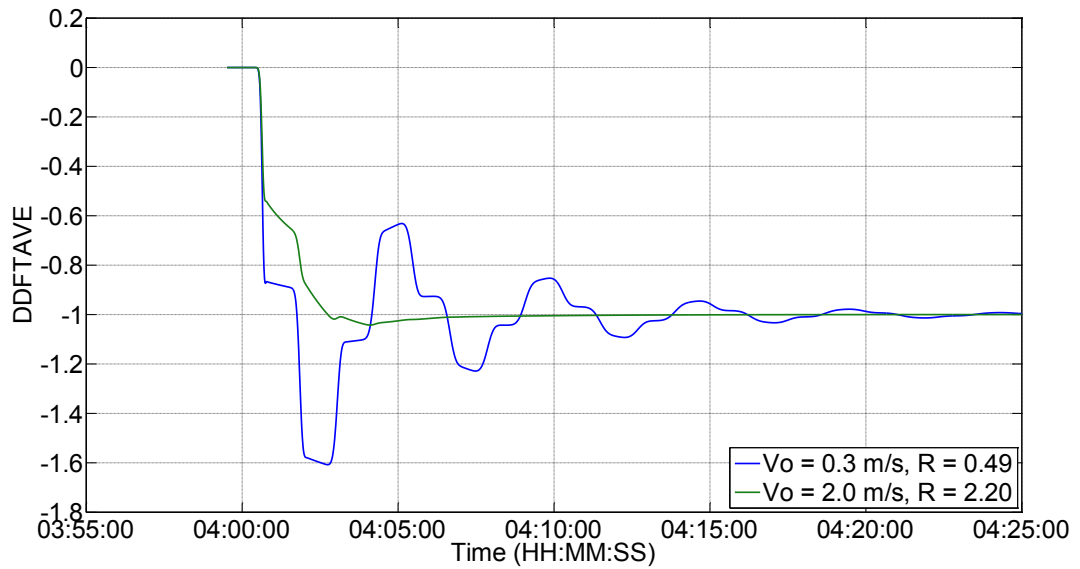


Figure C.16. Non-dimensional diagnostic flow over time for different R factors, Perfect data, steady state condition, LR = 30%, leak at L/4.

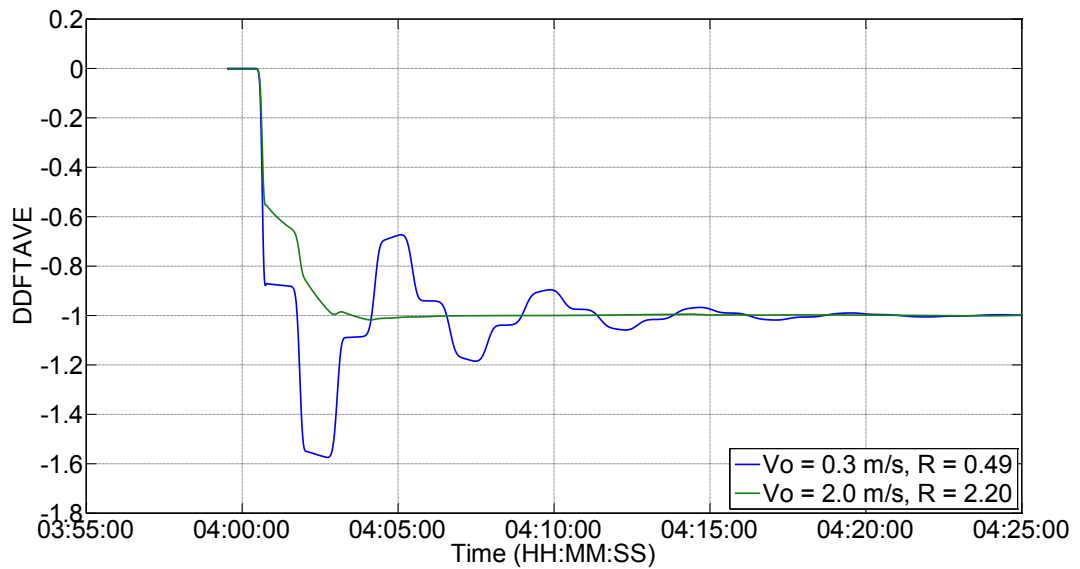


Figure C.17. Non-dimensional diagnostic flow over time for different R factors, Perfect data, steady state condition, LR = 1%, leak at 3L/4.

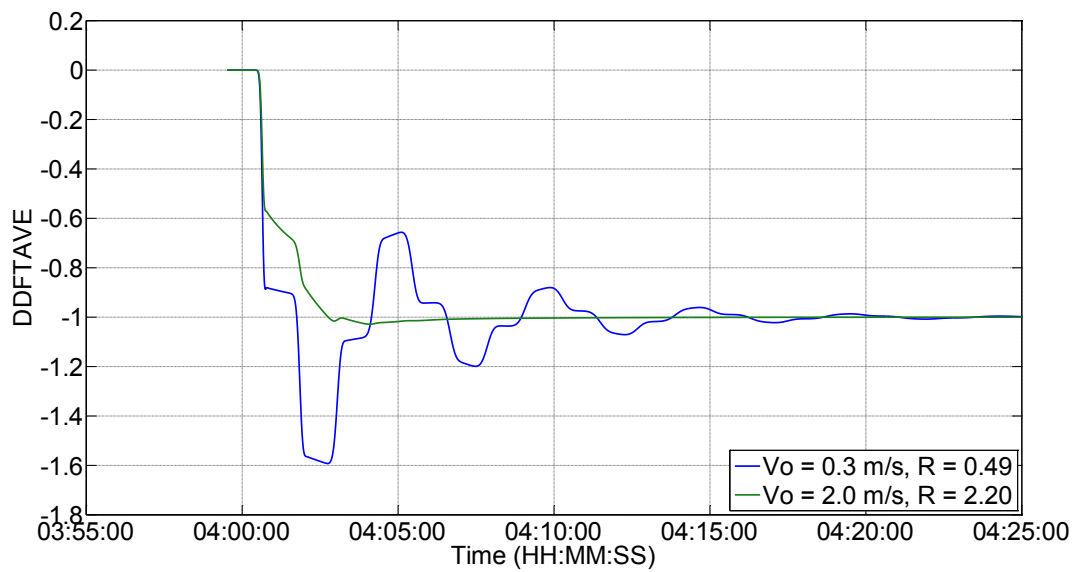


Figure C.18. Non-dimensional diagnostic flow over time for different R factors, Perfect data, steady state condition, LR = 30%, leak at 3L/4.

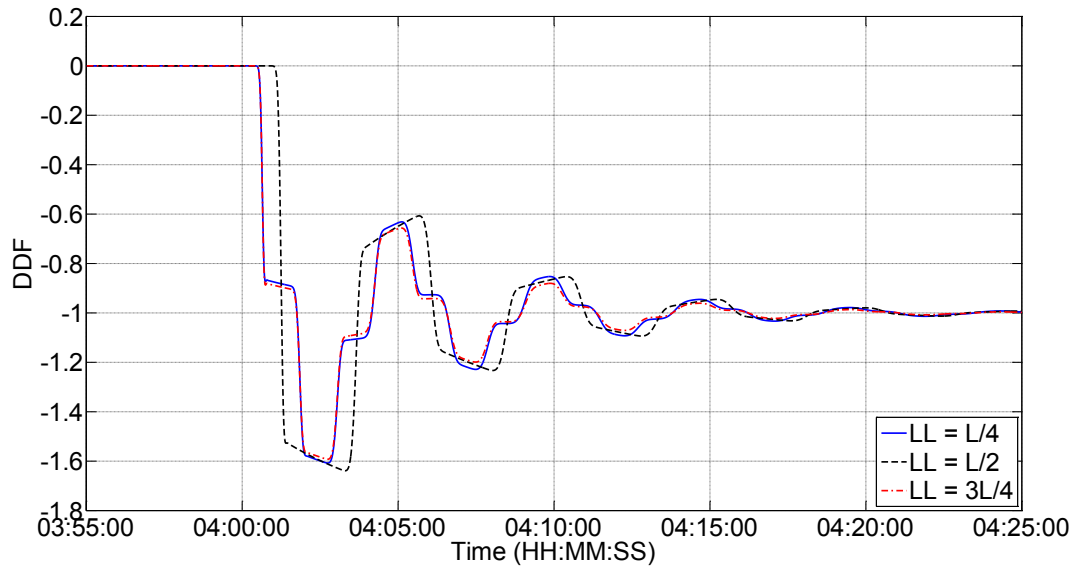


Figure C.19. Non-dimensional diagnostic flow over time for different leak locations, steady state condition,  $V_o = 0.3$  m/s,  $R = 0.49$ ,  $LR = 30\%$ . Perfect data.

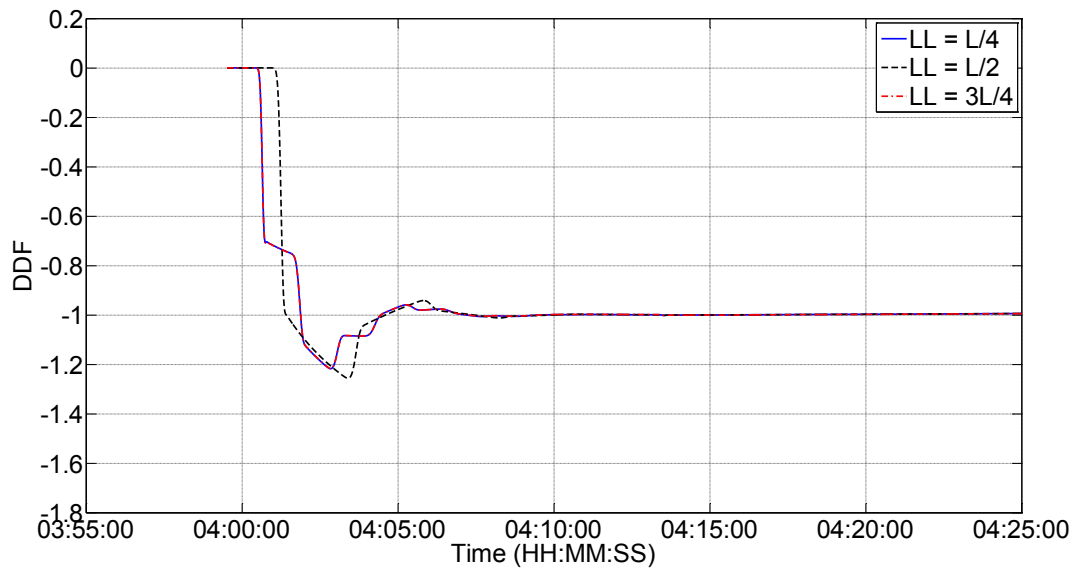


Figure C.20. Non-dimensional diagnostic flow over time for different leak locations, steady state condition,  $V_o = 1.0$  m/s,  $R = 1.26$ ,  $LR = 1\%$ . Perfect data.

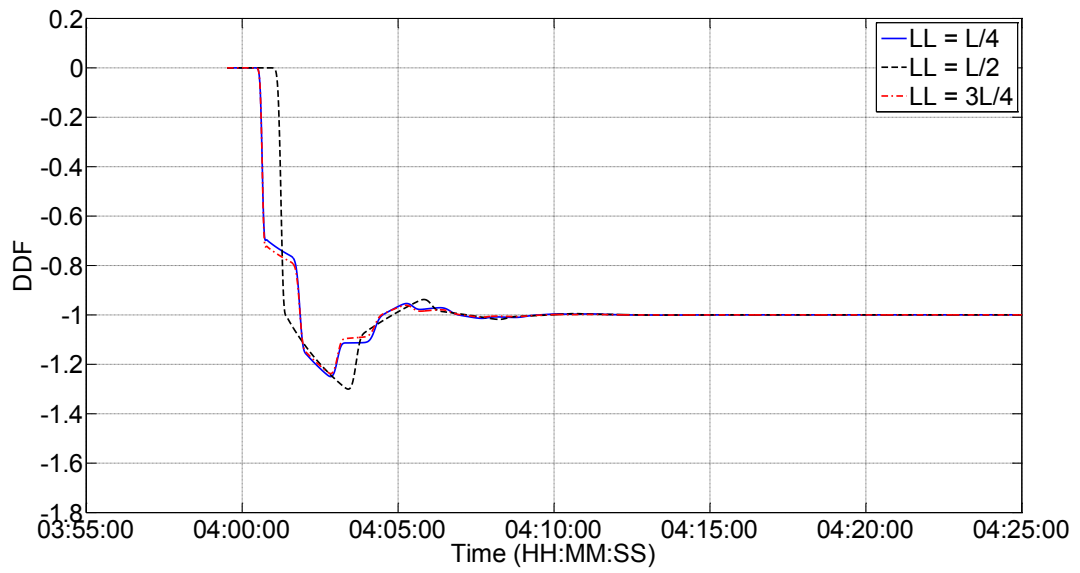


Figure C.21. Non-dimensional diagnostic flow over time for different leak locations, steady state condition,  $V_o = 1.0$  m/s,  $R = 1.26$ ,  $LR = 30\%$ . Perfect data.

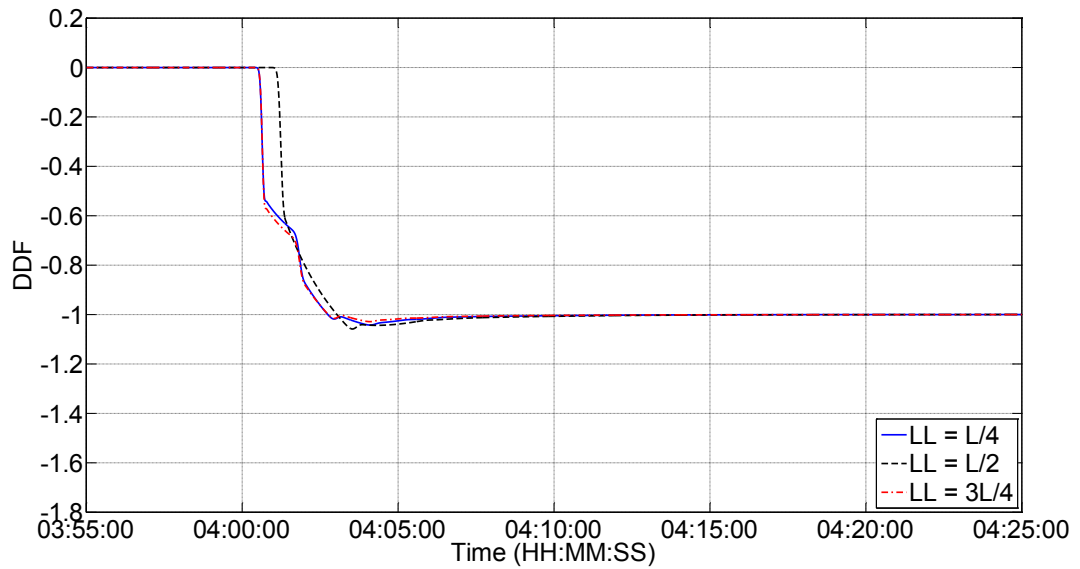


Figure C.22. Non-dimensional diagnostic flow over time for different leak locations, steady state condition,  $V_o = 2.0$  m/s,  $R = 2.20$ ,  $LR = 30\%$ . Perfect data.

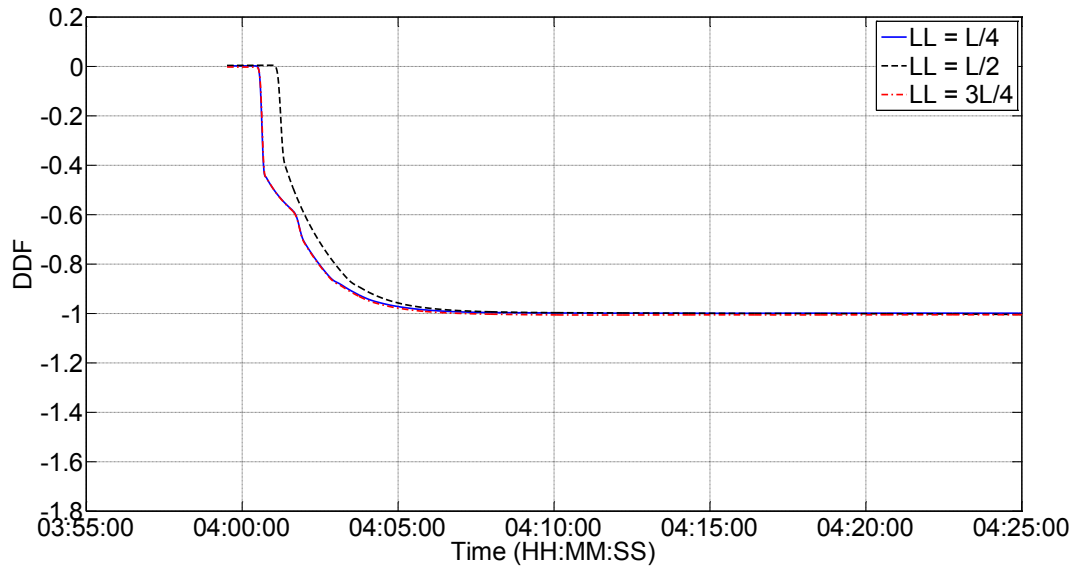


Figure C.23. Non-dimensional diagnostic flow over time for different leak locations, steady state condition,  $V_o = 3.0$  m/s,  $R = 3.08$ ,  $LR = 1\%$ . Perfect data.

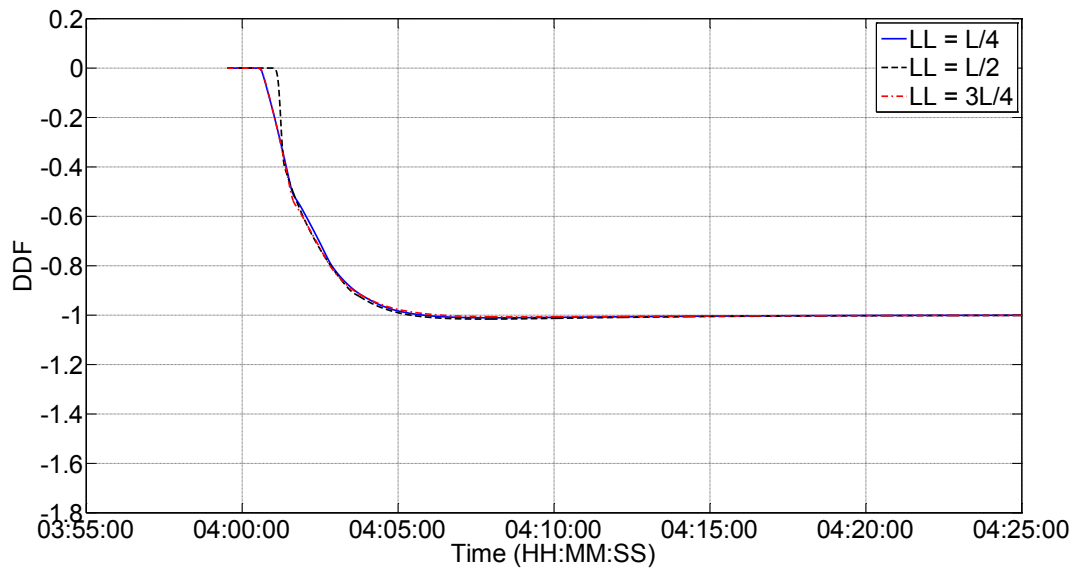


Figure C.24. Non-dimensional diagnostic flow over time for different leak locations, steady state condition,  $V_o = 3.0$  m/s,  $R = 3.08$ ,  $LR = 30\%$ . Perfect data.

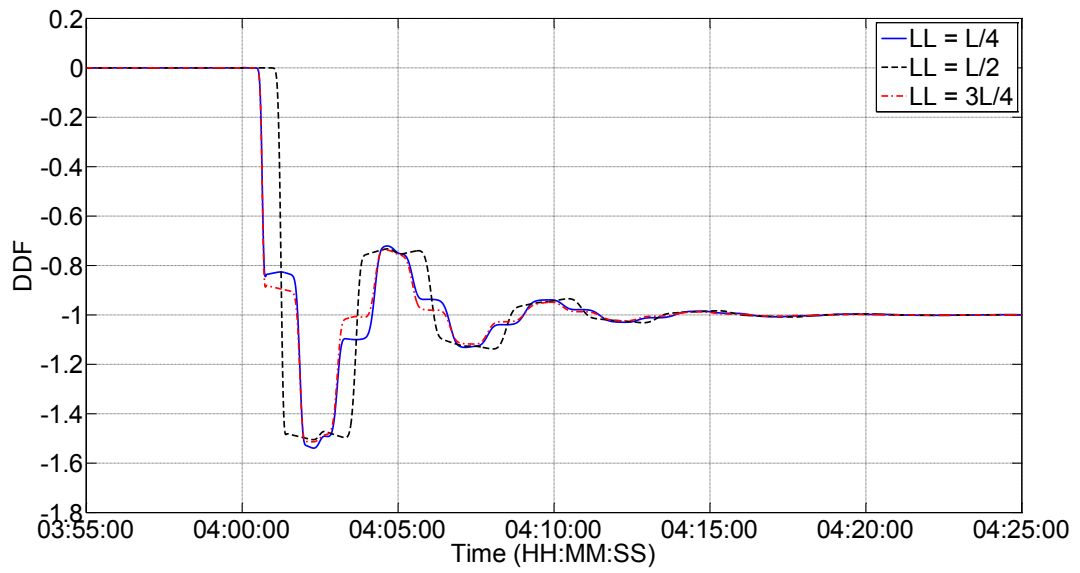


Figure C.25. Non-dimensional diagnostic flow over time for different leak locations. Flow increase condition, duration = 5 s, TSV = 0.5,  $R = 0.49$ ,  $V_0 = 0.3$  m/s, LR = 30%. Perfect data.

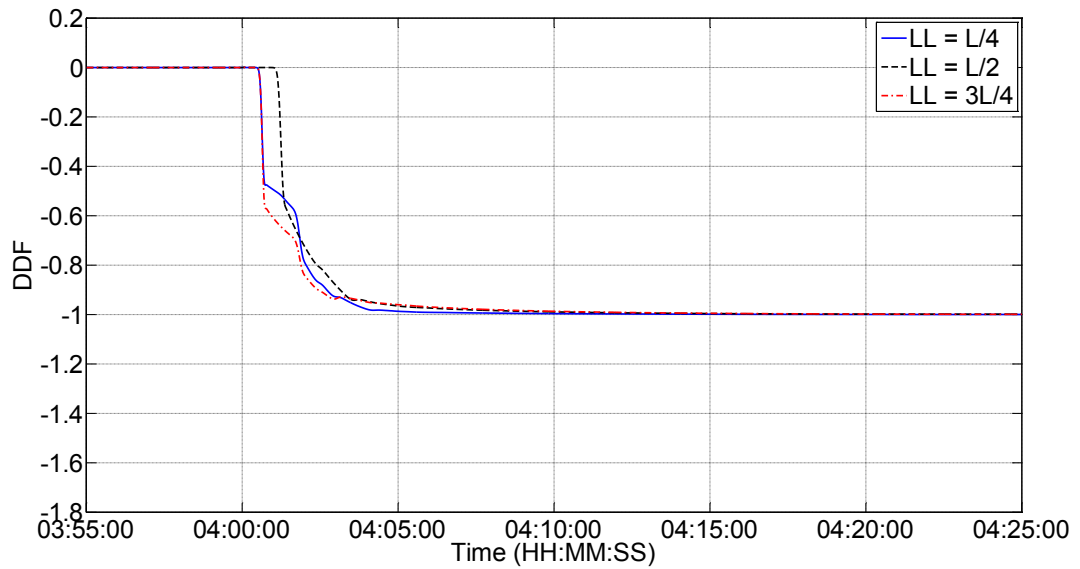


Figure C.26. Non-dimensional diagnostic flow over time for different leak locations. Flow increase condition, duration = 5 s, TSV = 0.5,  $R = 2.20$ ,  $V_0 = 2.0$  m/s, LR = 30%. Perfect data.

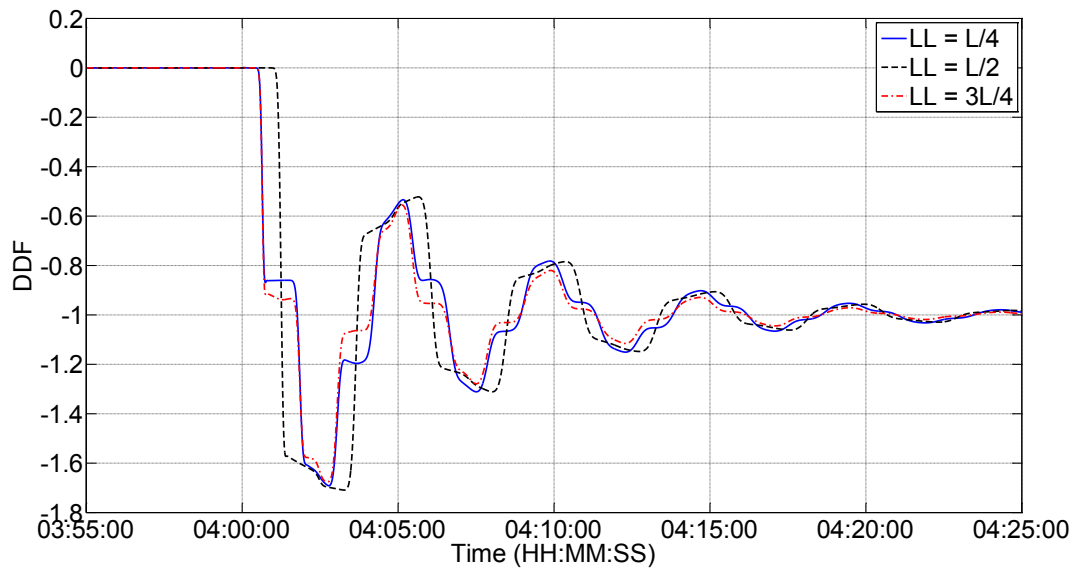


Figure C.27. Non-dimensional diagnostic flow over time for different leak locations. Flow decrease condition, duration = 5 s, TSV = 0.5,  $R = 0.49$ ,  $V_0 = 0.3$  m/s, LR = 30%. Perfect data.

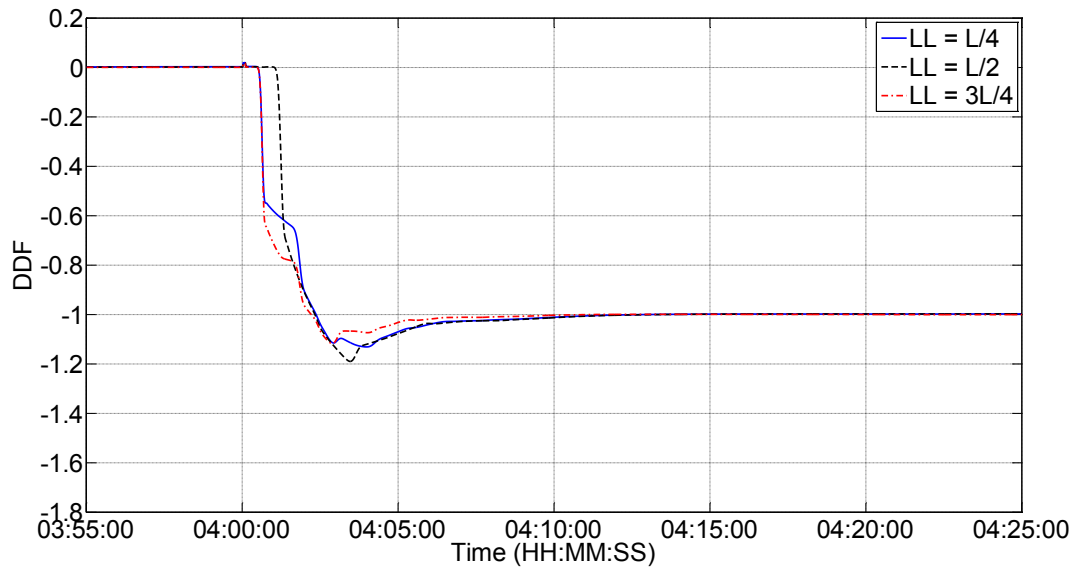


Figure C.28. Non-dimensional diagnostic flow over time for different leak locations. Flow decrease condition, duration = 5 s, TSV = 0.5,  $R = 2.20$ ,  $V_0 = 2.0$  m/s, LR = 1%. Perfect data.

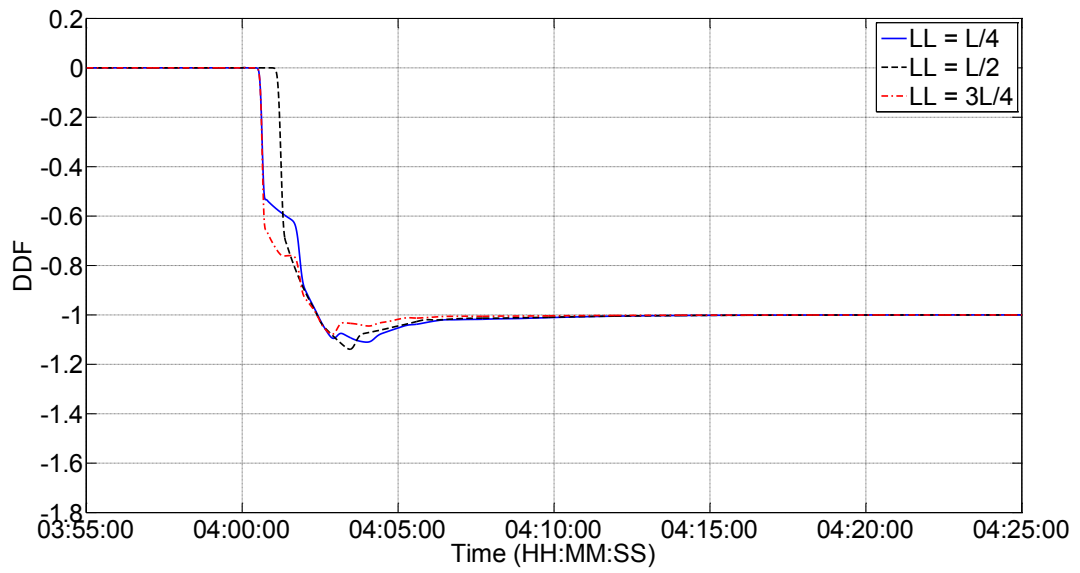


Figure C.29. Non-dimensional diagnostic flow over time for different leak locations. Flow decrease condition, duration = 5 s, TSV = 0.5, R = 2.20, Vo = 2.0 m/s, LR = 30%. Perfect data.

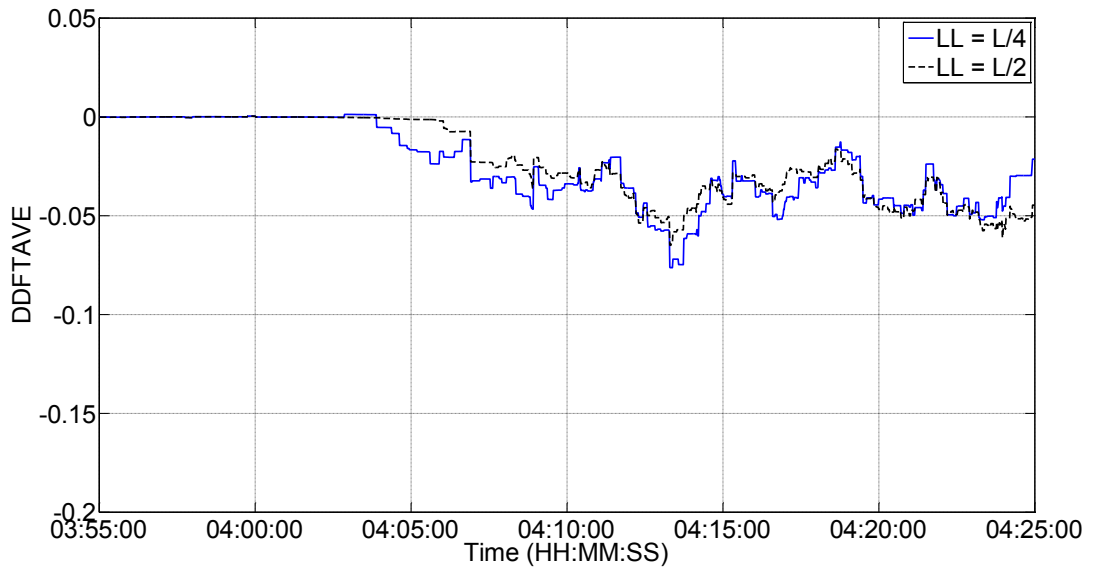


Figure C.30. Non-dimensional time-averaged diagnostic flow over time for different leak locations, steady state condition, Vo = 3 m/s, R = 3.08, LR = 1%. Noisy data, Noise in pressure and flow of 1%.

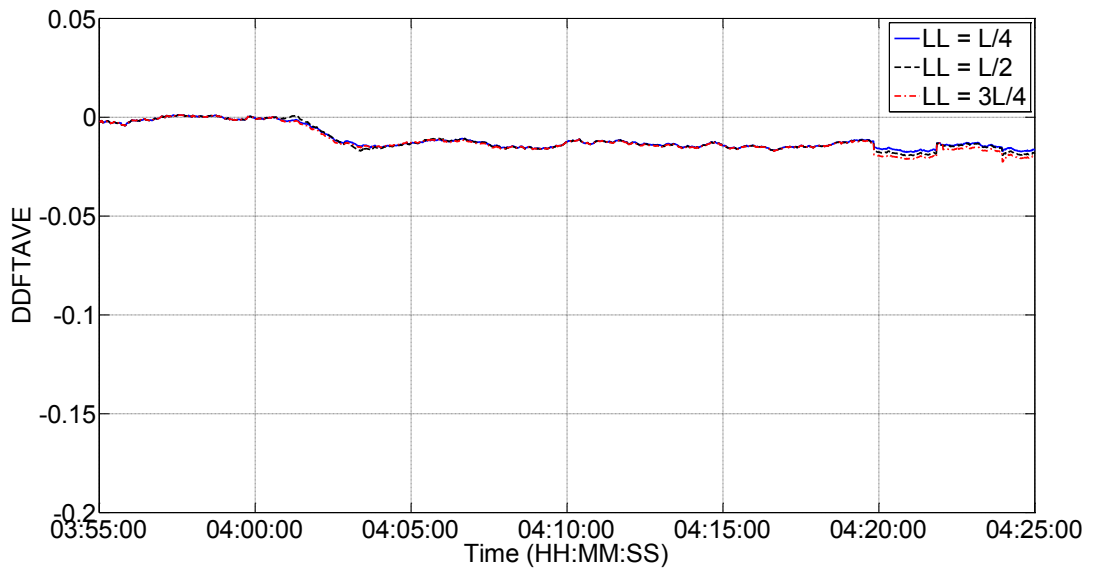


Figure C.31. Non-dimensional time-averaged diagnostic flow over time for different leak locations, steady state condition,  $V_o = 0.3$  m/s,  $R = 0.49$ ,  $LR = 1\%$ . Noisy data, Pressure noise of 1% and flow noise of 3%.

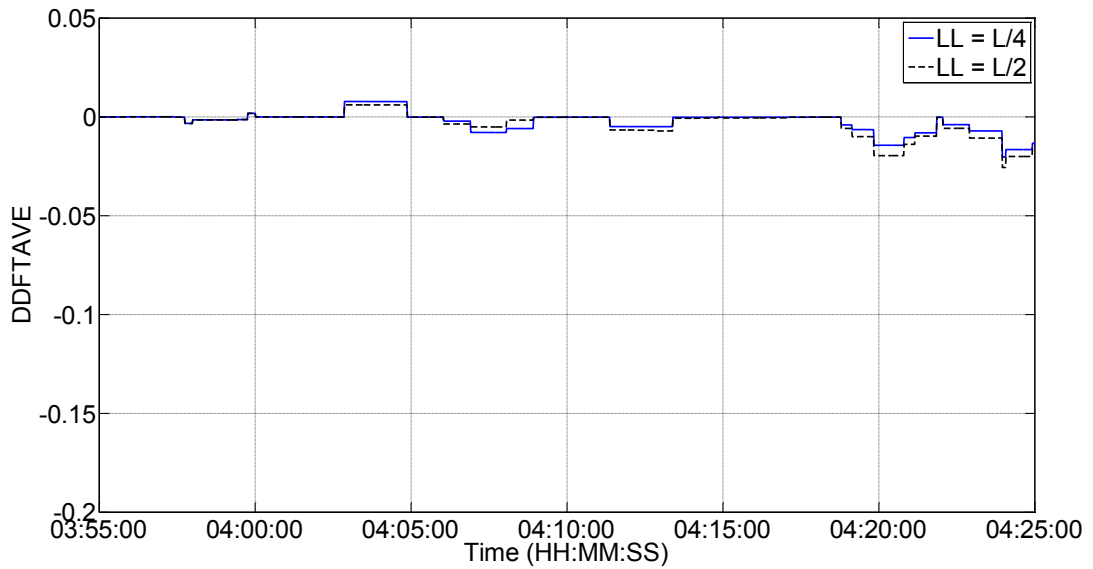


Figure C.32. Non-dimensional time-averaged diagnostic flow over time for different leak locations, steady state condition,  $V_o = 3$  m/s,  $R = 3.08$ ,  $LR = 1\%$ . Noisy data, Pressure noise of 1% and flow noise of 3%.

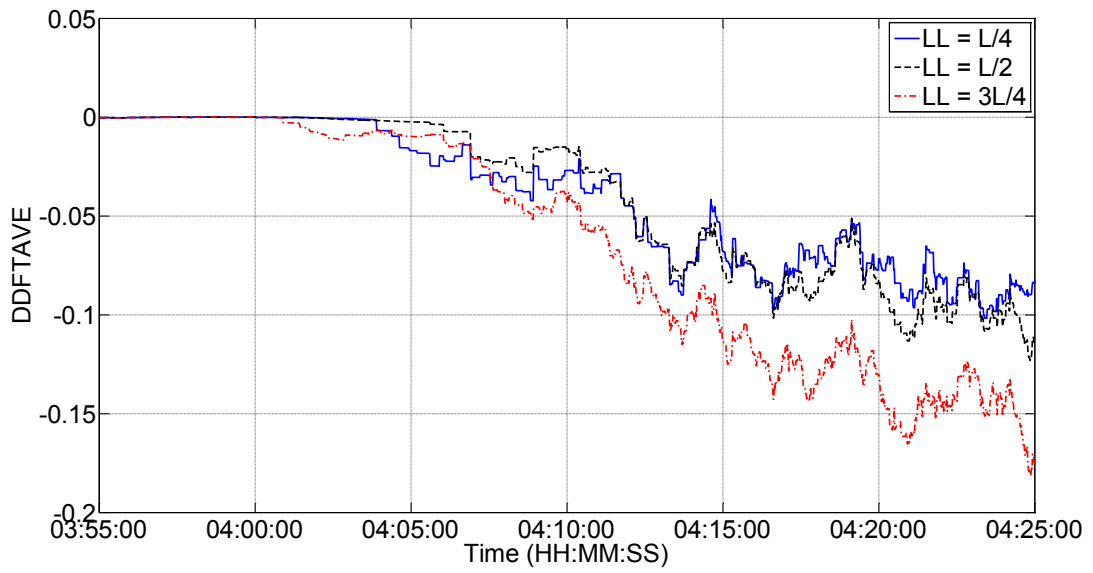


Figure C.33. Non-dimensional time-averaged diagnostic flow over time for different leak locations. Flow decrease condition, duration = 8 min, TSV = 0.12,  $R = 2.20$ ,  $V_o = 2.0$  m/s,  $LR = 1\%$ . Noise in pressure and flow of 1%.

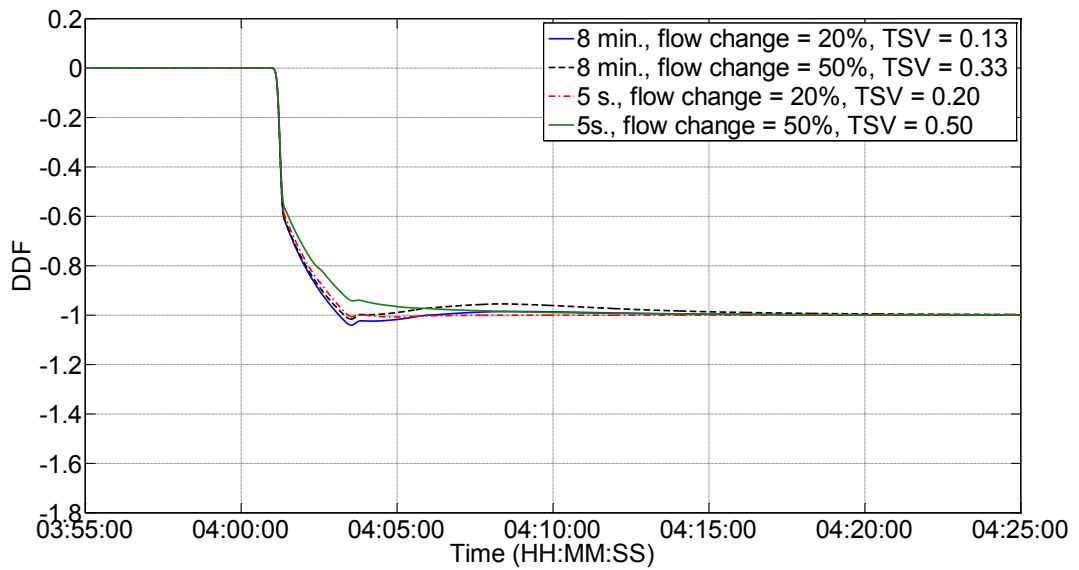


Figure C.34. Non-dimensional diagnostic flow over time for different transient severities, Perfect data. Flow increase condition,  $R = 2.20$ ,  $V_o = 2$  m/s,  $LR = 30\%$ . Leak at midpoint.

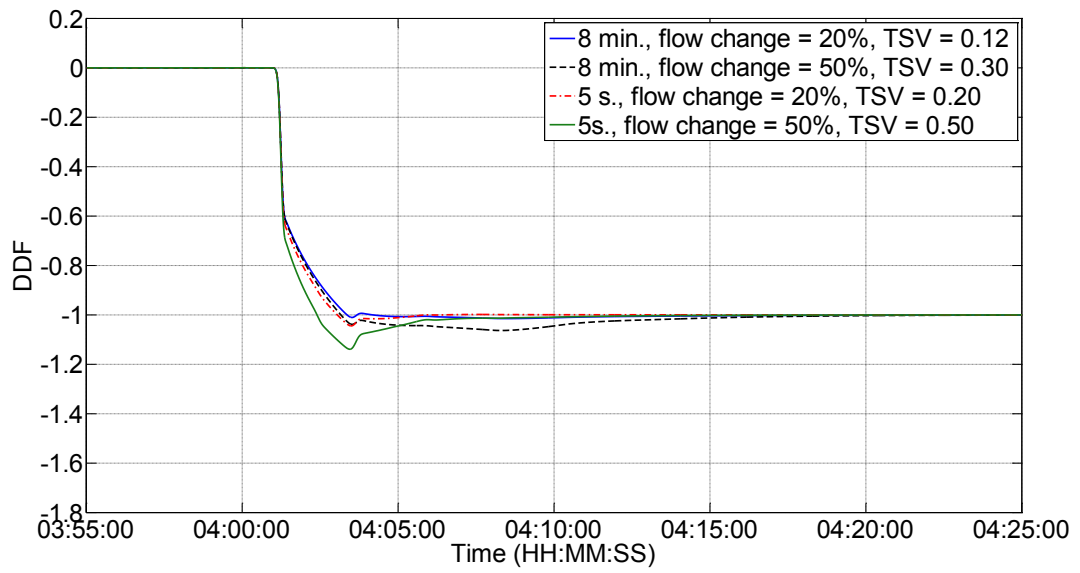


Figure C.35. Non-dimensional diagnostic flow over time for different transient severities, Perfect data. Flow decrease condition,  $R = 2.20$ ,  $V_o = 2$  m/s,  $LR = 30\%$ . Leak at midpoint.

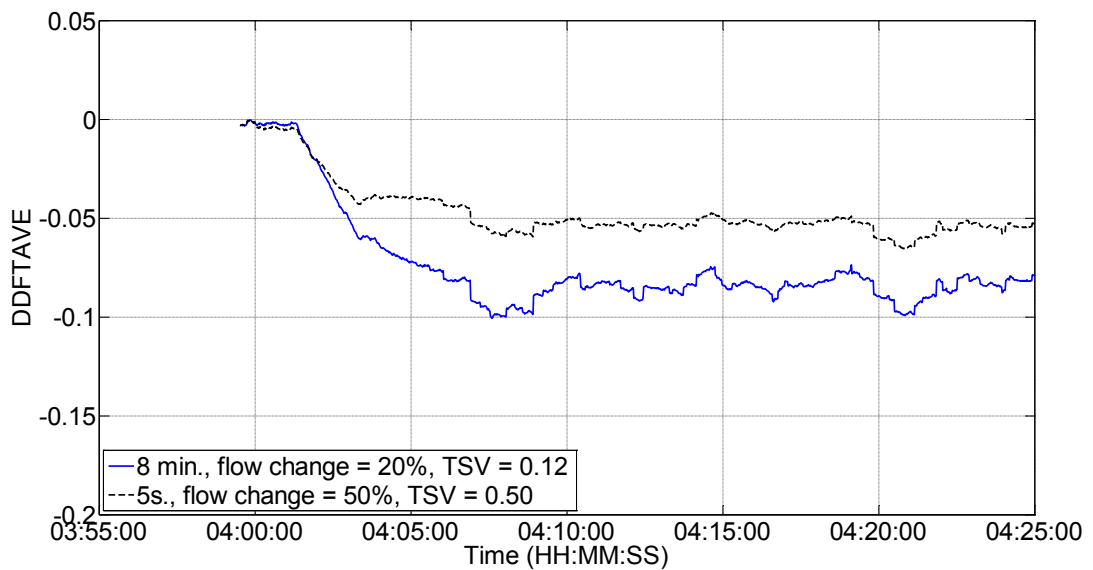


Figure C.36. Non-dimensional time-averaged diagnostic flow over time for different transient severities. Flow increase condition,  $R = 0.49$ ,  $V_o = 0.3$  m/s,  $LR = 1\%$ . Noise in pressure and flow of 1%. Leak at midpoint.

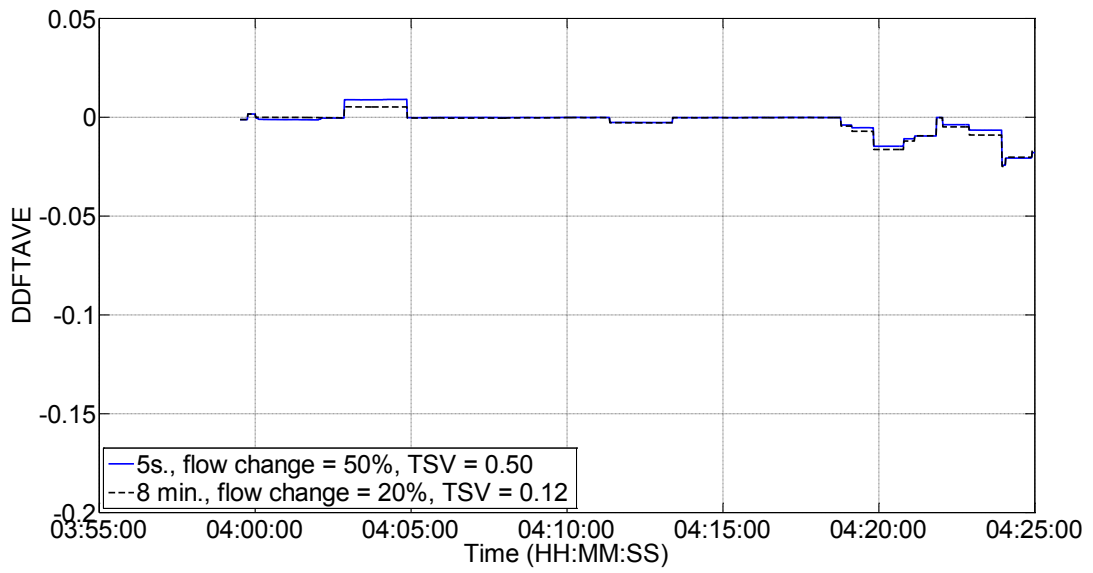


Figure C.37. Non-dimensional time-averaged diagnostic flow over time for different transient severities. Flow increase condition,  $R = 2.20$ ,  $V_o = 2$  m/s,  $LR = 1\%$ . Pressure noise of 1%, flow noise of 3%. Leak at midpoint.

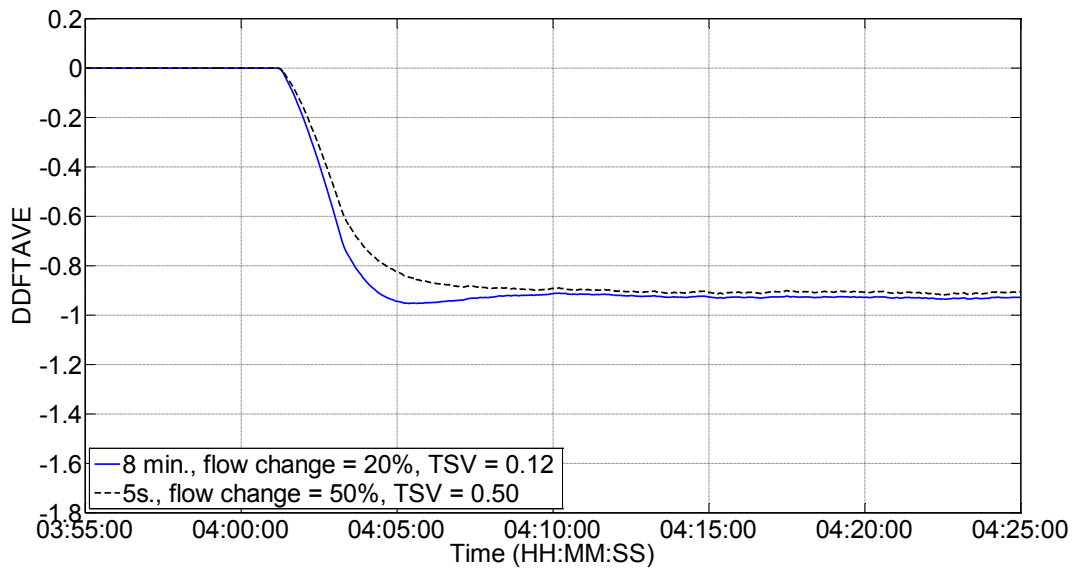


Figure C.38. Non-dimensional time-averaged diagnostic flow over time for different transient severities. Flow increase condition,  $R = 2.20$ ,  $V_o = 2$  m/s,  $LR = 30\%$ . Pressure noise of 1%, flow noise of 1%. Leak at midpoint.

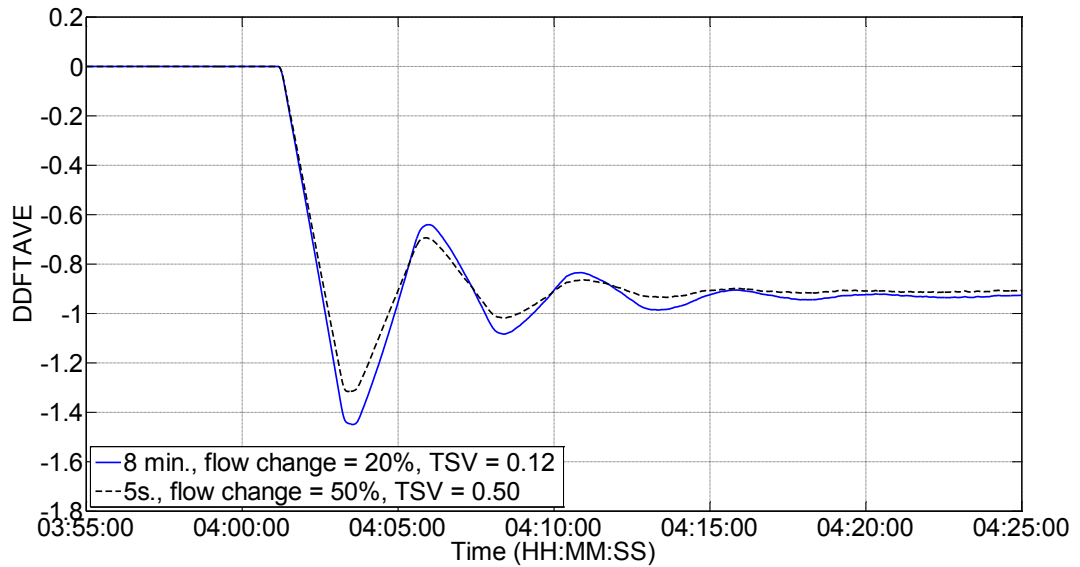


Figure C.39. Non-dimensional time-averaged diagnostic flow over time for different transient severities. Flow increase condition,  $R = 0.49$ ,  $V_o = 0.3$  m/s,  $LR = 30\%$ . Pressure noise of 1%, flow noise of 1%. Leak at midpoint.

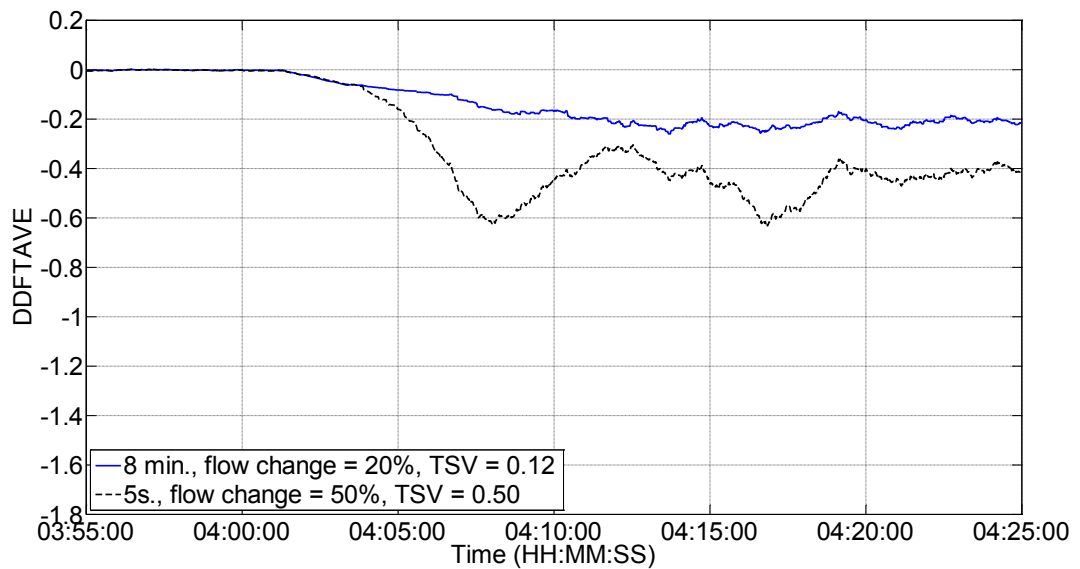


Figure C.40. Non-dimensional time-averaged diagnostic flow over time for different transient severities. Flow decrease condition,  $R = 0.49$ ,  $V_o = 0.3$  m/s,  $LR = 1\%$ . Pressure noise of 1%, flow noise of 1%. Leak at midpoint.

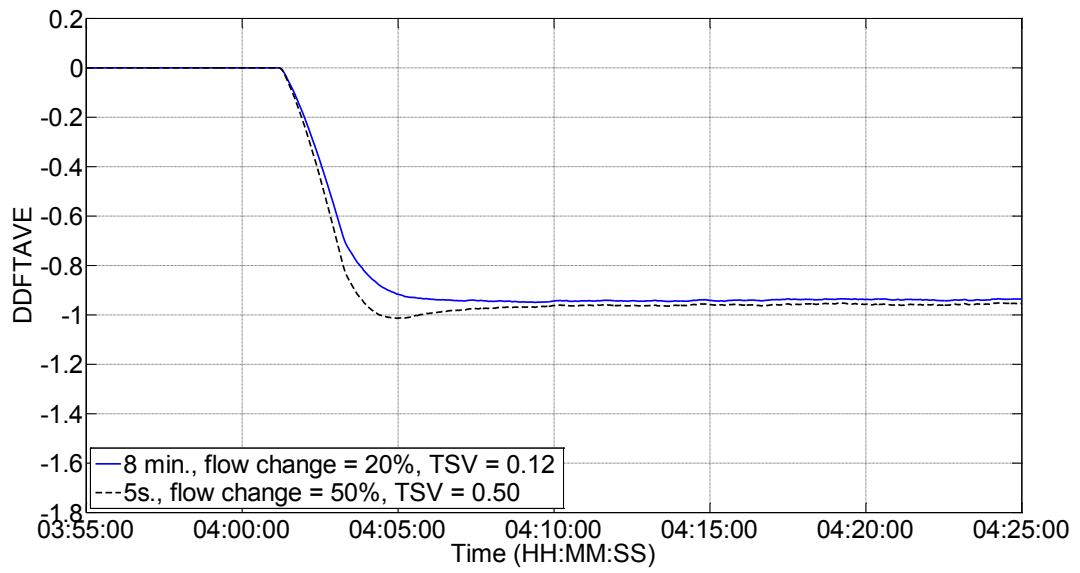


Figure C.41. Non-dimensional time-averaged diagnostic flow over time for different transient severities. Flow decrease condition,  $R = 2.20$ ,  $V_o = 2$  m/s,  $LR = 30\%$ . Pressure noise of 1%, flow noise of 1%. Leak at midpoint.

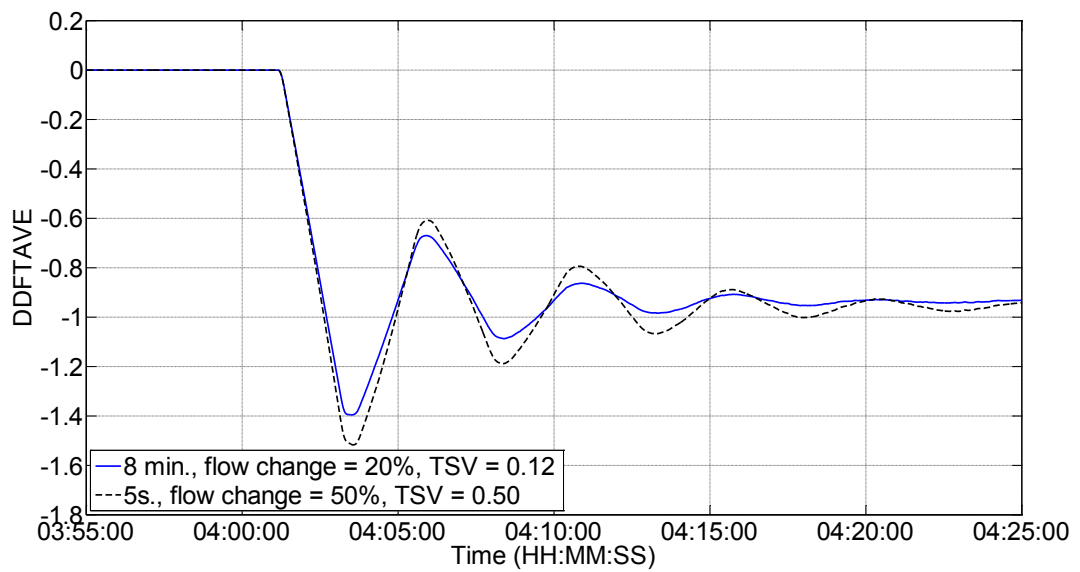


Figure C.42. Non-dimensional time-averaged diagnostic flow over time for different transient severities. Flow decrease condition,  $R = 0.49$ ,  $V_o = 0.3$  m/s,  $LR = 30\%$ . Pressure noise of 1%, flow noise of 1%. Leak at midpoint.

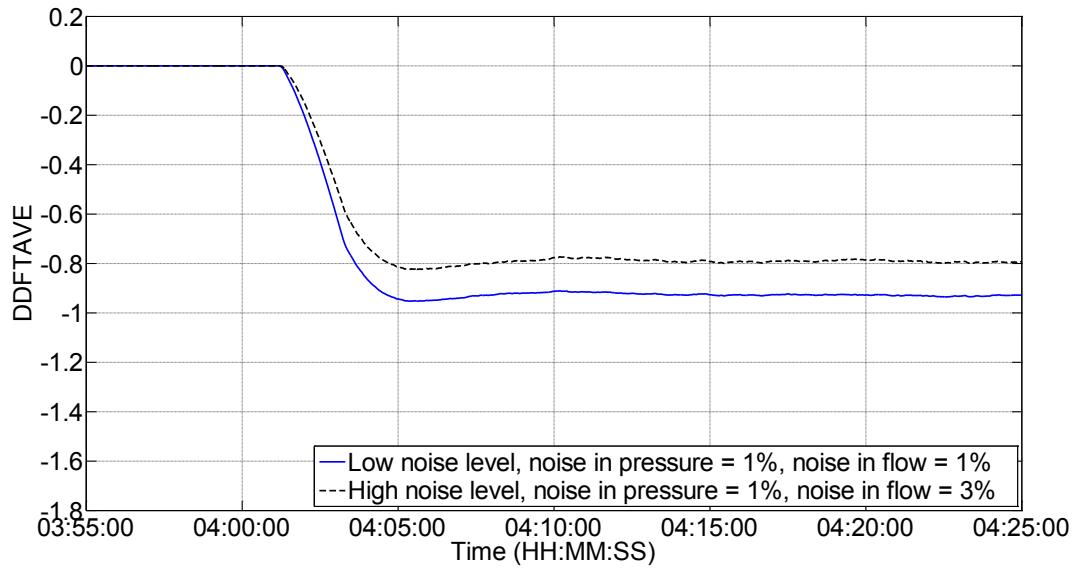


Figure C.43. Non-dimensional time-averaged diagnostic flow over time for different noise levels in flow, Noisy data. Flow increase condition,  $R = 2.20$ ,  $V_o = 2.0$  m/s,  $V_f = 2.4$  m/s,  $LR = 30\%$ , leak at midpoint,  $TSV = 0.2$ , duration = 8 min.

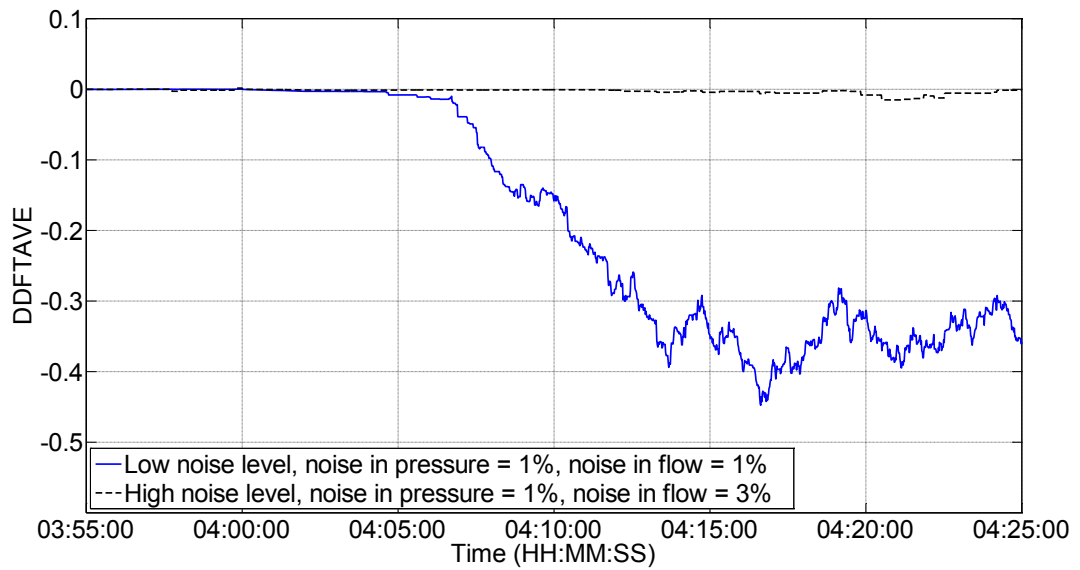


Figure C.44. Non-dimensional time-averaged diagnostic flow over time for different noise levels in flow, Noisy data. Flow decrease condition,  $R = 2.20$ ,  $V_o = 2$  m/s,  $V_f = 1$  m/s,  $LR = 1\%$ , leak at midpoint,  $TSV = 0.5$ , duration = 5 s.

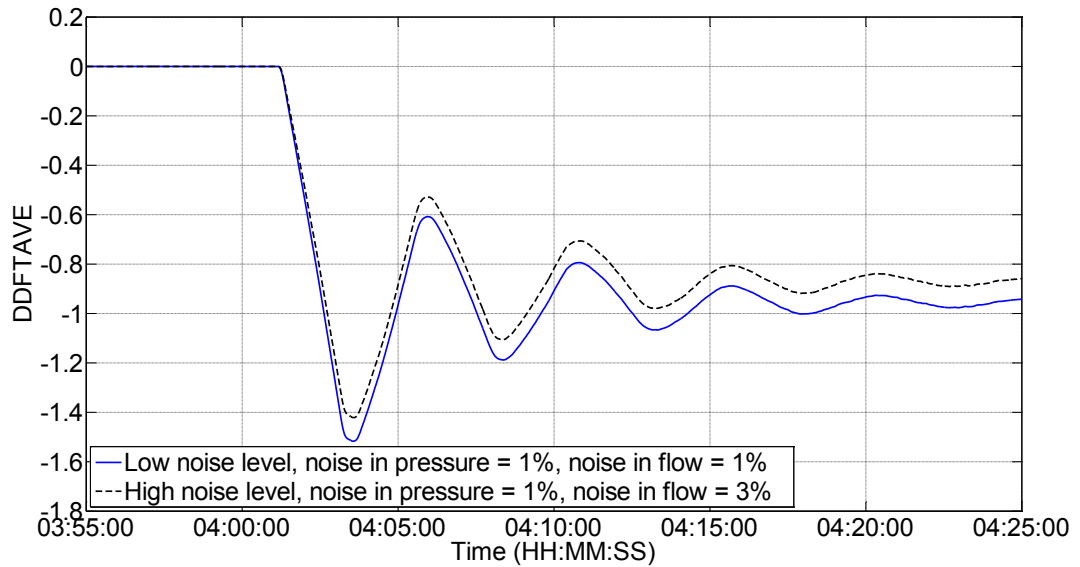


Figure C.45. Non-dimensional time-averaged diagnostic flow over time for different noise levels in flow, Noisy data. Flow decrease condition,  $R = 2.20$ ,  $V_o = 0.30$  m/s,  $V_f = 0.15$  m/s,  $LR = 30\%$ , leak at midpoint,  $TSV = 0.5$ , duration = 5 s.

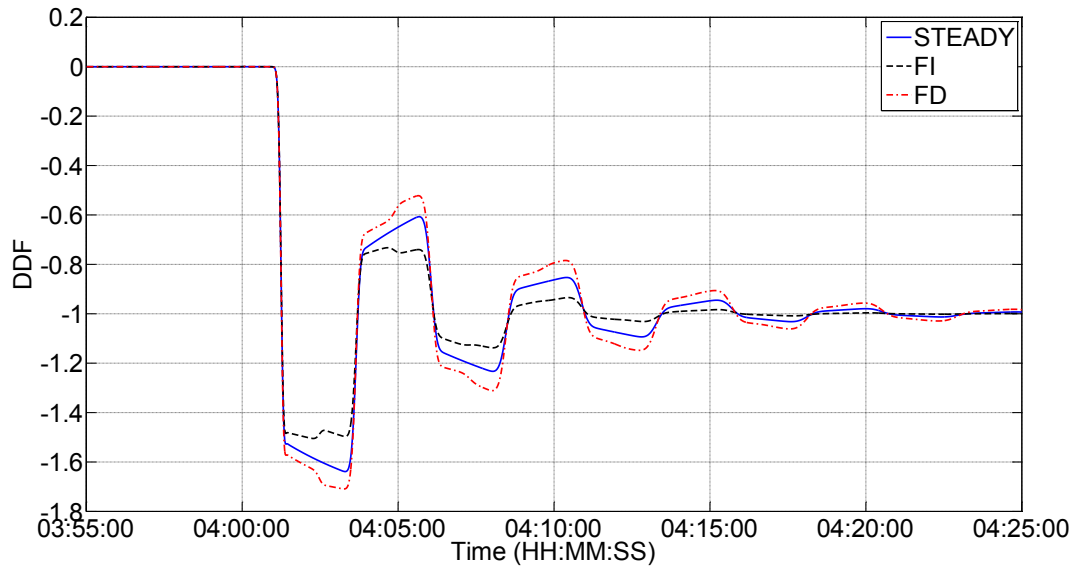


Figure C.46. Non-dimensional diagnostic flow over time for different flow states, Perfect data.  $V_o = 0.3$  m/s,  $R = 0.49$ ,  $LR = 30\%$ , leak at midpoint, transient duration = 5 s,  $TSV = 0.5$ .

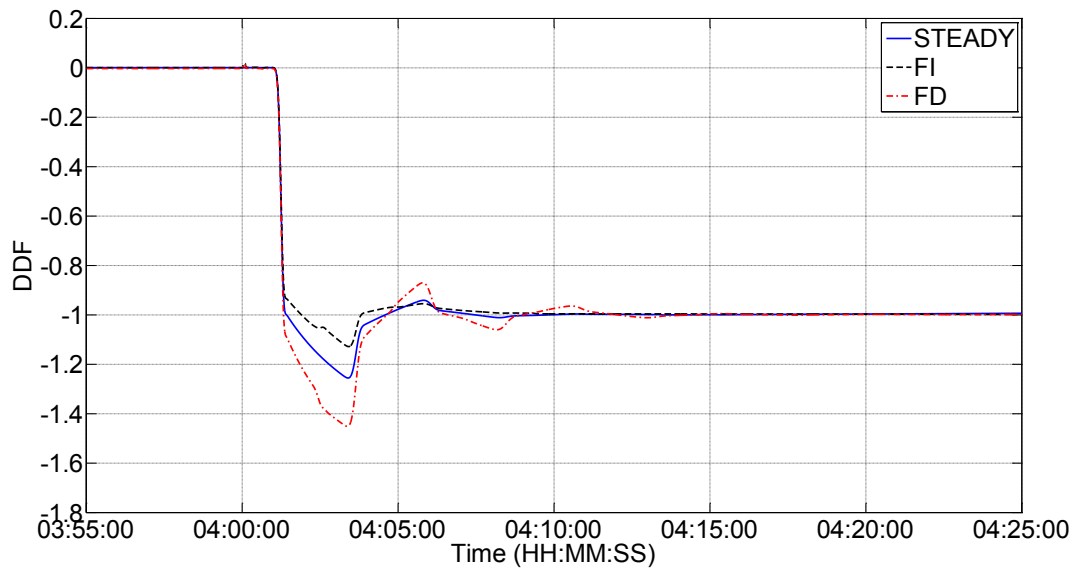


Figure C.47. Non-dimensional diagnostic flow over time for different flow states, Perfect data.  $V_o = 1.0$  m/s,  $R = 1.26$ ,  $LR = 1\%$ , leak at midpoint, transient duration = 5 s,  $TSV = 0.5$ .

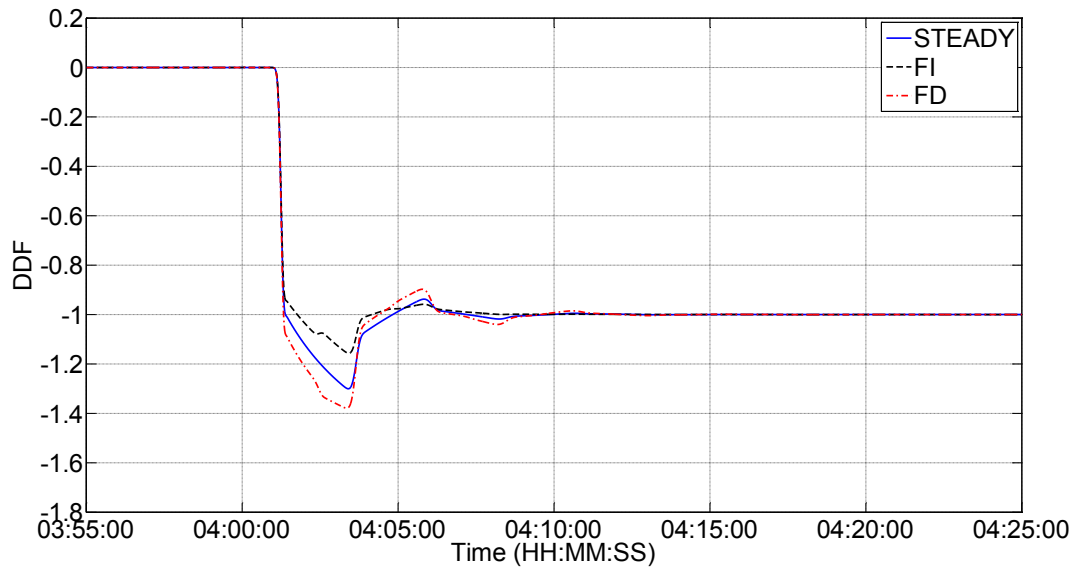


Figure C.48. Non-dimensional diagnostic flow over time for different flow states, Perfect data.  $V_o = 1.0$  m/s,  $R = 1.26$ ,  $LR = 30\%$ , leak at midpoint, transient duration = 5 s,  $TSV = 0.5$ .

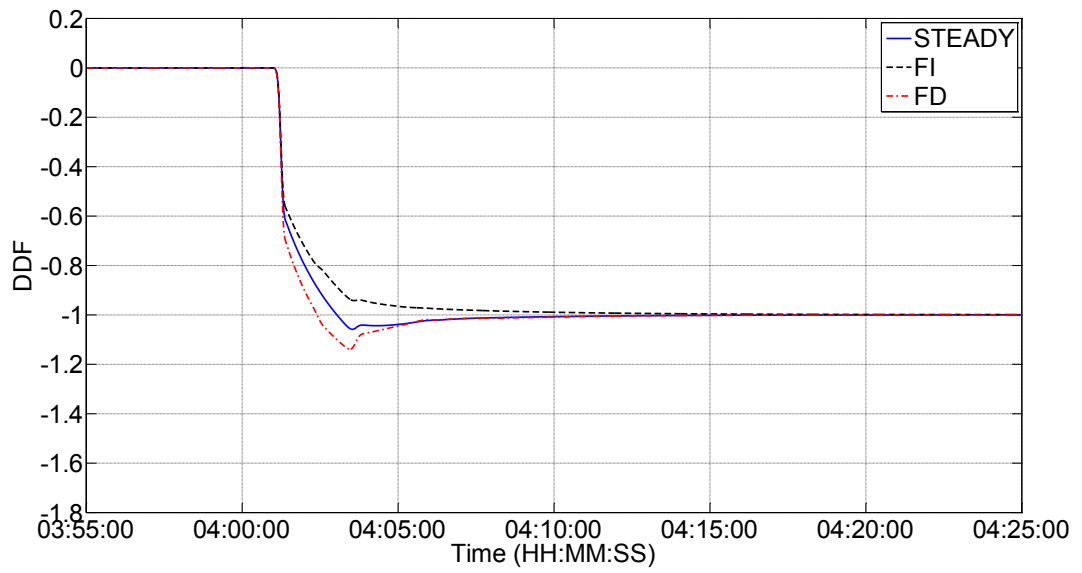


Figure C.49. Non-dimensional diagnostic flow over time for different flow states, Perfect data.  $V_o = 2.0$  m/s,  $R = 2.2$ ,  $LR = 30\%$ , leak at midpoint, transient duration = 5 s,  $TSV = 0.5$ .

Appendix D: Best tuning parameters of the leak detection system, With Perfect Data

<i>Check the following in inprep file</i>						
data.type	MACRO(data.type, perfect )					
SELECT (YES or NO)	PDF	YES	BMC	NO	SPANS	YES
<i>Check the following in intran file</i>						
BEGIN Tolerance	PRES.TOLER = 0 PSIG		TEMP.TOLER = 0			
Repeatability	FLOW_UNCRT = 0.00		PRES_UNCRT = 0.00 PSIG			
Time Error Bound	G.Q.TEB = 0 min		G.P.TEB = 0 min			
Repeatability decay	G.Q.RDR = 0 m3/hr/min		G.P.RDR = 0 PSIG/min			
Rate bound	G.Q.RB = 60,000 m3/hr/min		G.P.RB = 60,000 PSIG/min			
Elevation error	:EE = 0 ft.					
Friction correction bound for :FC	PFC.BOUND = 0					
Batch friction correction bound	BFC.BOUND = 0					
Bound for bulk modulus correction	BMC.BOUND = 0					

Appendix D: Best tuning parameters of the leak detection system, With Noisy Data

<i>Check the following in inprep file</i>						
data.type	MACRO(data.type, noise )					
SELECT (YES or NO)	PDF	YES	BMC	NO	SPANS	YES
<i>Check the following in intran file</i>						
BEGIN Tolerance	PRES.TOLER = 0 PSIG		TEMP.TOLER = 0			
Repeatability	FLOW_UNCRT = 0.01		PRES_UNCRT = 0.01 PSIG			
Time Error Bound	G.Q.TEB = 0 min		G.P.TEB = 0 min			
Repeatability decay	G.Q.RDR = 0 m3/hr/min		G.P.RDR = 0 PSIG/min			
Rate bound	G.Q.RB = 60,000 m3/hr/min		G.P.RB = 60,000 PSIG/min			
Elevation error	:EE = 0 ft.					
Friction correction bound for :FC	PFC.BOUND = 0					
Batch friction correction bound	BFC.BOUND = 0					
Bound for bulk modulus correction	BMC.BOUND = 0					

Appendix D: Best tuning parameters of the leak detection system, With Perfect and Noisy Data

Number	Parameter Description	Tuning Parameter	Units	Input values	Files
<b>Model parameters</b>					
1	include PDF in state estimation	PDF	NA	YES	inprep
2	include BMC in state estimation	BMC	NA	NO	inprep
3	for autocalibration	SPANS	NA	YES	inprep
4		PRES.TOLER	PSI	0.0	intran
5	error tolerance for solving non-linear equations	TEMP.TOLER	PSI/DF	0.0	intran
6	max iterations	OL.MAXITR	NONE	1000	intran
7	friction correction bound for :FC	PFC.BOUND	%	0	intran
8	batch friction correction bound	BFC.BOUND	%	0	intran
9	bound for bulk modulus correction	BMC.BOUND	%	0	intran
<b>Tuning parameters</b>					
10	expected density uncertainty on fluid	DENSITY.ERROR	%	DER=4	inprep
11	expected viscosity uncertainty on fluid	VISCOSITY.ERROR	%	VER=5	inprep
12	expected bulk modulus uncertainty on fluid	BULK.MOD.ERROR	%	BMER=20	inprep
13	on transfer pipe	ELEV.ERR	FT	0,0,0,0	inprep
<b>JTS weight</b>					
14	pressure deviation	JTSWT(1)	NONE	1	intran
15	rate of pressure change	JTSWT(2)	NONE	10	intran
16	flow deviation	JTSWT(3)	NONE	1	intran
17	diagnostic flow	JTSWT(4)	NONE	5	intran
18	rate of PDF change	JTSWT(5)	NONE	500	intran
19	bulk modulus error	JTSWT(6)	NONE	1000	intran
20	magnitude of frictional PDF	JTSWT(7)	NONE	10000	intran
21	pressure differences	JTSWT(8)	NONE	10000	intran
22	rate of gravitational PDF	JTSWT(9)	NONE	500	intran
23	magnitude of gravitational PDF	JTSWT(10)	NONE	1000	intran
24	leakless monitors	LM.WT	NONE	1	intran
<b>SCADA limits</b>					
25	Timeout	TOUT	MINUTES	1.5	inprep
26	Autocalibration periods	ACP	MINUTES	4320	inprep
27	Repeatability (based on noise level)	REP	USER UNITS	P=0, DN=4, D=1, T=1, C=5	inprep for others and intran for P
27a	Flow repeatability	FLOW_UNCTRL	%	0 for perfect data; 1 for noisy data	inprep based on noise level
27b	Pressure repeatability	FLOW_UNCTRL	%	0 for perfect data; 1 for noisy data	inprep based on noise level
28	Accuracy	ACC	USER UNITS	P = 1, T = 1, D = 1, DN = 3, C = 5	inprep
28a	Flow accuracy	ACC	%	0.2	inprep
29	Scan period	SP	MINUTES	0.1, except for V=1, and P,Q = 0.05 to 1/60	inprep for others and intran for P,Q
30	Time tag error bound	TEB	MINUTES	0	intran
31	Rate bound	RB	USER UNITS/TIME	P = 60000, Q = 60000, T = 50, D = 100	inprep
32	Repeatability decay rate	RDR	USER UNITS/TIME	0	intran
33	simulation behine real-time	LF.MAXWAIT	MINUTES	0.5	intran
34	for extrapolation	MAXSCANS	NONE	5	intran